



UNIFORMED SERVICES UNIVERSITY OF THE HEALTH SCIENCES  
F. EDWARD HÉBERT SCHOOL OF MEDICINE  
4301 JONES BRIDGE ROAD  
BETHESDA, MARYLAND 20814-4799



November 23, 2009

GRADUATE PROGRAMS IN  
THE BIOMEDICAL SCIENCES  
AND PUBLIC HEALTH

*Ph.D. Degrees*

Interdisciplinary  
-Emerging Infectious Diseases  
-Molecular & Cell Biology  
-Neuroscience

Departmental  
-Clinical Psychology  
-Environmental Health Sciences  
-Psychology  
-Medical Zoology

Physician Scientist (MD/Ph.D.)

Doctor of Public Health (Dr.P.H.)

*Master of Science Degrees*

-Public Health

*Masters Degrees*

-Health Administration & Policy  
-Military Medical History  
-Public Health  
-Tropical Medicine & Hygiene

*Graduate Education Office*

Eleanor S. Metcalf, Ph.D., Associate Dean  
Bettina Arnett, Support Specialist  
Roni Bull, Support Specialist  
Katie Hall, Support Specialist

*Web Site*

<http://www.usuhs.mil/graded/>

*E-mail Address*

[graduateprogram@usuhs.mil](mailto:graduateprogram@usuhs.mil)

*Phone Numbers*

Commercial: 301-295-9474 / 3913  
Toll Free: 800-772-1747  
DSN: 295-9474  
FAX: 301-295-6772

DISSERTATION APPROVAL  
FOR THE DOCTORAL DISSERTATION  
IN THE EMERGING INFECTIOUS DISEASES  
GRADUATE PROGRAM

Title of Dissertation: "Defining the Antigenic Structure of the Henipavirus Attachment (G) Glycoprotein: Implications for the Fusion Mechanism"

Name of Candidate: Andrew C. Hickey  
Doctor of Philosophy Degree  
December 11, 2009

DISSERTATION AND ABSTRACT APPROVED:

Dr. Gerald V. Quinman, Jr., MD  
PREVENTIVE MEDICINE AND BIOMETRICS DEPARTMENT  
Committee Chairperson

DATE:

3/10/10

Dr. Christopher C. Broder, Ph.D.  
MICROBIOLOGY AND IMMUNOLOGY DEPARTMENT  
Dissertation Advisor

1-22-2010

Dr. Brian C. Schaefer, Ph.D.  
MICROBIOLOGY AND IMMUNOLOGY DEPARTMENT  
Committee Member

1/25/10

Dr. R. Joel Lowey, Ph.D.  
Science Research Department, AFRR1  
Committee Member

1/22/2010

Dr. Dimitar S. Dimitrov, Ph.D.  
Senior Investigator, Protein Interactions Group, NCI  
Committee Member

1/22/2010

Report Documentation Page				Form Approved OMB No. 0704-0188	
Public reporting burden for the collection of information is estimated to average 1 hour per response, including the time for reviewing instructions, searching existing data sources, gathering and maintaining the data needed, and completing and reviewing the collection of information. Send comments regarding this burden estimate or any other aspect of this collection of information, including suggestions for reducing this burden, to Washington Headquarters Services, Directorate for Information Operations and Reports, 1215 Jefferson Davis Highway, Suite 1204, Arlington VA 22202-4302. Respondents should be aware that notwithstanding any other provision of law, no person shall be subject to a penalty for failing to comply with a collection of information if it does not display a currently valid OMB control number.					
1. REPORT DATE <b>2009</b>		2. REPORT TYPE		3. DATES COVERED <b>00-00-2009 to 00-00-2009</b>	
4. TITLE AND SUBTITLE <b>Defining the Antigenic Structure Of The Henipavirus Attachment (G) Glycoprotein:Implications For The Fusion Mechanism</b>				5a. CONTRACT NUMBER	
				5b. GRANT NUMBER	
				5c. PROGRAM ELEMENT NUMBER	
6. AUTHOR(S)				5d. PROJECT NUMBER	
				5e. TASK NUMBER	
				5f. WORK UNIT NUMBER	
7. PERFORMING ORGANIZATION NAME(S) AND ADDRESS(ES) <b>Uniformed Services University Of The Health Sciences,Bethesda,MD,20814</b>				8. PERFORMING ORGANIZATION REPORT NUMBER	
9. SPONSORING/MONITORING AGENCY NAME(S) AND ADDRESS(ES)				10. SPONSOR/MONITOR'S ACRONYM(S)	
				11. SPONSOR/MONITOR'S REPORT NUMBER(S)	
12. DISTRIBUTION/AVAILABILITY STATEMENT <b>Approved for public release; distribution unlimited</b>					
13. SUPPLEMENTARY NOTES					
14. ABSTRACT <b>Epidemics of communicable disease such as the Medieval Black Death (Yersinia pestes) or the introduction of smallpox to the Aztecs decimated human populations interrupted trade routes, and transformed social and economic conventions (reviewed in 69, 105, 136). However, communicable diseases remained enigmatic until the advancement of germ theory suggested these illnesses resulted from discrete biological sources. In 1928, Sir Alexander Flemming discovered penicillin and proved communicable disease could be treated and cured (54). Further, development of the smallpox and rabies vaccines by Edward Jenner and Louis Pasteur, respectively demonstrated illness was preventable. These scientific advances ushered in an era of rapid development in prophylactic and therapeutic modalities resulting in significant global decreases in the health burden of infectious agents. As early as the mid 1940s widespread achievement in the control of infectious disease prompted public health leaders in the United States and elsewhere to declare the global threat of infectious disease had passed (140).</b>					
15. SUBJECT TERMS					
16. SECURITY CLASSIFICATION OF:			17. LIMITATION OF ABSTRACT <b>Same as Report (SAR)</b>	18. NUMBER OF PAGES <b>203</b>	19a. NAME OF RESPONSIBLE PERSON
a. REPORT <b>unclassified</b>	b. ABSTRACT <b>unclassified</b>	c. THIS PAGE <b>unclassified</b>			

The author certifies that the use of any copyrighted material in the dissertation manuscript entitled:

“Defining the Antigenic Structure of the Henipavirus Attachment (G) Glycoprotein: Implications for the Fusion Mechanism”

is appropriately acknowledged and, beyond brief excerpts, is with the permission of the copyright owner.



Andrew Christopher Hickey  
Emerging Infectious Diseases Graduate Program  
Uniformed Services University

# **ABSTRACT**

## **Defining the Antigenic Structure of the Henipavirus Attachment (G) Glycoprotein: Implications for the Fusion Mechanism**

Andrew Christopher Hickey, Ph.D., M.P.H., 2009

Thesis Supervisor: Dr. Christopher C. Broder, Professor and Director, Emerging  
Infectious Diseases Graduate Program

Henipaviruses undergo class I viral fusion at the cell surface orchestrated by the collective action of the immunodominant fusion (F) and attachment (G) glycoproteins. Immunization of Balb/cJ mice with soluble G (sG) glycoprotein induced a strong humoral response that targeted diverse epitopes and inhibited HeV- and NiV- glycoprotein mediated membrane fusion. To characterize the antigenic structure of the henipavirus G glycoprotein, we generated 27 monoclonal antibody (mAb) secreting hybridoma cell lines derived from immunized mice. The library of mAbs target diverse epitopes common to both sG and the native wild type glycoprotein and 12 mAbs inhibited viral glycoprotein-mediated membrane fusion at concentrations less than 200 µg/ml. Competitive-binding assays indicated the neutralizing mAbs targeted 4 common (sites II, III, V, and VI) and 3 virus-specific (sites I, IV, and VII) antigenic sites. Notably, mAbs targeting only a single antigenic site (VI) competitively blocked ephrinB2 and -B3 binding. These results confirmed the B class ephrin receptors target a single overlapping domain common to both HeV G and NiV G. In addition, the conformation and disulfide

bridges were requisite for recognition by inhibitory mAbs. Additional analysis with the library of mAbs uncovered 6 murine mAbs and 1 human mAb that differentially bound full-length G in the presence or absence of soluble viral receptor, sEphrinB2. The subpanel includes 2 mAbs which mediate virus neutralization and target 2 independent antigenic sites (sites I and III) and the remaining 5 mAbs target 2 additional independent antigenic sites (sites A and B) of the G glycoprotein. Co-expression of F did not alter mAb recognition of receptor induced antigenic changes in the G glycoprotein indicating formation of oligomeric complexes associated with F does not modulate the structure of the G glycoprotein. Immunoprecipitation analyses and comparison of the amount of soluble antigen precipitated revealed the mAbs efficiently bound sG in the presence and absence of sEphrinB2, demonstrating these epitopes are readily exposed on the sG glycoprotein. Taken together, these results reveal a multistep model of henipavirus envelope glycoprotein function that physically links post-attachment processes in the G glycoprotein with the activation of the F glycoprotein mediated fusion process.

**DEFINING THE ANTIGENIC STRUCTURE OF THE  
HENIPAVIRUS ATTACHMENT (G) GLYCOPROTEIN:  
IMPLICATIONS FOR THE FUSION MECHANISM**

**By**

**Andrew Christopher Hickey**

**Dissertation submitted to the Faculty of the  
Emerging Infectious Diseases Graduate Program  
Uniformed Services University of the Health Sciences  
in partial fulfillment of the requirements for the degree of  
Doctor of Philosophy 2009**

## Preface

Portions of this manuscript have been published as:

**Hickey, A.C., and C.C. Broder.** 2009. The Mechanism of Henipavirus Fusion: Examining the Relationships between the Attachment and Fusion Glycoproteins. *Virologica Sinica* **24**(2): 110-120.

and

**Li, Y., Wang, J., Hickey, A.C., Zhang, Y., Li, Y., Wu, Y., Zhang, H., Yuan, J., Han, Z., McEachern, J., Broder, C.C., Wang, L.F., and Z. Shi.** 2008. Antibodies to Nipah or Nipah-like viruses in bats, China. *Emerging Infectious Diseases* **14**(12): 1974-1976.

Human monoclonal antibodies were supplied by Dr. Zhongyu Zhu and Dr. Dimitar Dimitrov of the National Cancer Institute, National Institutes of Health. Murine monoclonal antibodies 3A5.D2, 8H4, 17A5, and H2.1 were supplied by Dr. John White of the Australian Animal Health Laboratory, Australian Commonwealth Scientific and Research Organization (AAHL, CSIRO). Dr. Linfa Wang and Dr. Brian Eaton, both of the AAHL, supplied the henipavirus envelope glycoproteins for cloning and characterization by Dr. Katharine Bossart. Dr. Bossart created recombinant S-tagged sG and Dr. Kimberly A. Bishop-Lilly created the recombinant S-peptide tagged sEphrinB2 construct. Purified mAb and soluble glycoproteins were prepared by Yanru Feng and myself.

## **Dedication**

I thank past and present members of the laboratory, particularly Dr. Kimberly Bishop-Lilly and Stephanie Petzing, for the laughter and help. I thank Dr. Katharine Bossart for her friendship, mentoring, and guidance. I also thank Dr. Julie Pavlin, a friend and advocate who has opened many doors for me and other students of the EID program. I owe a special debt of gratitude to both Dr. Christopher C. Broder and Dr. Eleanor Metcalf who mentored me in the program.

I thank my friends and I look forward to your continued friendship and following your successes. Most of all, I thank my parents and my family. You supported me through years of school and it would not have been possible to have succeeded without you.



## Table of Contents

List of Figures .....	xii
List of Tables .....	xiv
Chapter 1: Introduction .....	1
Preface .....	1
Emerging infectious diseases .....	2
Emerging zoonotic diseases .....	5
Emerging viral diseases .....	7
Paramyxoviridae family .....	8
Organization .....	8
Biology .....	10
Henipavirus epidemiology .....	24
Emergence .....	24
Epidemiology .....	26
Endemic henipavirus infection .....	27
Henipavirus biology .....	32
Disease and pathogenesis .....	33
Humoral immune response .....	40
Paramyxovirus membrane fusion .....	43
Virus attachment .....	44
Interaction of the envelope glycoproteins .....	45
Activation of the fusion glycoprotein .....	47
Membrane merger .....	49

Specific aims and hypotheses .....	50
Chapter 2: Materials and Methods .....	54
Tissue culture .....	54
Tissue sample collection and RNA isolation .....	54
NiV Taqman reverse transcriptase PCR .....	55
Recombinant proteins .....	56
Immunization of mice and hybridoma .....	56
Monoclonal antibody preparation .....	57
Indirect ELISA and competitive-binding assay .....	58
Serology and data collection .....	59
Data analysis .....	60
Virus neutralization assays .....	60
Viral glycoprotein mediated membrane fusion assays .....	61
Immunoprecipitation assays.....	62
Metabolic labeling and receptor induced changes assays .....	63
Chapter 3: Characterizing the neutralizing epitopes of the henipavirus G glycoprotein .	65
Introduction.....	65
Results.....	67
Murine polyclonal B cell response following sG glycoprotein immunization .....	67
Generating the library of mAb-secreting hybridomas .....	72
Identification of neutralizing mAbs .....	72
Characterization of neutralizing mAbs .....	73
Competitive-binding analysis of neutralizing mAbs .....	81

Antigenicity of the receptor-binding domain.....	82
Model of the virus neutralizing henipavirus G glycoprotein antigenic sites .....	85
Discussion.....	91
Chapter 4: Receptor induced changes in the antigenic structure of henipavirus G. ....	97
Introduction.....	97
Results.....	99
Conformational and antigenic changes in the henipavirus G glycoprotein following receptor binding.....	99
Characterization of G glycoprotein specific mAbs.....	100
Competitive binding analysis of the G glycoprotein specific mAbs .....	106
Antigenic structural analysis of henipavirus sG glycoprotein .....	110
Antigenic changes in oligomeric forms of the henipavirus G glycoprotein .....	113
Receptor-induced antigenic changes in henipavirus G glycoprotein co-expressed with the F glycoprotein .....	114
Model of henipavirus fusion .....	121
Discussion.....	122
Chapter 5: Discussion .....	129
Preface .....	129
Experimental results in the context of the project aims.....	131
Contributions to the study of Paramyxoviruses .....	135
Antibody library and assay development.....	135
The host virus neutralizing humoral response .....	138
Mechanisms of antibody-mediated virus neutralization .....	140

Receptor induced antigenic changes in the paramyxovirus attachment	
glycoproteins .....	148
Unanswered questions .....	150
Limitations and future directions .....	152
Limitations .....	152
Future directions .....	153
Concluding remarks .....	159
Chapter 6: Appendices .....	160
Chapter 7: References .....	166

## List of Figures

Figure 1. Diagram of the paramyxovirus replication cycle .....	11
Figure 2. Genomic and structural organization of the <i>Paramyxovirinae</i> .....	13
Figure 3. Structural features of henipavirus G.....	20
Figure 4. Diagram of the paramyxovirus F.....	22
Figure 5. Age, gender, and school distribution of children in Kamphaeng Phet province, Thailand with serologic evidence of prior henipavirus exposure.....	30
Figure 6. Relative quantity of NiV genome in blood fractions derived from African Green monkeys challenged with NiV. ....	36
Figure 7. Relative quantity of NiV genome among organ samples harvested from African Green monkeys challenged with NiV. ....	38
Figure 8. Model of henipavirus glycoprotein mediated class I fusion.....	51
Figure 9. Diagram of the immunization of mice with sG glycoprotein.....	68
Figure 10. Polyclonal humoral response among mice immunized with purified henipavirus sG .....	70
Figure 11. Inhibition of HeV- and NiV- entry by mAb hAH1.3 .....	75
Figure 12. Neutralizing mAb reactivity with soluble and full-length recombinant G.....	77
Figure 13. Competitive-binding assays indicated the collection of neutralizing mAbs targeted 7 antigenic sites of the henipavirus G glycoprotein.....	83
Figure 14. Neutralizing mAbs that block ephrinB2 and -B3 targeted a single antigenic site.....	86
Figure 15. Venn diagram of the henipavirus G glycoprotein antigenic sites.....	89

Figure 16. Immunoprecipitation of HeV and NiV G glycoprotein in the presence and absence of sEphrinB2 .....	101
Table 6. Ratio of G glycoprotein precipitated by each mAb in the presence and absence of ephrinB2 .....	103
Figure 17. The mAb specificity for the henipavirus G glycoprotein.....	104
Figure 18. Competitive-binding assays indicate the subset of mAbs target 4 antigenic sites .....	108
Figure 19. EphrinB2 binding did not alter the amount of sG glycoprotein precipitated with the sub-panel of receptor-modulated mAbs.....	111
Figure 20. Precipitation of covalently- and noncovalently associated henipavirus G glycoprotein .....	115
Figure 21. Co-expression of F glycoprotein does not alter mAb precipitation of henipavirus G glycoprotein.....	119
Figure 22. Model of henipavirus receptor binding and membrane fusion.....	136
Figure 23. Ribbon diagram of the henipavirus G noose epitope .....	141
Figure 24. Deletion of cysteine residues forming a disulfide bridge near the base of the HeV G glycoprotein noose epitope disrupts hAH1.3 and receptor binding. ....	144
Figure 25. Scanning alanine mutations of the HeV G glycoprotein noose epitope disrupt hAH1.3 virus neutralization and the fusogenic promoting activity of the viral envelope glycoproteins .....	146
Appendix A. Binding of mAbs with henipavirus sG antigens in ELISA .....	161

## List of Tables

Table 1. Factors promoting the emergence or reemergence of infectious diseases .....	3
Table 2. Organization of the <i>Paramyxoviridae</i> family of negative-sense RNA viruses. ...	9
Table 3. Frequency of henipavirus sG specific antibody among serologic samples collected from schoolchildren in Kamphaeng Phet province, Thailand .....	29
Table 4. MAb inhibition of viral glycoprotein-mediated membrane fusion.....	74
Table 5. Characteristics of neutralizing mAbs and the target epitopes of the sG glycoprotein .....	80
Table 6. Ratio of G glycoprotein precipitated by each mAb in the presence and absence of ephrinB2 .....	103
Table 7. Ratio of covalently and non-covalently associated tetramers of the G glycoprotein precipitated by each mAb in the presence and absence of ephrinB2.....	117
Appendix B. Characteristics of the mAbs derived from mice immunized with henipavirus sG antigens and the targeted epitopes .....	163

# Chapter 1: Introduction

## Preface

Epidemics of communicable disease such as the Medieval Black Death (*Yersinia pestes*) or the introduction of smallpox to the Aztecs decimated human populations, interrupted trade routes, and transformed social and economic conventions (reviewed in 69, 105, 136). However, communicable diseases remained enigmatic until the advancement of germ theory suggested these illnesses resulted from discrete biological sources. In 1928, Sir Alexander Flemming discovered penicillin and proved communicable disease could be treated and cured (54). Further, development of the smallpox and rabies vaccines by Edward Jenner and Louis Pasteur, respectively, demonstrated illness was preventable. These scientific advances ushered in an era of rapid development in prophylactic and therapeutic modalities resulting in significant global decreases in the health burden of infectious agents. As early as the mid 1940s, widespread achievement in the control of infectious disease prompted public health leaders in the United States and elsewhere to declare the global threat of infectious disease had passed (140).

Leaders proclaimed the end to human pestilence prematurely and the incidence of infectious illnesses accelerated in subsequent years. In fact, 87 (6.1%) of the 1,415 recognized communicable human pathogens were discovered following 1980 (149, 152). The World Health Organization (WHO) reports communicable diseases as the leading cause of morbidity and mortality among persons under the age of 50, accounting for approximately 26% of all deaths in 2002 (120). In 1992, the Institute of Medicine (IOM) first reported continued evolution of infectious diseases threatens public health in the



United States, prompting the IOM to formally recognize the fields of emerging infectious diseases (EID) and re-emerging infectious diseases (rEID) (91, 93).

### **Emerging infectious diseases**

Broadly defined, EIDs are illnesses caused by novel pathogenic organisms that spread beyond traditional geographic or species boundaries; whereas rEIDs are illnesses caused by previously known pathogenic organisms associated with rapidly rising incidence (reviewed in 108). Importantly, emerging pathogens evolve mechanisms to subvert medical and public health countermeasures as well as exploit weaknesses in the public health infrastructure, such as the rapid evolution and transfer of antibiotics resistance mechanisms among pathogenic bacteria. Consequently, epidemics of EIDs and rEIDs (or simply EIDs) can be difficult to control and effectively prevent.

Furthermore, globalization of population and trade diminish natural impediments that restrict the geographic distribution and epidemic potential of some diseases (27). Rapid technological and social/political changes during the last half of the 20<sup>th</sup> century have generated fundamental global transitions in human society and the environment (such as increasing population density, altering sources and deteriorating quality of food, as well as changes in biodiversity) with the unintended consequence of promoting factors favorable to microbial pathogens (reviewed in 27, 111, 156).

The IOM arranges factors that contribute to the emergence of infectious illnesses into four broad categories (**Table 1**), these include biological, environmental, ecological, and social/political (120). The biological domain refers to factors of the emerging organism or the host that increase pathogen fitness or host susceptibility. Ecological and

**Table 1. Factors promoting the emergence or reemergence of infectious diseases. †**

Domain	Factor	Example
Biological	pathogen evolution	<i>Escherichia coli</i> 0157:H7
	microcidal resistance	Methicillin-resistant <i>Staphylococcus aureus</i>
	mutation/genetic reassortment	SARS-coronavirus
	broad host range	Nipah virus
Environmental	climate change	Yellow fever virus
	de-/re- forestation	Guanarito virus
	land use/urban sprawl	<i>Borrelia burgdorferi</i>
	weather patterns	Sin Nombre virus
	water quality	<i>Vibrio cholerae</i>
Ecological	biodiversity shift	<i>Ehrlichia chaffeensis</i>
	population expansion (human)	HIV
	invasive species	Dengue virus
	animal migration	H5N1 Influenza virus
Social/Political	pop. aging/demographics/density	<i>Streptococcus pneumoniae</i>
	agricultural practices	Bovine Spongiform Encephalitis
	food quality/malnutrition	Norovirus
	behavior changes	<i>Treponema pallidum</i>
	bioterrorism	<i>Bacillus anthracis</i>
	commerce/trade	Monkeypox virus
	construction/infrastructure	Coccidioidomycosis
	public health deterioration	<i>Mycobacterium tuberculosis</i>
	intravenous drug use	Hepatitis C virus
	medical care/treatment	<i>Clostridium difficile</i>
	organ transplantation/transfusion	<i>Trypanosoma cruzi</i>
	pathogen co-infections	Human herpesvirus 8
	pathogen detection/ identification	Human metapneumovirus
	technology	Group A <i>Streptococcus</i> (toxic shock syndrome)
	domestic and international travel	Malaria
	religious/cultural practices	Ebola virus
	vaccination failures	<i>Bordetella pertussis</i>
	war/conflict/famine	<i>Acinetobacter baumannii</i>

† Examples of specific factors linked to certain infectious agents. The table is not intended to be exhaustive and agents are only listed once even though some could be linked to more than one domain.

environmental factors are changes in environment, climate, and ecosystems, including wildlife population density and biodiversity, that alter natural barriers and promote greater interaction between a pathogen and host. Social/political factors refer to human demographics, population density, and societal elements that change the way people interact with the environment. Although the biological, ecological, and environmental domains project nonhuman factors for EIDs, anthropogenic aspects underlie or aggravate the majority of contributing factors. Statistical analyses indicated that human population density was a significant predictor of infectious disease emergence, offering additional evidence that the EID problem is born of anthropogenic origins (80). Jones *et al.* refer to this as the cost of human economic development (80). Importantly, the entire global community bears the public health threat of EIDs regardless of mechanisms of emergence at the local level.

Although the IOM only recently defined EIDs, repeated periods of increased pathogen emergence correlate with significant historic transitions in human society. McMichael *et al.* categorized these transitions into two major evolutions, the prehistoric and the historical transitions (reviewed in 34, 101). The emergence of some arthropod-borne and enzootic infections occurred during the prehistoric transition with the movement of hominids from tree dwelling to land based hunter-gatherers that formed small tribal groups (101). The transition to the historical period follows the domestication of animals and development of agriculture. Creation of reliable food sources allowed settlements to form while subsequent advances in agriculture and science promoted increasing size and density of human settlements. McMichael *et al.* further sub-divided the historical transition into four successive transitional periods based on the

size and inter-relationship of the settlements: the local (5,000-10,000 years ago), continental (1,000-3,000 years ago), intercontinental (1500-1900s), and global (present) transitions (101).

Numerous human-specific pathogens of significant historical importance likely emerged during the local transition (34). During the local transition, humans began to keep animals, particularly ungulates, for food /work and consequently established the foundation for the emergence of pathogens emanating from domestic animals. Progenitor species of communicable diseases such as measles and smallpox emerged during this time and, over time, evolved in humans to the present human-specific forms (34, 101). However, most pathogens did not adapt to become human specific (only 50 -100 known pathogens in total) and the vast majority of contemporary human pathogens are transmitted from environmental (sapronoses) or animal (zoonoses) reservoirs (160).

#### *Emerging zoonotic diseases*

Infections transmitted between vertebrate hosts and humans (zoonoses) account for 61% of known human pathogens and 75% of EIDs (149, 152). While domesticated animals remain important reservoirs of emerging pathogens, wildlife are the most significant reservoirs of emerging pathogens in the present global transition (22). Social, demographic, and environmental changes rapidly expand development and promote conditions favorable for pathogen emergence among immunologically naïve human hosts. The necessity for constant transmission events from animal reservoirs to support epidemics forms a wide spectrum related to the number of secondary cases that arise from a single infection, the reproductive ratio ( $R$ ) (reviewed in 160). Low pathogen reproductive ratios ( $R_0 < 1$ ) indicate the pathogen fitness for the human host is weak and

epidemics are not sustainable. High pathogen reproductive ratios ( $R_0 \geq 1$ ) indicate greater potential for self-sustaining epidemics and transmission of the pathogen among humans independent of the animal reservoir.

Biological traits of the pathogen, humans, and/or the route of transmission limit the conveyance of some zoonotic pathogens from animal reservoirs to human hosts. These pathogens, obligate zoonoses, are accidental pathogens of human hosts and human-to-human transmission is restricted, but account for 67% of zoonotic pathogens (149, 160). Many important EIDs, such as emerging hemorrhagic fever viruses and avian influenza (H5N1), are obligate zoonoses where geography and demographics limit the susceptible population. Facultative zoonoses are transmitted both by animal-to-human and human-to-human cycles. As epidemics of facultative zoonoses become less reliant on animal reservoirs, these organisms more readily overcome geographic and ecological limitations leading to national and international dissemination (160). Evolution of facultative zoonoses with human hosts may promote host fitness adaptations resulting in increased human specificity.

Statistical analyses indicate host range, taxa of the pathogenic organism, and route of transmission are the important risk factors associated with the emergence of novel pathogens (reviewed in 34, 149, 161). Further characterization indicates a broad host range (able to infect species from multiple taxonomic orders) increases the emerging potential of the organism (161). Among zoonoses, the relative risk (RR) of emergence is greatest among wildlife populations ( $RR=2.75$ ) and, more specifically, among bats ( $RR=2.64$ ), primates ( $RR=2.23$ ), or ungulates ( $RR=2.09$ ) (34). Furthermore, ecological factors such as animal density, introduction of invasive species, habitat fragmentation,

and host species richness are correlated with the emergence of zoonotic diseases (2, 80). Importantly, biodeversity and habitat fragmentation are inversely correlated with the emergence of zoonotic pathogens in human populations (2).

Most strikingly, taxonomic division of the pathogen is associated with the greatest potential for emergence. Specifically, emerging organisms are most strongly associated with the viral (RR=4.43) and protozoan (RR=2.49) taxonomic divisions (149). Transmission through direct contact (RR=1.47) or by a vector (RR=2.35) are associated with increased potential for emergence; however they are not independent of host range and taxonomic division (149).

#### *Emerging viral diseases*

Increasing media reference to viruses is common and demonstrates the importance of virus taxa as emerging pathogens. Recent examples include the 2009 H1N1 pandemic, SARS-Coronavirus epidemic, HIV-1, and looming threat of Avian influenza (H5N1). In fact, nearly 44% of the recognized emerging human pathogens are viruses (149). Furthermore, no other EID impacted global health as significantly as the current HIV-1 pandemic. The United Nations estimates, as of 2007, 25 million people died and more than 33 million people are infected with HIV (79). In comparison, the number of HIV-1 related deaths (ending 2007) approaches the estimated 50 million deaths resulting from the Medieval Black Death or the Spanish flu pandemic (105). Among viruses, the risk of RNA and DNA virus emergence is nearly equivalent (RR=2.8 and 2.5, respectively); however, RNA viruses are more strongly associated with emerging zoonoses (34).

The order *Mononegavirale* encompasses viruses with a non-segmented negative-sense RNA genome that share a similar replication strategy and structural conservation of the viral polymerase (123, 154). The order contains four families of viruses, including *Rhabdoviridae*, *Bornaviridae*, *Filoviridae*, and *Paramyxoviridae* (23). Each of these families contains multiple highly pathogenic mammalian viruses, such as Rabies virus, Ebola virus, and Measles virus (MeV). In addition, some Mononegavirales (such as Ebola virus and the henipaviruses) are among the most lethal human pathogens and are potential agents of bioterrorism.

Among the mononegavirales, the *Paramyxovirinae* is the most extensive family of known animal pathogens and novel viruses isolated from mammals and exhibit features that promote viral emergence (23, 87). The viral RNA polymerase exhibits a high error rate during replication which can lead to mutation and rapid virus evolution. Paramyxoviruses commonly spread via aerosol or contaminate the surfaces of fomites and food. In addition, paramyxoviruses target a variety of receptor molecules including protein receptors that are highly conserved among multiple mammalian species and in some cases facilitate intra- and inter-species transmission. Together, these traits facilitate cross-species transmission of viruses and adaptation to new hosts.

## **Paramyxoviridae family**

### *Organization*

The *Paramyxoviridae* family is divided into two sub-families (**Table 2**), the *Pneumovirinae* and the *Paramyxovirinae* (reviewed in 87). The prototypic human pneumoviruses, human Respiratory syncytical virus (hRSV) and human Metapneumovirus (hMPV), are respiratory pathogens. Infection with these pathogens is

**Table 2. Organization of the *Paramyxoviridae* family of negative-sense RNA viruses.**

Sub-family	Genus	Type Species
Paramyxovirinae	Avulavirus	Newcastle disease virus
	Henipavirus	Hendra virus Nipah virus
	Jeilongvirus <sup>1</sup>	Beilong virus J-virus
	Morbillivirus	Measles Virus Canine Distemper virus Rinderpest virus
	Respirovirus	Bovine Parainfluenzavirus 3 Human Parainfluenzavirus 1,3 Sendai virus
	Rubulavirus	Human Parainfluenzavirus 2, 4 Mumps virus
	Unclassified	Menangle virus Mossman virus Tioman virus
Pneumovirinae	Metapneumovirus	Avian Metapneumovirus Human Metapneumovirus
	Pneumovirus	Bovine Respiratory Syncytial virus Human Respiratory Syncytial virus

<sup>1</sup> Proposed genus



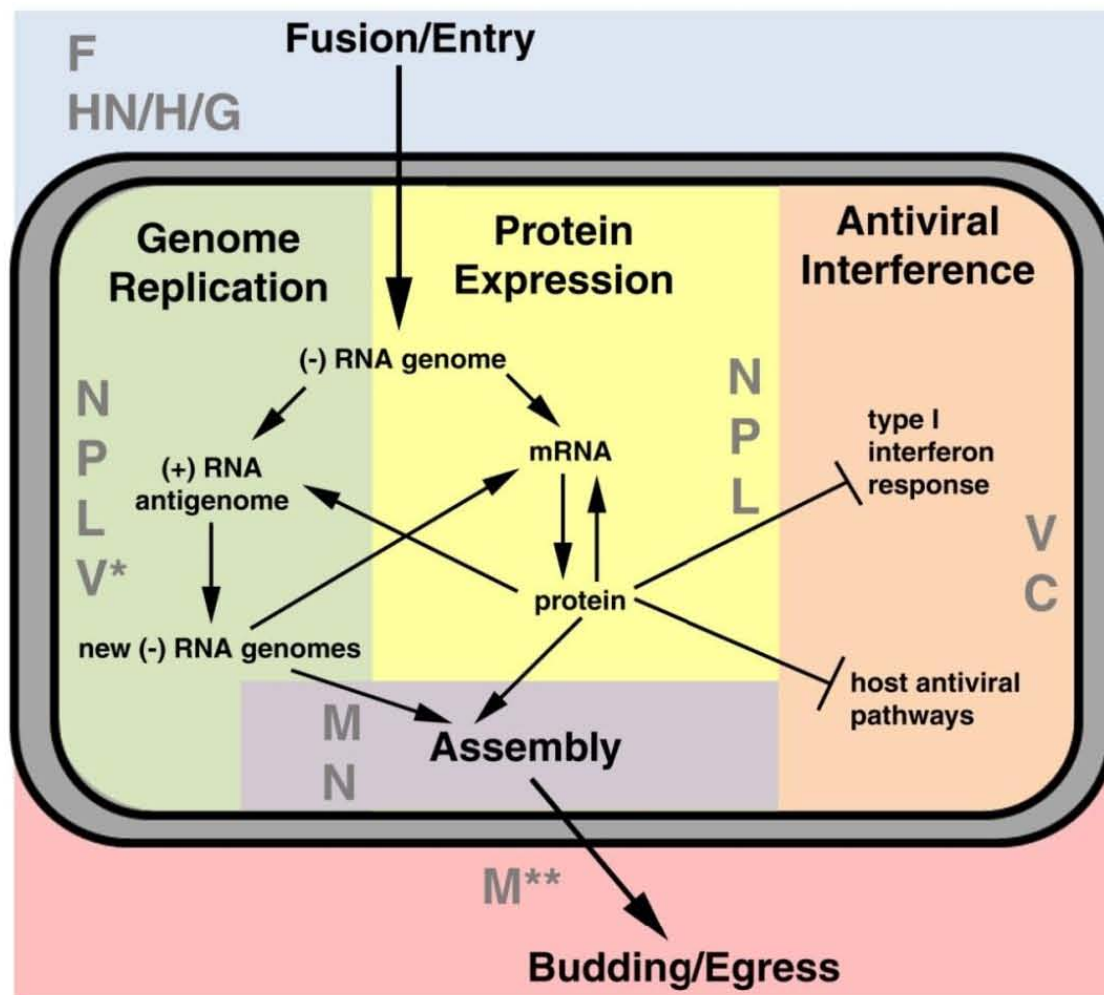
often mild, but can progress to bronchitis and pneumonia. Serologic studies revealed near universal prevalence of hRSV and hMPV antibody by adolescence (35). The *Paramyxovirinae* sub-family comprises five genera (*Avulaviruses*, *Henipaviruses*, *Morbilliviruses*, *Respiroviruses*, *Rubulaviruses*), the proposed genus *Jeilongvirus*, along with many unclassified paramyxoviral species. Significant variation in disease is present among the paramyxovirinae, ranging from mild respiratory illness to fatal disease. The *Henipavirus* genus is the most recent division of the Paramyxovirinae, formally recognized by the International Committee on Taxonomy of Viruses in 2002 (45). Currently, *Hendra virus* (HeV) and *Nipah virus* (NiV) are the only recognized henipaviruses (23).

### *Biology*

To perpetuate themselves, paramyxoviruses must enter host cells, replicate, assemble their structural and non-structural components containing the genomic material, exit the host cell, and avoid the host immune response (**Figure 1**). To accomplish these tasks, paramyxoviruses encode six essential genes organized similarly among all species (**Figure 2**) including (3' to 5') the nucleocapsid (N), phosphoprotein (P), matrix (M), fusion (F), attachment (HN/H/G), and the large (L) protein (reviewed in 87). In addition, multiple overlapping open reading frames (ORFs) in the P gene are common (encoding the C, V, and W genes) and the GX overlapping ORF was recently identified in the G gene of the jeilongviruses (87, 95). Furthermore, genes identified among only some paramyxovirus species include the short hydrophobic protein (SH; PIV5, MuV, and the pneumoviruses), the transmembrane protein (TM; jeilongviruses), and additional non-structural proteins found only among the pneumoviruses (87, 95).

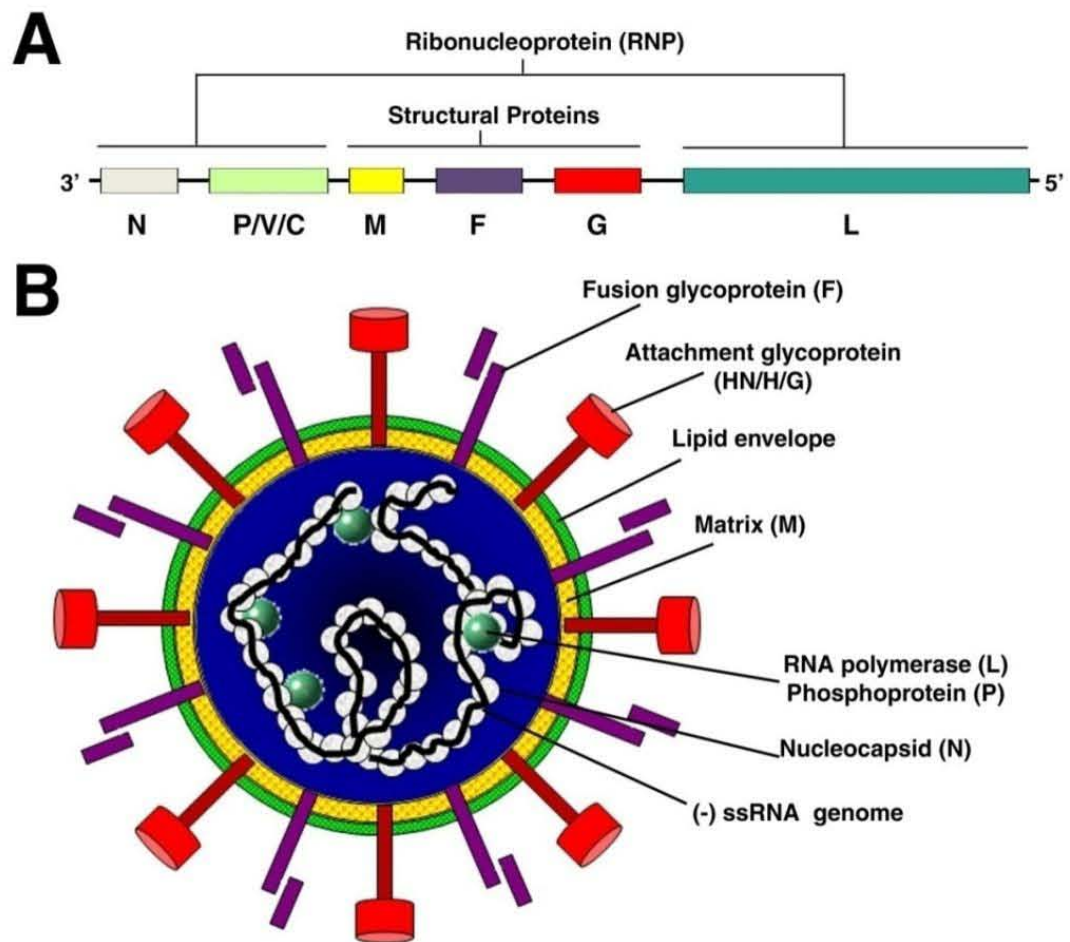
**Figure 1. Diagram of the paramyxovirus replication cycle.**

The paramyxovirus replication cycle occurs in stages, including entry/fusion, genome replication/protein expression, abating host responses, virion assembly, and budding/egress from the host cell. Direct parasitism of the host resources and interaction with host responses occurs in the cytoplasm and nucleus of the host cell, whereas entry and assembly/egress occur at the cell surface. The light grey text indicates the viral determinants important during each stage. (\*) The V protein may contribute to the polymerase complex. (\*\*) M is required for optimal particle formation and packaging of the essential viral components to form infectious virions.



**Figure 2. Genomic and structural organization of the *Paramyxovirinae*.**

A: Diagram of the large (approx. 18.2 kb) henipavirus negative-sense RNA genome representative of the paramyxoviruses. The genetic features are shown, proportionally, including 3'- and 5'-untranslated regions, intragenic regions, and the ORFs encoding the nucleocapsid (N), phosphoprotein (P), matrix (M), fusion (F), attachment (G), and RNA-dependent RNA polymerase (L) proteins. B: Structural organization of the pleomorphic paramyxovirus virion, including the lipid bi-layer envelope derived from the host cell membrane during budding. The virus particle is formed by the structural elements (M, F, G) and the non-structural elements of the ribonucleocomplex (genome, N, P, and L) which form the viral replication machinery.



The release of the non-structural viral components into the host cell cytoplasm initiates paramyxovirus replication. The ribonucleoprotein complex (RNP), the core viral genomic and non-structural proteins, is the central viral transcriptase and replicase apparatus for this intracellular phase of the virus life-cycle. The RNP for all paramyxoviruses consists of the RNA genome, N, P, and L gene products (reviewed in 87, 126).

Paramyxovirus genomes are linear non-segmented single-stranded RNA of negative polarity that range in size from 15 kilobases (kb) to slightly more than 19 kb (87). Short noncoding regions usually no more than 50 to 150 nucleotides in length flank the N and L genes forming the 3'-leader and 5'-trailer sequence (87, 151). Additional sequences flank each gene forming extracistronic noncoding regions of varying length (usually no more than 50 nucleotides) (87). The extracistronic regions contain sequences that are conserved among paramyxoviruses, important for regulating transcription and initiating genome replication. Found between the gene end and gene start sequences is a short (less than 70 nucleotides) intergenic region that contains a conserved sequence among isolates of the same species (87).

The RNA genome serves as a template for transcribing mRNA which begins following viral entry. Cis-acting elements following each gene regulate re-initiation as the viral polymerase moves toward the 5'-end of the genome (reviewed in 87, 126). Inefficient re-initiation produces a gradient of mRNA transcription levels and resultant protein products, with the most abundant products encoded toward the 3'-genomic end. After mRNA and protein synthesis has initiated, the viral polymerase will switch to producing full-length positive-polarity copies of the genome that serve as the template for

replicating the viral genome. The molecular mechanism that promotes the change from mRNA to the antigenome synthesis is not clearly understood, but is dependent on the relative abundance of the N protein in the host cell (151).

During all stages of viral entry and replication, the viral genome remains protected by the RNA-binding protein N. The N protein is highly conserved among the paramyxoviruses ranging in size from approximately 480 to 550 amino acid residues (87). The N protein coat forms a helical structure (the number of N protein subunits per helical turn varies between species) that appears as a repeated herringbone when viewed during electron microscopy (EM). Each N protein subunit covers six nucleotides and, consequently, every paramyxovirus genome is a multiple of six nucleotides in length, a property commonly known as the “rule of 6” (138). In addition to protecting the viral RNA genome, the N protein is necessary for replication and transcription of both the (-)- and (+)- sense viral RNA material as well as incorporating the viral RNA genome into the budding virion (87, 151). However, the N subunit does not exhibit enzymatic activity and must interact with the RNA-dependent RNA polymerase to initiate transcription and replication.

The L protein is largest gene product encoded by paramyxovirus genome and is the main unit of the viral RNA polymerase. The L protein is also the least abundant transcript produced during infection and only approximately 50 copies of the nearly 2,200 residue polypeptide are incorporated in each budding virion (87). In addition to polymerase activity, the L protein possesses enzymatic activity necessary for polyadenylation and capping of mRNA at the 3' and 5' ends, respectively (87). The L protein contains six regions of significant homology with the RNA-dependent RNA

polymerase of other Mononegavirales (reviewed in 126). Each of these domains (I-VI), defined by Poch *et al.* (reviewed in 126), is found near the center of the protein forming three regions linked by non-conserved hinge regions: the first region contains Poch domains I and II, the second containing Poch regions III, IV, and V, and the last region containing domain VI (100, 126). The conserved domains are responsible for each of the different enzymatic activities of the protein (100).

The L protein alone does not mediate the polymerase enzymatic activities and requires the P protein for function. The P protein forms a tetrameric multimer heavily phosphorylated at serine and threonine residues near the N-terminus of the polypeptide (87). The P gene product, approximately 400 amino acids in length, contains docking regions for both the N protein and L protein that bridge the L protein and the N/RNA genome complex to promote transcription and replication of the viral genome (151). Further, the P gene is the site of multiple overlapping ORFs encoding the V, W, and C proteins (87). These proteins may participate in replication of the RNA genome by inhibiting transcription of the antigenome via an unknown mechanism. More significantly, the V, W, and C products are viral factors implicated in abating the host antiviral response. In particular, these polypeptides bind signal transducer and activation of transcription (STAT)-1 and -2 molecules sequestering them in the cytoplasm and blocking the transduction of interferon signals to the nucleus (84, 127, 134). Additional studies suggest the proteins interfere with downstream toll-like receptor-3 (TLR-3) and -4 signal molecules to inhibit NF-kappaB signal transduction and the cellular response to the invading virus (73, 97, 135, 137).



The non-structural components ensure the perpetual reproduction of the viral components and subvert host responses, but must be organized into infectious virion particles and delivered to susceptible cells. The structural components of the virus are responsible for organization of the virion, budding from the plasma membrane, targeting susceptible cells, and membrane fusion with the host cell to release the viral RNP into the cytoplasm of the target cell. The viral structural determinants minimally include the matrix (M), and the glycosylated fusion (F), and attachment glycoproteins. Some paramyxoviruses encode additional membrane proteins, such as the small hydrophobic protein (SH); however, non-conserved membrane proteins are not essential to maintaining virus infectivity and their function is currently unknown (87).

The M protein is central to facilitating the organization of the remaining viral determinants into the budding particle. The M protein is a small (approx. 350 amino acids in length) and highly basic in nature and, although associated with the lipid membrane, the M protein is not an integral protein (87). Instead, the M protein forms a paracrystalline array underlying the lipid bilayer on the cytoplasmic face where viral assembly occurs (87). Evidence shows the M protein interacts with the structural proteins via the cytoplasmic tail and also with the N protein. Once assembled, some M protein species have been shown to interact with host proteins of multivesicular bodies (MVB) to promote membrane budding and release of infective virions (87). However, recent data did not find a direct association of NIV M protein with host cell determinants of the MVB complex suggesting the henipaviruses may mediate budding from the host cell by a novel mechanism (118).

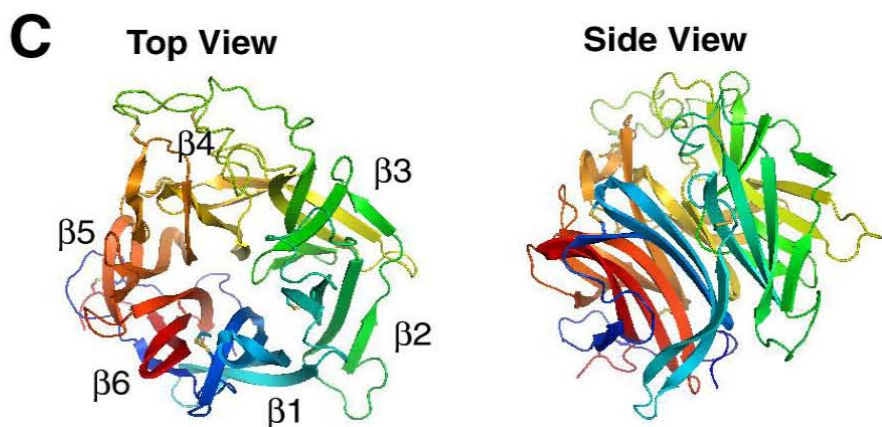
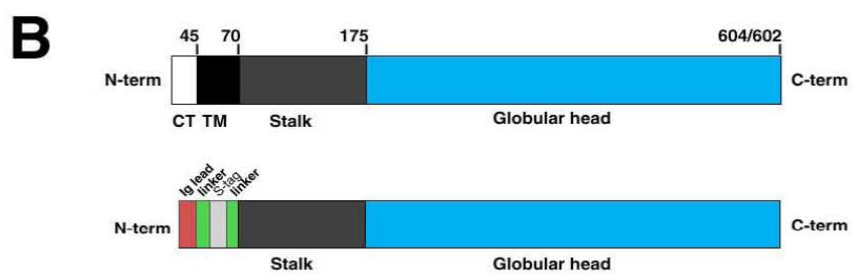
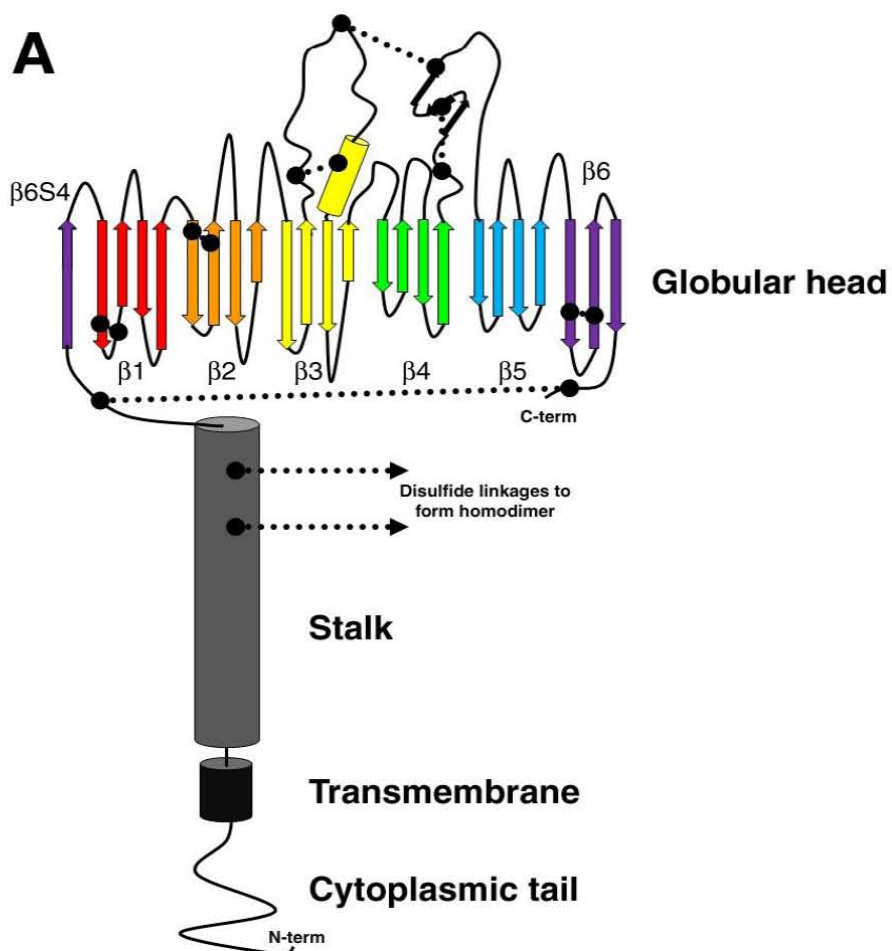
The fusion and attachment glycoproteins are the only essential viral determinants found integral in the virion envelope. Both the F and the attachment proteins are glycosylated and are oriented with the major catalytic surfaces toward the solvent exposed extra-virion space (87). The virion must incorporate both the F glycoprotein and the attachment glycoprotein to mediate attachment and membrane fusion to initiate the replication cycle.

The paramyxovirus attachment glycoprotein (**Figure 3**) facilitates viral attachment to host cells and is divided into three lineages based on hemagglutinating (agglutinates red blood cells) and neuraminidase (hydrolysis of sialic acid moieties on glycoproteins) enzymatic activities. The glycoprotein is designated hemagglutinin–neuraminidase (HN), hemagglutinin protein (H), or a glycoprotein (G) when the attachment glycoprotein lacks both hemagglutinating and neuraminidase activities (reviewed in 87). The paramyxovirus attachment glycoprotein is composed of a globular head domain, stalk region, transmembrane domain, and a short cytoplasmic tail (16, 165). The globular head domain of the attachment glycoprotein contains all enzymatic activities of the molecule and mediates viral attachment with the target cell via receptor engagement (reviewed 107). The stalk domain contains important cysteine residues necessary to form the disulfide-linked dimers (89, 165). The covalently associated dimers further associate to form tetrameric oligomers (dimer of dimers) on the virion surface (16, 89).

The F glycoprotein (**Figure 4**) directly mediates the merger of the virus and host cell membranes (reviewed in 14). The Pneumovirus F glycoprotein (and PIV-5 F

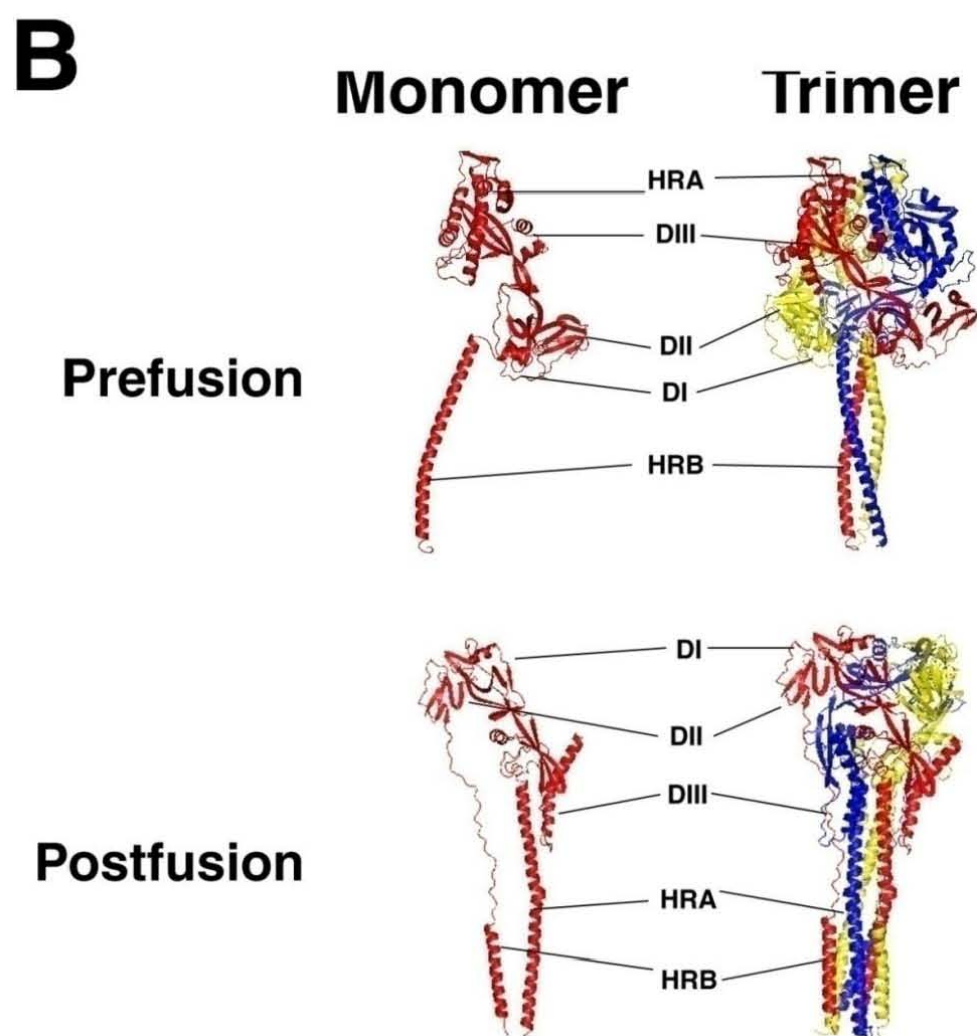
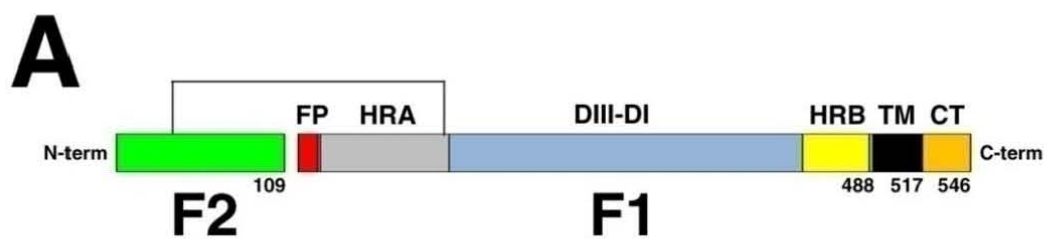
**Figure 3. Structural features of henipavirus G.**

A: Diagram showing the N-terminus cytoplasmic tail, transmembrane domain, stalk region, and large C-terminus globular head domain of henipavirus G. The stalk region contains two cysteine residues important in forming disulfide-linked dimers of G. The globular head conforms with the 6-bladed  $\beta$ -propeller structure common to the neuraminidase super-family of proteins. Each of the six  $\beta$ -sheets ( $\beta_1 - \beta_6$ ) is composed of four anti-parallel  $\beta$ -strands ( $\beta_x S_1 - \beta_x S_4$ ) connected by a single loop ( $\beta_x L_{12} - \beta_x L_{34}$  and intersheet loops  $\beta_{61} L - \beta_{56} L$ ). Henipaviruses contain six disulfide bridges in the globular head (dashed lines) essential for maintaining the structure of the glycoprotein. B: The henipavirus G gene showing regions of the molecule and relative nucleotide position (numbers along top). Soluble G (sG) was created by replacing the initial 70 nucleotides encoding the CT and TM domains with a secretion sequence and S-peptide epitope tag (S-tag) joined by linker regions. C: Ribbon diagram showing top and side views of the NiV G globular head. The  $\beta$ -sheets (indicated on the top view) form a circular array. Ribbon diagram was created using the crystal structure of NiV G (PDB ID: 3D11 and 3D12) with Pymol software (39, 162).



**Figure 4. Diagram of the paramyxovirus F.**

A: Diagram of the henipavirus F polypeptide showing the disulfide-linked F<sub>1</sub> and F<sub>2</sub> cleavage products. Important functional domains are shown, including the hydrophobic fusion peptide (FP), heptad-repeat structures (HRA and HRB), transmembrane, cytoplasmic tail (CT), and structural domains (DI-DIII). B: Ribbon diagram of the PIV-5 F showing the monomeric peptide (red) and the homo-trimeric native form (red, blue, and yellow). The PIV5 F glycoprotein trimer is shown in the pre-fusion form with the HRA disorganized toward the top of F and post-fusion form with alpha-helical 6-helix bundle composed of HRA/HRB. Ribbon diagrams created using the crystal structure of PIV5 (prefusion; PBD ID: 2B9B) and hPIV3 (post fusion; PBD ID: 1ZTM) with Pymol software (39, 163, 164).



glycoprotein when over-expressed) can mediate membrane merger in the absence of the attachment glycoprotein; however, paramyxovirus fusion is most efficient when both the attachment and F glycoproteins are present (139). The F glycoprotein is synthesized as an inactive precursor ( $F_0$ ) that is cleaved by host cell proteases forming the active molecule, composed of the disulfide linked  $F_1$  and  $F_2$  cleavage products (reviewed in 139). Located adjacent to the fusion peptide,  $F_1$  possesses an important domain referred to as the N-terminal heptad or heptad repeat A (HRA) and a second HR region proximal to the transmembrane domain referred to as the C-terminal heptad or heptad repeat B (HRB) (88). Experimental evidence indicates that the trimeric henipavirus F glycoprotein spike is associated with the tetrameric G glycoprotein spike prior to receptor binding, similar to other well-characterized paramyxoviruses (12).

## **Henipavirus epidemiology**

### *Emergence*

HeV was identified in 1994 as the etiologic agent of severe respiratory disease among horses and humans in Queensland, Australia (reviewed in 46, 47). The first outbreak of HeV occurred in the Brisbane suburb of Hendra where 21 horses developed severe respiratory disease and two human caretakers fell ill, one a nationally recognized horse trainer (133). A second spillover occurred in Mackay, Australia was discovered retrospectively after a horse owner died following the development of neurologic disease (reviewed in 52). Here, the horse owner had previously recovered from a meningitic illness after helping with necropsies of two horses that died on his ranch (52). The owner then relapsed with encephalitis 14 months later and died (52). Researchers detected HeV antigen in tissue obtained from the patient following his death.

NiV was discovered in 1999 during a large outbreak of severe encephalitis among pig farmers in peninsular Malaysia (reviewed in 28, 31). Early in the epidemic, public health leaders implicated Japanese encephalitis virus (JEV) as the causative agent, which delayed implementation of effective intervention strategies to control the outbreak. Although investigators recognized HeV infection in multiple mammalian and avian species (including rats, chickens, house shrews, dogs, and cats), infected pigs were the intermediate hosts that amplified and transmitted the virus to humans (50, 115, 154). During the course of the epidemic, there were 265 confirmed human infections and 105 deaths (reviewed in 45). In addition, NiV infected abattoir workers in neighboring Singapore following the importation of infected swine from Malaysia (45). The Malaysian government intervened to alleviate the epidemic and ordered the culling more than one million pigs in peninsular Malaysia (86).

The preponderance of evidence implicated frugivorous bat species commonly known as flying foxes (order *Chiroptera*, family *Pteropodidae*, genus *Pteropus*) as the principle host reservoir of henipaviruses (reviewed in 10, 52). These bats are widely distributed throughout Australia, Oceania, and Southeast Asia to Madagascar (63). Serological studies revealed henipavirus specific antibody or other evidence of infection among several Chiroptid species throughout these geographic regions (reviewed in 10). Most recently, multiple groups reported serologic evidence of henipavirus exposure in bats sampled from West Africa and China (68, 94). In summary, indications of henipavirus exposure have been found in 24 species across 10 genera of bats (10, 68, 94).

Anthropogenic factors appear to have altered the interaction between humans and the reservoir bat species allowing henipaviruses to emerge. Although all events



contributing to the emergence of the henipaviruses are not known, several theories attempt to explain the appearance of NiV in 1998. Chua *et al.* suggested rapid and extensive deforestation throughout Malaysia and Borneo drought related effects of the local El niño southern oscillation (ENSCO) event limited available foodstuffs and roosting habitat for the bats (30). Ultimately, the bats began foraging for food at orchards often found in close proximity to large piggeries, facilitating the transmission of the virus to pigs. Unpublished data suggests the 1998-1999 epidemic erupted after the local trade of infected pigs to farms housing a greater proportion of previously unexposed pigs (38). The virus spread rapidly in the susceptible swine population amplifying the virus and infecting human caretakers (38).

### *Epidemiology*

There have been 13 recognized outbreaks of HeV which have occurred in Australia since the virus was first recognized (4-7, 52, 53, 64, 133). All documented spillovers occurred in Queensland, Australia except for a single outbreak in New South Wales, Australia (4). During each emergence, human infection resulted from close contact with clinically ill horses demonstrating the horse is an important intermediate host for HeV spillovers into humans. To date, more than 33 horses have died or were euthanized due to HeV infection and HeV has resulted in seven confirmed human infections and four deaths (57% case-fatality) (5, 6, 53, 133). The most recent death occurred in September of 2009 when a veterinarian fell ill after performing an endoscopy on a horse originally believed to be suffering from a snake bite (5). Respiratory illness was the predominate clinical feature of individuals infected during the 1994 Hendra,

Australia epidemic (133); however, progressive encephalitis was a predominant clinical feature of subsequent human cases (47).

Since its discovery, NiV has killed hundreds of people, and outbreaks of NiV occur in Bangladesh nearly annually (reviewed in 8, 45, 66, 85). Importantly, recent NiV outbreaks have been associated with higher case fatality rates (>75%), increased incidence of acute respiratory distress syndrome with neurological disease, evidence of person-to-person transmission, and direct transmission of the virus from natural reservoirs to humans via contaminated food sources (62, 66, 98). In addition, serologic analysis of fruit bats, the reservoir host of NiV, has shown NiV or a NiV-like virus is spread throughout Southeast Asia and Oceania, including Thailand, Cambodia, China, Indonesia, and Australia as well as parts of Africa, including Madagascar and Ghana (10, 68, 94). The wide geographic seroprevalence of NiV or NiV-like viruses suggests billions of people are potentially at risk for NiV exposure.

#### *Endemic henipavirus infection*

Limited information is available to determine the rate of endemic or non-lethal infection in regions where henipaviruses are present. The most extensive data available evaluates exposure among high risk populations in two separate studies, including 668 samples collected from abattoir workers in Malaysia from 1998-1999 (130) and 1,412 samples from individuals involved with culling of pigs during the first outbreak in Malaysia (3). Serologic analysis indicates 7% of Singapore abattoir sampled and 0.4% Malaysian outbreak responders exhibited evidence of NiV exposure (3, 130). Among the Malaysian cohort, two individuals developed serious illness and were hospitalized (130). Additional samples collected from eight researchers following close association with

infected bats did not show any serologic evidence of henipavirus exposure (32).

Together, the low prevalence of sero-conversion among high-risk populations suggests transmission leading to productive infection may require significant levels of virus exposure.

Newer studies, carried out by myself and Dr. J. Pavlin, suggest henipaviruses may cause endemic infection among people in regions of Southeast Asia. As part of a study to examine the incidence of Dengue virus among children, public health nurses collected blood samples from school-aged children in a rural northern Thailand province following the onset of acute febrile illness and following convalescence from 1998-2002 (48, 49, 119). Analysis of samples was performed by ELISA using a recombinant soluble form of the NiV G glycoprotein of NiV (sG<sub>NiV</sub>) in which the cytoplasmic tail and transmembrane domain were replaced by an Ig kappa protein secretion sequence and S-peptide epitope tag for purification (16). These ELISA analyses with sG<sub>NiV</sub> revealed a low prevalence of exposure to NiV or a NiV-like virus among the cohort of children in the rural Thai province (**Table 3**). Detection of antibodies among samples collected in 1998 demonstrate NiV or a NiV-like virus infected individuals in this region prior to the onset of the Malaysian outbreak.

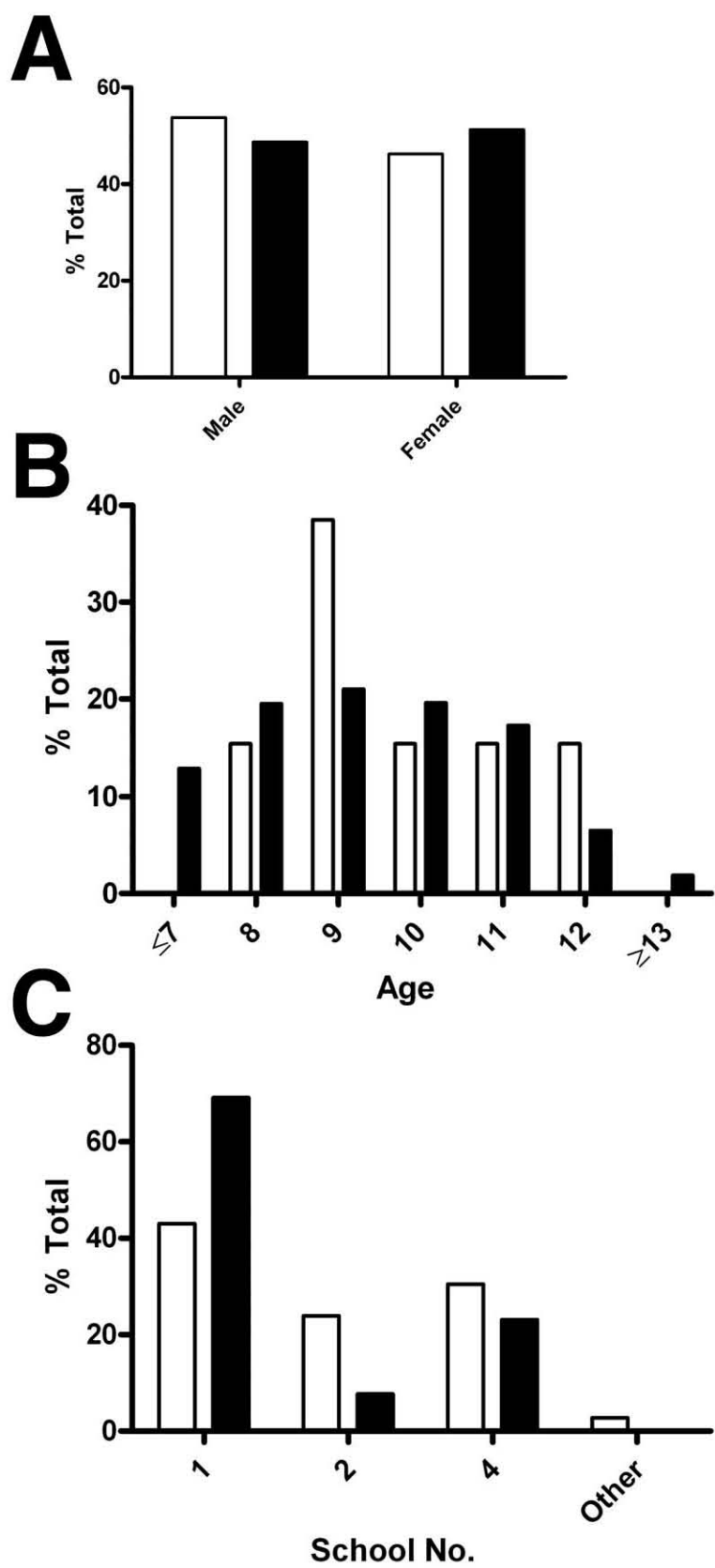
The prevalence odds ratio (POR), a statistical comparison of the frequency of risk factor(s) among NiV sero-positive children (cases) and sero-negative children (controls), was determined for age at the time of illness, gender, and school the child attended using data collected from the family of each child. The POR did not indicate a significant relationship between the cases and any of the factors examined; however, seroprevalence was highest among 9-year-old children and those that attended school 1 (**Figure 5**).

**Table 3. Frequency of henipavirus sG specific antibody among serologic samples collected from schoolchildren in Kamphaeng Phet province, Thailand.**

Year	Freq.	N	%
1998	2	186	1.1
1999	4	224	1.8
2000	6	283	2.1
2002	1	108	0.9
<b>Total</b>	<b>13</b>	<b>801</b>	<b>1.6</b>

**Figure 5. Age, gender, and school distribution of children in Kamphaeng Phet province, Thailand with serologic evidence of prior henipavirus exposure.**

Proportion of children with serologic evidence of prior henipavirus exposure (n=13; open bars) and without serologic evidence henipavirus exposure (n=788; closed bars) stratified by gender (A), age (B), and school (C). Numeric codes were given to each of the schools from which children were sampled.



Importantly, these results suggest that endemic exposure to NiV or a NiV-like virus may occur in areas of Southeast Asia resulting in an asymptomatic infection or mild illness. These data underscore the need to initiate and extend research to evaluate the potential patterns of exposure, transmission, and characterize endemic henipaviruses to define the risk to populations in southern Asia and elsewhere.

### **Henipavirus biology**

Henipaviruses have distinguished themselves among paramyxoviruses as highly pathogenic viruses with a broad host tropism. Henipaviruses also possess the second largest genome among paramyxoviruses and HeV and NiV, the prototype species of the genus, share significant nucleotide identity (approx. 78%) (reviewed in 47). Although the literature contains reference to only one lineage of HeV, evidence to date suggests there are at least three distinct known lineages of NiV: Malaysia (29), Bangladesh (65) and Cambodia (125). In addition, it is likely that the eventual isolation of virus from the recently identified reservoirs in Madagascar and China will yield phylogenic additions to the Henipavirus genus.

Available data suggests transmission of the virus occurs by contaminated aerosols, contact with biological fluids from infected animals, or ingestion of tainted fruit and fruit juices (reviewed in 33, 47, 62, 98). Further, analysis of cases during outbreaks in Bangladesh strongly indicates person-to-person transmission is possible (62); however, person-to-person transmission has not been a recognized feature during any of the HeV spillover events. Following exposure, acute disease in humans typically develops within two weeks, but onset of clinical illness can occur as late as 45 days following exposure for some individuals (reviewed in 47). Although limited information is available,

differences in the transmissibility and in case-fatality rates could indicate differences in the virulence among the various NIV lineages, route of exposure, dose of inoculum, and/or host responses to infection. Regardless, disease progression and pathogenesis is similar among all recognized henipavirus outbreaks.

#### *Disease and pathogenesis*

Henipavirus infection commonly results in acute febrile illness followed by multiple organ system involvement. The estimated rate of asymptomatic infection during the NiV epidemic in Malaysia was between 8-15% (28). The disease presents with the onset of fever, cough, headache, drowsiness, and myalgia (31, 71, 159). The condition progresses with the patient experiencing reduced level of consciousness, disorientation, drowsiness, aflexia, hypertension, tachycardia, and abnormal doll's eye reflex (47, 55). These symptoms are consistent with increased involvement of the central nervous system (CNS) including the brain and brain stem (159). The infected patient often succumbs of meningoencephalitis and/or atypical pneumonia. The mean duration of illness (from the onset of symptoms until death) during the 1998-1999 NiV outbreak in Malaysia ranged from 5 to 29 days (average of 10.3 days) (55). Recovery followed by potentially fatal relapse episodes of encephalitis occurred as long as four years following the initial infection (55, 147). In these cases, the source of the virus in the host is not known, but presumably disease results from viral resurgence.

Inflammation and pathology following viral infection predominates in the respiratory system and CNS (reviewed in 47). However, inflammation and/or pathologic findings are also present in the spleen, kidney, adrenal gland, heart, and throughout the vascular endothelium (159). While the dynamics of virus spread within an infected



individual are still unknown, current data suggests the virus spreads hematogenously from the initial infection site to then infect and replicate in the vascular endothelium throughout the host (47, 159). Secondary replication in the vascular system produces a high viremia allowing spread to multiple organ systems (159). Vascular involvement correlated most strongly with arteries, arterioles, capillaries, and venules in the lung, heart, kidney, and extensive involvement in the CNS (159). Vasculitis, thrombosis, viral cytopathic effects (CPE), and necrosis in the parenchyma, grey and white matter of the brain as well as in the brain stem, were predominant features of CNS disease among individuals that died following NiV infection during the Malaysian epidemic(47, 159) . In addition, analysis of lung samples revealed hemorrhage and fibrinoid necrosis with pulmonary edema were prominent in alveolar tissues (47, 159). Other prominent features include necrotizing inflammation disrupting splenic organization as well as vasculitis, necrosis, inflammation, and/or hemorrhage in the lymph nodes, kidney, heart, adrenal gland, and pancreas (47, 159).

Broad viral tropism among mammalian species has facilitated the development of several animal models of henipavirus infection; however, only a few species appear to be good representative models of human disease (reviewed in 155). Recently, novel models of NiV and HeV infection utilizing African Green Monkeys (AGM; *Chlorocebus sabaeus*) have been developed (Geisbert and Broder, unpublished). The disease in AGMs closely reproduces the disease and pathological findings observed in humans following infection with henipaviruses. To define the viral tissue tropism, the relative quantity of NiV genome was determined by Taqman reverse transcriptase PCR (RT-PCR) performed as previously described (18, 99).

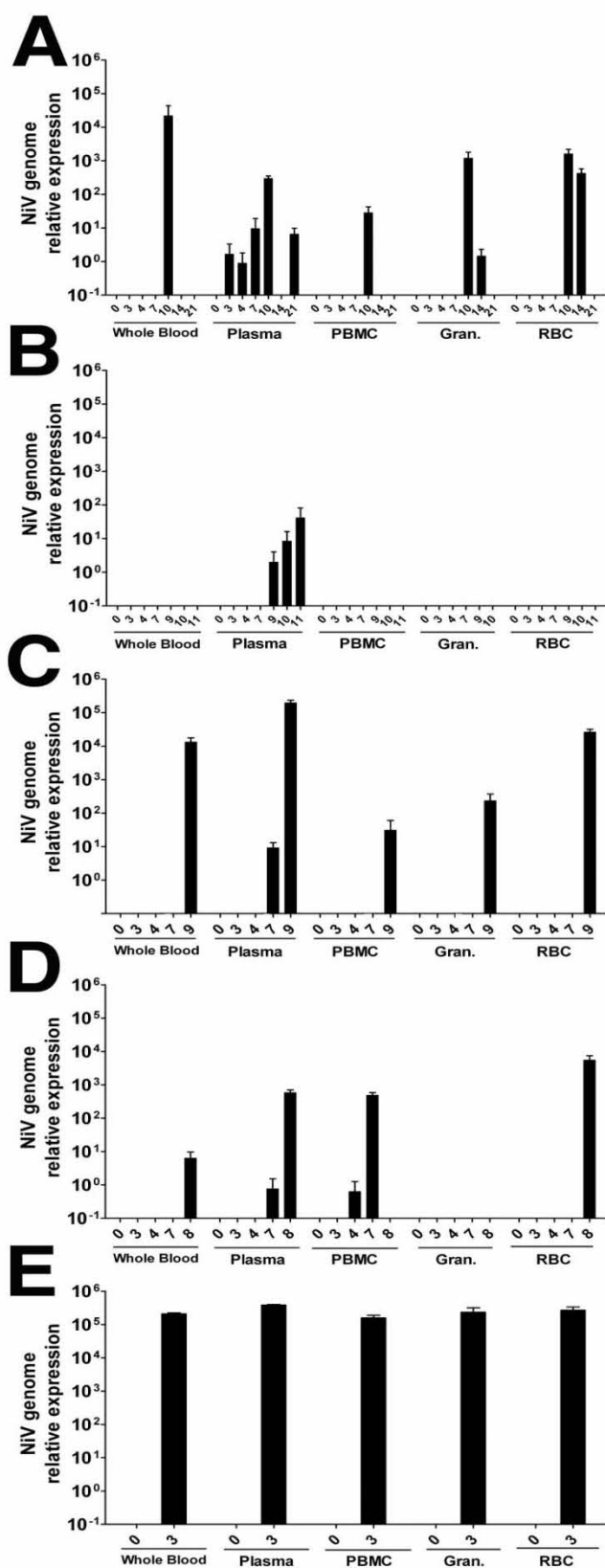
Detection of viral genome in these samples corresponded closely with the onset of clinical illness and disease progression (**Figure 6**). NiV RNA was present in the plasma of each of the challenged animals and is the first clear demonstration of plasma-borne viremia in experimentally infected animals. These data suggest the virus can spread hematogenously via the cell-free blood component. In all cases the highest viremic level detected corresponds with the day of euthanasia or death of the animal. Furthermore, the presence of NiV genomic material in all blood fractions correlated with the day associated with the most significant morbidity. In all animals, appearance of the viral genome occurs as a single peak suggesting a progressive infection seeding multiple organs simultaneously from the initial site of infection.

The distribution of B class ephrin molecules, the host cell protein molecules that serve as the receptor molecules during viral entry, contributes to the vasculitis and broad tissue tropism of the henipaviruses (46). Detection of viral genome among tissue samples following necropsy demonstrates the virus spread to nearly every organ system sampled (**Figure 7**). Notably, NiV RNA was highest among the spleen, adrenal gland, axillary lymph node, and pancreas samples from infected monkeys. Further study is required to establish the time course of infection of these organ systems and disease progression.

Person-to-person as well as food-borne transmission of the virus following contamination of fruit or date palm sap by bats may be the result of virus secreted in urine and at the mucosal surfaces during the course of infection (33). Viral genome was commonly detected in nasal and throat swabs. These results indicate the virus can be found at multiple mucosal surfaces along the respiratory system. Given the broad organ distribution and ulcerative pathology noted in the bladder, it is likely that virus detected

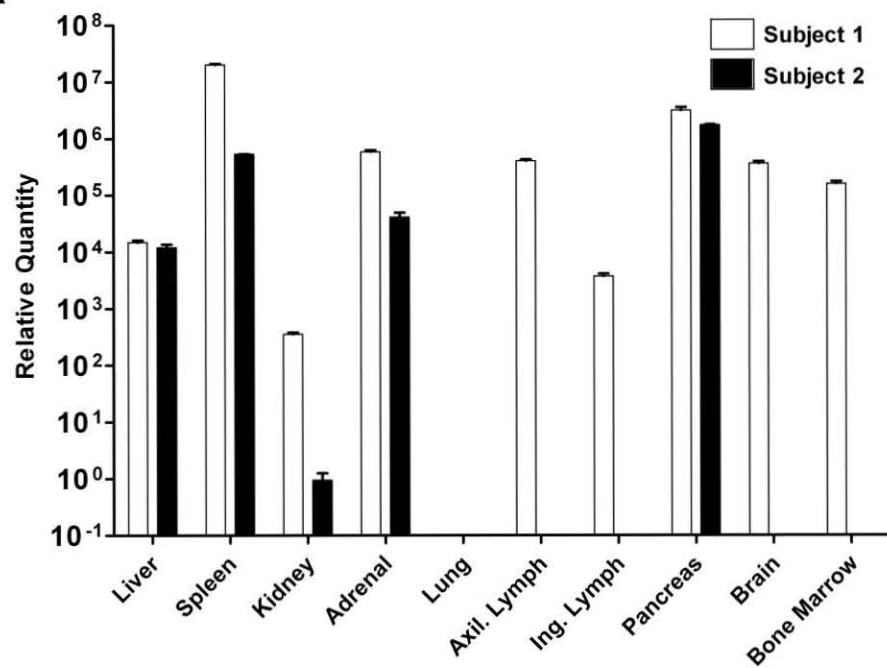
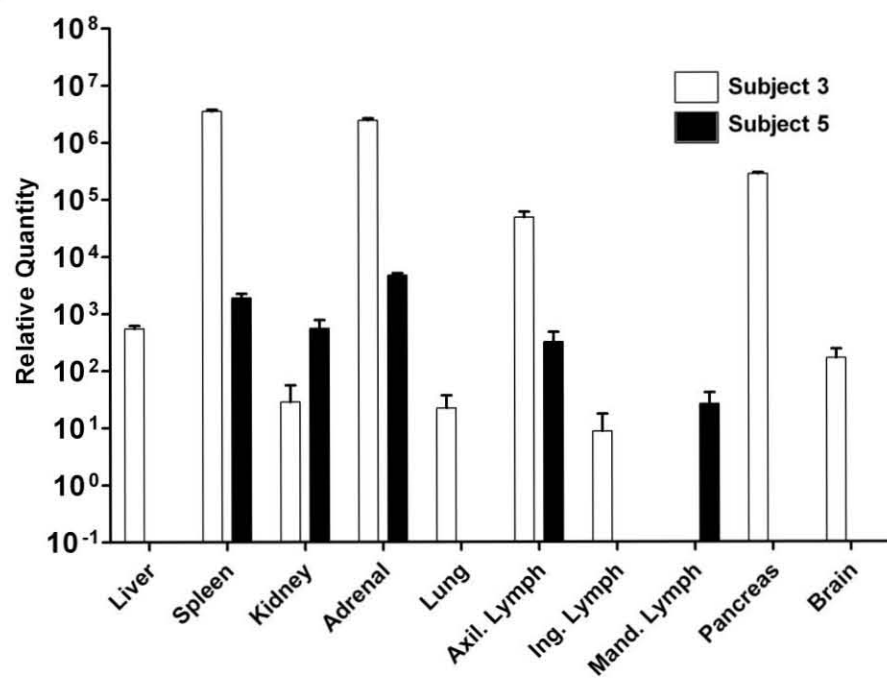
**Figure 6. Relative quantity of NiV genome in blood fractions derived from African Green monkeys challenged with NiV.**

Taqman RT-PCR was used to determine the relative NiV genome level among samples of whole blood or blood components separated by Ficoll density centrifugation. Low challenge dose,  $<5 \times 10^4$  (A, subject 4); medium challenge dose,  $>5 \times 10^4$  and  $<1 \times 10^8$  pfu (B, subject 5 and C, subject 3); and high challenge dose,  $>1 \times 10^8$  pfu (D, subject 2 and E, subject 1).



**Figure 7. Relative quantity of NiV genome among organ samples harvested from African Green monkeys challenged with NiV.**

The relative quantity of NiV genome detected by Taqman RT-PCR among AGM tissue samples obtained at necropsy. Tissue samples were stored in TriPure reagent and total RNA from each sample was isolated according to the manufacturer's directions following homogenization. Shown are the grouped results from AGM specimens receiving either a medium challenge dose ( $>5 \times 10^4$  and  $<1 \times 10^8$ , A) or high challenge dose ( $>1 \times 10^8$ , B). Abbreviations: Axillary lymph node (axil. lymph), inguinal lymph node (ing. lymph), and mandibular lymph node (mand. lymph).

**A****B**

from rectal swabs is the result of significant local pathology allowing the virus to enter the lumen.

### *Humoral immune response*

Multiple examples demonstrate a strong neutralizing humoral response targets both paramyxovirus envelope glycoproteins and is sufficient to confer resistance on subsequent challenge. Passive transfer of antibody from mother to infant during nursing protects the infant from MeV infection until virus specific antibody wanes (reviewed in 19, 57) and, similarly, neutralizing mAb protects hamsters against challenge with Mumps virus (MuV) (158). Infection with hRSV induces higher levels of secretory IgA and serum IgG which confer short-lived resistance to hRSV re-infection (reviewed in 35). Repeated reinfection generates greater cytotoxic T lymphocyte (CTL) responses and sustained IgA secretory titers in the lungs that confer longer-lived protection (35). In addition, multiple IgG mAb preparations have been approved for hRSV prophylaxis and are the only FDA approved viral antibody prophylaxis currently available (reviewed in 25). Together these results demonstrate the humoral response to paramyxovirus antigens can be an important host determinant that can modulate infection and disease severity.

Virus inhibitory mAbs recognize multiple distinct epitopes of the attachment glycoprotein, regardless of the paramyxovirus species (19, 24, 35, 51, 57, 112, 151). Often, neutralizing mAbs interact with the attachment glycoprotein at regions associated with specific function, i.e. hemagglutinin or neuraminidase activities, or receptor-binding. However, the host B cell response can also generate neutralizing antibodies that do not interfere with these functions. The nature and conservation of these attachment- or

enzymatic- independent neutralizing antigenic sites remain poorly characterized, but could provide additional insight for modeling the paramyxovirus fusion mechanism.

The humoral response to the henipaviruses can also confer resistance to viral infection with both the homo- and the heterotypic species (99, 110). Plasma from a NiV moribund monkey that fully recovered from infection exhibited high titer to sG<sub>NiV</sub> and moderate reactivity with sF<sub>NiV</sub> in ELISA as well as potently neutralized NiV in a virus plaque reduction assays (Geisbert and Broder, unpublished). Passive transfer of immune plasma to non-immune monkeys provided complete protection against subsequent lethal challenge with NiV (Geisbert and Broder, unpublished). The data from this monkey model of NiV infection and disease clearly demonstrated that protective immunity to henipaviruses develops following infection and, more specifically, the humoral response to henipaviruses is sufficient to confer protection from subsequent virus exposure. Although, both F and G glycoproteins can elicit neutralizing antibodies that participate in host resistance to viral infection, the G glycoprotein appears to be the immunodominant target suggesting the G glycoprotein-specific response may confer protection.

To detail the protective humoral response to the henipavirus G glycoprotein, recombinant soluble constructs were generated for each henipavirus species by replacing the CT and TM domains with the nucleotide sequence encoding an Ig kappa secretion signal and S-peptide epitope tag for purification (16). Bossart *et al.* demonstrated the recombinant soluble protein is conformationally similar to native glycoprotein and forms disulfide-linked dimers (16). Additional study demonstrated immunization of rabbits with sG glycoprotein elicits a strong cross-reactive polyclonal response that potently inhibits viral glycoprotein-mediated membrane fusion *in vitro* (16).



Subsequent *in vivo* studies demonstrated vaccination of cats with purified recombinant sG glycoprotein generated variable antibody endpoint ELISA titers, but protected the animals from challenge with the homo- and heterotypic henipavirus species (99, 110). Although the cat vaccination studies clearly showed protection following vaccination with sG glycoprotein, additional characterization of the antigenic structure of the henipavirus G glycoprotein is required to define structural and functional determinants that correlate with resistance to viral infection.

Earlier work by White *et al.* reported the isolation of five neutralizing mAbs from mice immunized with inactivated HeV virus (157). These five mAbs bind HeV specifically and competitive-binding indicated these mAbs target four epitopes topographically located in the globular head of the G glycoprotein. In addition, Zhu *et al.* described seven neutralizing mAbs isolated by panning a large naïve human antibody phage library with recombinant sG glycoprotein (169). Competitive binding indicates these cross-reactive human mAbs target two distinct antigenic sites (169). Further, additional analysis revealed the mAbs targeting one site strongly inhibited receptor binding. Recently we demonstrated passive transfer of one of the human mAbs, m102.4, to ferrets reduced morbidity and mortality following challenge with NiV (18). The prominent role the G glycoprotein maintains for both virus attachment and triggering F activation suggests the G glycoprotein is an ideal target for vaccine and therapeutic interventions. Further characterization is necessary to determine the specific features the G glycoprotein targeted during a protective response. Moreover, evaluation of the antigenic composition of the henipavirus G glycoprotein will also provide additional insights into structural and functional aspects of the viral glycoprotein.

### **Paramyxovirus membrane fusion**

Enveloped viruses have developed multiple mechanisms to overcome energy barriers to membrane fusion with a target cell (9, 44, 67, 83, 139). Generally, these mechanisms fall into three broad classes based on the structure and organization of the proteins catalyzing the membrane fusion process. Class I viral fusion is mediated by proteins arranged in trimers perpendicular to the virion surface with the fusion peptide near the N-terminal end of the polypeptide (44, 83). The major secondary structure observed in the pre- and post-fusion states of class I fusion molecules are  $\alpha$ -helices (83). Class II viral fusion proteins are dimeric prior to fusion and lay parallel to the cell surface of the virion and reveal an internal fusion peptide or fusion loop when triggered (83). Triggering the fusion glycoprotein results in a series of conformational changes resulting in a post-fusion form consisting largely of  $\beta$ -sheets (83). Recently, a third type, class III viral fusion, was advanced for viruses such as Vesicular Stomatitis virus (VSV) with proteins that exhibit properties of both class I and class II fusion proteins (9). These proteins form pre-fusion trimer spikes perpendicular to the cell surface that contain extensive  $\alpha$ -helical and  $\beta$ -sheet secondary structures (9). In addition, class III proteins also do not require pre-fusion cleavage to generate an active protein as seen with both class I and class II fusion proteins.

Included among viruses that undergo class I viral fusion are influenza (family *Orthomyxoviridae*) and HIV-1 (family *Retroviridae*) as well as the paramyxoviruses (67, 83). However, while a single protein determinant mediates attachment and fusion for the orthomyxoviruses and retroviruses, the paramyxoviruses separate each of these functions into distinct glycoprotein components. Division of attachment and fusion functions into

separate proteins allows independent study of these processes advancing paramyxoviruses as unique model system to study class I viral fusion.

#### *Virus attachment*

Henipavirus G mediates attachment to host cells by the interaction with one of the alternate viral receptors, ephrinB2 or ephrinB3 (13, 113). EphrinB2 and B3 are members of a large family of surface expressed glycoprotein ligands that bind Eph receptor tyrosine kinases (41, 116, 122). The Eph receptors and their ephrin ligand partners make up an important group of bi-directional signaling molecules that participate in a variety of cell-cell interactions including those of vascular endothelial cells and are the modulators of cell remodeling events, especially within the CNS. EphrinB2, in particular, is highly conserved across the metazoa and widely expressed in vertebrate animal tissues (reviewed in 70, 153, 168). Its identification as a major receptor for the henipaviruses has helped clarify the broad species and tissue tropisms of the henipaviruses as well as the pathological features observed in both humans and animal hosts.

The recent crystal structures of NiV G glycoprotein in complex with receptor indicate the interface of the receptor binding domain (RBD) is conformation-dependent and consists predominately of two regions: a large docking region of polar residues near the rim of the globular head and a distinct channel which accepts residues of the B class ephrin G-H loop (20, 162). Interestingly, detailed analysis of the channel revealed a small hydrophobic pocket homologous to the 2-deoxy-2, 3-dehydro-N-acetylneuraminic acid (sialic acid) binding site of human Parainfluenza virus type 3 (hPIV-3) HN glycoprotein (162). Sequence analysis of the HeV G glycoprotein shows the molecule is

more similar to hPIV-3 HN glycoprotein than MeV H glycoprotein which also binds a protein receptor (165).

Site-directed mutagenesis and the crystal structure revealed residues W504, E505, Q530, T531, A532, E533, N557 of NiV G glycoprotein and residues D257, D260, G439, K443, G449, K465, and D468 of HeV G glycoprotein are important in the interaction of the G glycoprotein with the ephrin receptor molecules (12, 58, 162). Since both viruses use the same B class ephrin receptors, and given the significant level of structural conservation and similar susceptibilities to certain mAb neutralization, it is likely the majority of residues within the G glycoprotein essential for receptor binding will be similar for both viral species. Further, the crystal structure of NiV G glycoprotein in complex with ephrinB3 and -B2 confirms the importance of the B class ephrin G-H loop for binding within the channel of the globular head domain of NiV G glycoprotein and HeV G glycoprotein (20, 162). The importance of the G-H loop as the principle site of interaction between the G glycoprotein and the ephrinB2 and -B3 is similar to reports showing the importance of this loop among the B class ephrins in binding to their Eph receptor partners.

#### *Interaction of the envelope glycoproteins*

Multiple studies clearly demonstrate the necessity for both the attachment and fusion glycoproteins to promote efficient membrane fusion among paramyxoviruses. Expression of either glycoprotein without its envelope glycoprotein partner results in the absence of detectable fusion with few noted exceptions (reviewed in 87, 89). In addition, only envelope glycoproteins from the same or highly related viruses, such as the henipaviruses, mediate fusion when co-expressed in a heterotypic manner (17). We have

previously shown co-precipitation of the G and F glycoproteins in the absence of receptor suggesting these glycoproteins interact and remain associated on the surface of the virion or infected cell prior to attachment (12). Several reports have implicated regions in the stalk domain and/or the  $\beta$ 2 sheet region of various attachment glycoproteins as important elements of the molecule in its interaction with the F glycoprotein (40, 102, 142, 143, 148, 150). However, to date, these findings have not definitively shown the precise molecular elements involved in their association and uncertainty remains as to the specific regions in both the F glycoprotein and an attachment glycoprotein that are involved.

Certain isoleucine residues in the stalk domain of the attachment glycoprotein potentially form a HR- like structure important in the interaction between the attachment and fusion glycoproteins (143). Mutations made in this region of the Newcastle disease virus (NDV) HN glycoprotein have been shown to alter both the interaction of HN glycoprotein with the F glycoprotein and the capacity of the viral proteins to promote fusion (102, 143). However, mutations in the analogous region of MeV H glycoprotein also disrupted fusion, but did not disrupt the interaction of H glycoprotein with the F glycoprotein (36). As a result, Iorio *et al.* proposed that paramyxoviruses modulate F glycoprotein activation differently based on the nature (i.e. a sialic acid moiety or protein) of the target viral receptor (76).

Recently, we reported identification of a series of isoleucine residues in the stalk domain of the HeV G glycoprotein that appear important in the G glycoprotein's structure and fusion-promotion activity (11). Comparison of the amino acid sequence of NiV G glycoprotein and HeV G glycoprotein indicates these isoleucine residues are

conserved and form an imperfect HR-like arrangement (11). Individual site-directed mutagenesis of each isoleucine residue was performed and, although 9 of 12 of these HeV G glycoprotein mutants were expressed on the cell surface and retained receptor-binding competence, they were completely defective in their fusion-promotion activity. Additional analysis of these defective cell-surface expressed mutants revealed that they were differentially glycosylated with complex oligosaccharides and migrated as a slightly higher molecular weight species. However, analysis of the HeV G glycoprotein isoleucine mutants produced in the presence of 1-deoxymannojirimycin, HCl indicated that inhibiting of the addition of high molecular weight mannose species did not alleviate their fusion-promotion defect (11). Co-precipitation studies of these G glycoprotein mutants with the F glycoprotein revealed defects in F glycoprotein association in the absence of receptor, suggesting the isoleucine mutations were altering the conformation of the G glycoprotein and preventing its association with the F glycoprotein.

#### *Activation of the fusion glycoprotein*

The favored model of paramyxovirus fusion posits that specific receptor binding induces changes in the attachment glycoprotein, which triggers the activation of the F glycoprotein allowing fusion to proceed. In fact, structural studies by Takimoto *et al.* suggested the conformation of the outer face of the NDV HN glycoprotein globular head varied when bound to sialic acid (145). However, the subsequent crystal structures from other paramyxovirus attachment glycoproteins have not revealed major conformational variations when comparing receptor bound and unbound structures (20, 92, 162, 166). In particular, the structure of NiV G glycoprotein in complex with ephrinB3 shows remarkably little alteration in the conformation when compared with the structure of

unbound NiV G glycoprotein (162). The structures show alterations in conformation are principally restricted to the binding pocket and interface with ephrinB3 (162). It seems unlikely that these minor conformational differences alone would be sufficient to effect the interaction of the F glycoprotein and the G glycoprotein and the resultant triggering of the conformational alterations in the F glycoprotein leading to membrane fusion.

Iorio *et al.* proposed that paramyxoviruses may mediate the activation of the F glycoprotein by distinct mechanisms based on the nature of the receptor, e.g. carbohydrate moiety or protein (76). Experiments showing the co-immunoprecipitation of F and G glycoproteins indicate henipaviruses facilitate fusion activity via a mechanism consistent with NDV, which binds sialic acid, and is proportional to the extent of G glycoprotein and F glycoprotein association (11, 76, 103). However, in the case of MeV, which also utilizes a protein receptor, fusion activity appears inversely related to the extent of the association of the envelope glycoproteins (36, 121).

The incongruence of henipavirus protein receptor usage and F glycoprotein association with the model proposed by Iorio *et al.* can perhaps be somewhat clarified by examination of the NiV G glycoprotein crystal structures recently published. These structures show the site of interaction with the B class ephrins is located on the G glycoprotein in an analogous position to the sialic acid binding site of NDV (11, 76, 162). In contrast, the RBD described for MeV H glycoprotein is located in a position on the globular head further from the dimer interface than found with NDV HN glycoprotein (76). It is therefore plausible that the divergent mechanisms described by Iorio *et al.* are not resulting from the nature of the viral receptor, but rather the nature and location of the binding site on the attachment glycoprotein itself.

### *Membrane merger*

Following virus attachment and F glycoprotein activation, the F glycoprotein mediates the merger of the viral and host cell membranes. Conformational changes in the F glycoprotein trimer produce an extended molecule exposing the fusion peptide that inserts into the target cell membrane (reviewed in 88). After a physical link has been established between the membranes, the two HR domains undergo significant conformational rearrangements whereby the HRB domains fold into the grooves of the trimeric HRA domain core forming a hairpin bundle of  $\alpha$ -helices known as the 6-helix bundle (88). The formation of the 6-helix bundle structure is concomitant with membrane merger and appears to drive the fusion process. Once fusion occurs between the virion and host cell membranes, the virion contents are released into the cytoplasm initiating virus replication.

Molecular characterization of the fusion process has resulted in significant refinements of the theoretical model of membrane fusion mediated by paramyxoviruses. In particular, studies using specific peptides that mimic the HR regions shown capable of inhibiting fusion at defined steps (129). These experiments point to specific conformational changes in the F glycoprotein that proceed in a defined sequence. The solution structures of both pre- and post-fusion forms of two paramyxovirus F glycoproteins were found consistent with HR peptide fusion inhibition studies and have further detailed the conformational changes in the F glycoprotein in relation to the model of paramyxovirus membrane fusion (reviewed in 87). However, major gaps in our understanding of paramyxovirus membrane fusion process remain, particularly in the nature of the interaction between the attachment and fusion glycoproteins and precise



details of the receptor-induced processes leading to the activation and conformational changes in the F glycoprotein. A model of henipavirus fusion is shown in **Figure 8**.

### **Specific aims and hypotheses**

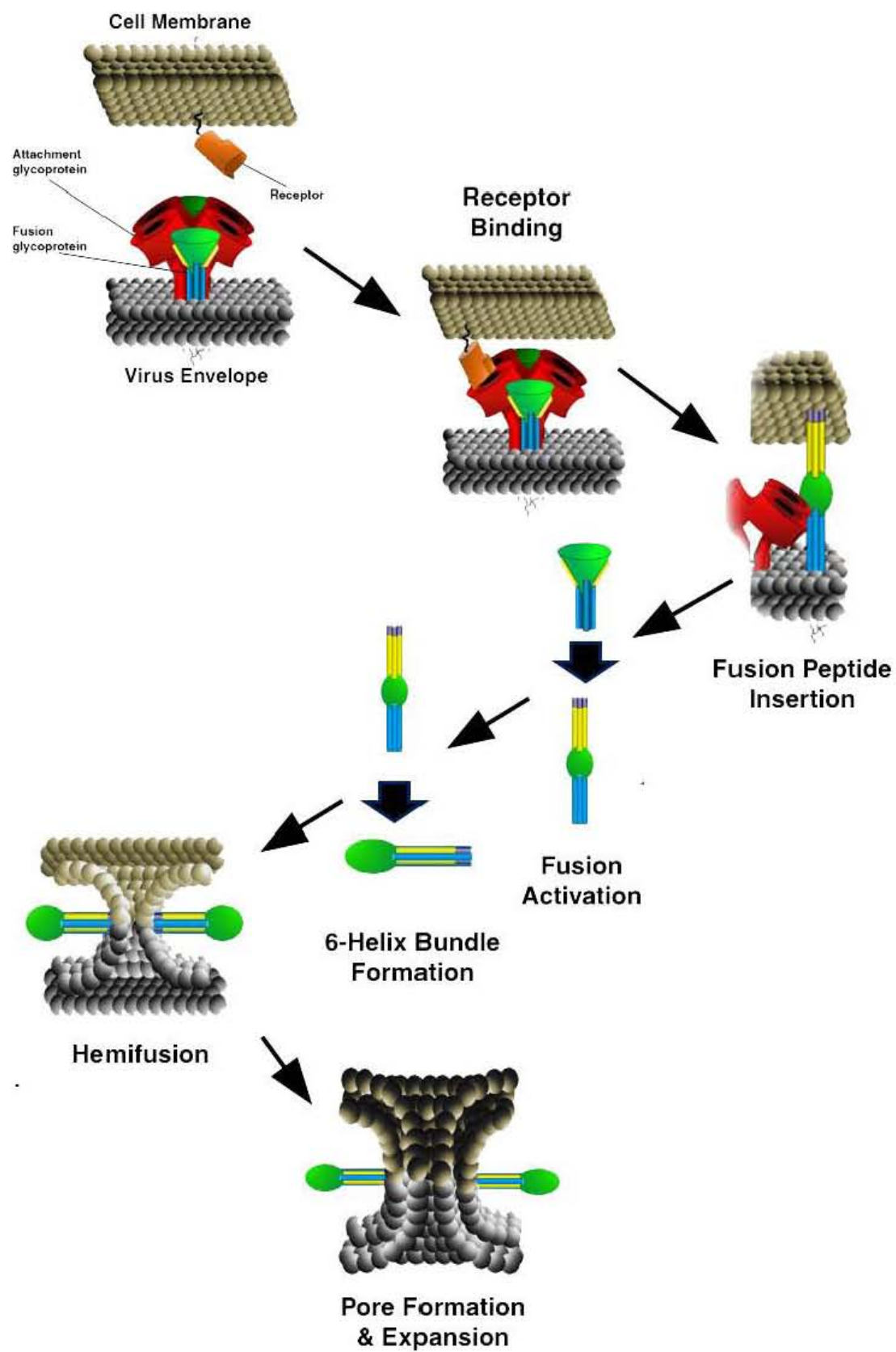
The henipavirus G glycoprotein is an essential viral component for host cell infection and an important immune target of the host response. Multiple studies clearly demonstrate that among paramyxoviruses the attachment glycoprotein is also the dominant target of the protective humoral response. Furthermore, recent publications have shown humoral response to the henipavirus G glycoprotein imparts potent protection from subsequent challenge with either henipavirus species. However, the majority of reports focus principally on the polyclonal humoral response and only limited characterization using monoclonal antibodies is available. As a result, the features of the henipavirus G glycoprotein targeted by neutralizing antibodies, mechanisms of neutralization, functional domains, and the antigenic structure remain poorly understood. The focus of this dissertation is characterization of the protective and functional features of the henipavirus G glycoprotein that elicit a humoral immune response. Specifically, I sought to:

**Specific Aim #1:** Generate hybridoma cell lines that elaborate monospecific henipavirus G glycoprotein immunoglobulin.

#### *Hypotheses*

- *Immunization of mice with recombinant soluble henipavirus G glycoprotein should induce a strong humoral response.*
- *Murine henipavirus monoclonal antibodies should target multiple diverse epitopes of the G glycoprotein.*

**Figure 8. Model of henipavirus glycoprotein mediated class I fusion.** Hetero-oligomeric complexes of henipavirus G glycoprotein (dimer of dimers) associated with F glycoprotein (trimer) protrude from the virion surface and target the virus particle to a susceptible host cell. The henipavirus G glycoprotein binds the extended G-H loop of the B class ephrin molecule (receptor binding) promoting G glycoprotein-dependent activation of the F glycoprotein by an uncharacterized mechanism (fusion activation). Activated F glycoprotein undergoes major conformation changes to reveal the hydrophobic fusion peptide which is inserted in the host cell membrane (F glycoprotein rearrangements). Once the F glycoprotein spans both membranes, the HR regions reorganize to form a hairpin structure (6-helix bundle) that positions the membranes in close proximity so the lipid bi-layers can mix (pore formation/expansion) eventually depositing the contents of the virus particle in the cytoplasm of the host cell.



**Specific Aim #2:** Characterize the features of the henipavirus G glycoprotein that elicit a protective humoral immune response.

*Hypotheses*

- *Neutralizing murine mAbs should target multiple independent antigenic sites of the henipavirus G glycoprotein.*
- *Neutralizing mAbs from sG<sub>HeV</sub> glycoprotein and sG<sub>NiV</sub> glycoprotein immunized mice should target antigenic sites common to both henipavirus species.*
- *Neutralizing mAbs may target antigenic sites of the henipavirus G glycoprotein that mediate as well as do not mediate the interaction of glycoprotein with the viral receptor.*

**Specific Aim #3:** Examine the antigenic structure of receptor bound and unbound henipavirus G glycoprotein.

*Hypotheses*

- *Receptor engagement may alter the structure of the henipavirus G glycoprotein changing the availability of antigenic sites in the globular head to interact with mAbs.*
- *Receptor induced conformational changes in the henipavirus G glycoprotein may occur at multiple independent antigenic sites.*
- *Receptor induced conformational changes in the henipavirus G glycoprotein should be independent of F glycoprotein co-expression.*

## Chapter 2: Materials and Methods

### *Tissue culture*

Human HeLa-USU, 293T, 293F, vervet monkey BS-C-1 cells, and AGM Vero cells were obtained as previously described and cultured in Dulbecco's modified Eagle's medium (DMEM; Quality Biologicals, Gaithersburg, MD) or Eagle's minimal essential medium (EMEM; Quality Biologicals) containing 10% cosmic calf serum (CCS; Hyclone, Logan, UT), 100 U/ml Penicillin, 100 µg/ml Streptomycin, and 2 mM L-glutamine (17). Growth media for stably transfected 293T and 293F cell lines was supplemented with hygromycin (Invitrogen Corp., Carlsbad, CA) to a final concentration of 500 µg/ml (26). Sp2/0 cells, a murine myeloma cell line, (American Type Culture Collection [ATCC], Manassas, VA) was cultured in Iscove's modified Dulbecco's medium (IMDM; Invitrogen) containing 10% cosmic calf serum, 100 U/ml Penicillin, and 100 µg/ml Streptomycin as previously described (43). All cultures were maintained at 37°C in humidified 5% CO<sub>2</sub> atmosphere.

### *Tissue sample collection and RNA isolation*

Blood samples were collected in tubes containing EDTA and a portion of each was separated into individual blood components (plasma, granulocytes, peripheral blood mononuclear cells, and lysed red blood cells) by gradient centrifugation using Ficoll 400 (Sigma-Aldrich, St. Louis, MO) at 400 x g for 45 min at 25°C. Tissue samples were harvested from animals AGM at the time of sacrifice and subsequently homogenized in TriPure reagent (Roche Applied Sciences, Indianapolis, IN) at 10% tissue weight by volume TriPure. Blood samples were immediately diluted in TriPure Isolation Reagent at a ratio of 1 part plasma to 4 parts TriPure reagent or 1 part whole blood, granulocytes,

lysed red blood cells, and PBMC sample to 8 parts TriPure reagent. TriPure diluted samples were stored at -80°C and transported frozen on dry ice. All samples were thawed at 25°C prior to isolation of total RNA. Total RNA was isolated from each TriPure dilute sample according to the manufacturer's directions and each sample was resuspended with 35 µl of ultrapure water treated with 0.1% diethylpyrocarbonate (DEPC; Invitrogen). Samples of purified RNA were stored at -20°C until use.

#### *NiV Taqman reverse transcriptase PCR*

Taqman PCR was performed using the primer sets and probes as previously described (18, 99). Briefly, samples were thawed at 25°C and 2 µl of sample was assayed in triplicate using Taqman One-Step Mastermix (Applied Biosystems, Foster City, CA). Each 25 µl reaction contained Nipah N specific primers (N1198F and N1297R) and 18s rRNA primers (18SrRNAF and 18SrRNAR) at a final concentration of 900 nM each (Applied Biosystems). In addition, each reaction contained 200 nm of both Nipah-1247-comp-FAM-labeled probe and 18SrRNA-VIC-labeled probe. Samples were amplified with a GeneAmp 7500 Sequence Detection System (Applied Biosystems) as follows: 48°C for 30 min, 1 cycle; 95°C for 10 min, 1 cycle; and 95°C for 15 sec and 60°C for 1 min, 50 cycles. Standard curves were calculated based on the threshold cycle (Ct) value for multiple dilutions of purified pCAGGS DNA containing the NiV N gene assayed in triplicate (data not shown). Reported is the mean NiV N RNA relative quantity or relative quantity per ml of sample determined by linear regression analysis of each sample assayed in triplicate.

### *Recombinant proteins*

Recombinant sG<sub>Hev</sub> glycoprotein and sG<sub>NiV</sub> glycoprotein were transiently expressed in BS-C-1 cells using the recombinant vaccinia virus system previously described (16). Soluble human ephrinB2 fused with an S-peptide epitope tag (12) was stably expressed in 293F cells as previously described (26). Supernatant from spent cultures was collected and clarified by centrifugation prior to filtration through a 0.22 µm low-protein binding membrane. Soluble protein was purified by S-protein agarose bead (Novagen Corp., Madison, WI) affinity chromatography and concentrated with centricon microconcentrator units with a 30,000 dalton molecular weight cutoff (Millipore, Billerica, MA) as previously described (16). The concentration of purified protein in PBS was determined using a Nanodrop spectrophotometer (NanoDrop, Wilmington, DE).

Recombinant soluble mouse ephrinB2/Fc, human ephrinB3/Fc, and biotinylated human ephrinB3/Fc were obtained commercially (R&D Systems, Minneapolis, MN). Biotinylated soluble ephrinB2/Fc was prepared using NHS-PEO-biotin bound to a nickel chelated support matrix according to the manufacturer's directions (Pierce, Rockford, IL).

### *Immunization of mice and hybridoma*

Balb/cJ mice (Jackson Laboratory; Bar Harbor, ME) were immunized with a suspension of 10 to 15 µg of purified sG glycoprotein and RiBi adjuvant (RiBi Immunochem Research Inc.; Hamilton, MN) prepared according to the manufacturer's directions. Mice were inoculated 3 times at 28-day intervals receiving half of the inoculum intraperitoneally and the remainder subcutaneously. Mice were inoculated with a final 10 to 15 µg of purified protein given in sterile PBS intraperitoneally 2 weeks

following the third immunization and sacrificed 3 days following. The spleen and, in some cases, inguinal lymph node were harvested at the time of death.

Single cell suspensions of splenocytes/lymphocytes were added to fresh cultures of murine myeloma Sp2/0 cell and fused using polyethylene glycol (PEG) in accordance with standard practices. The resultant cells were distributed at a limiting dilution in 96-well tissue culture plates as previously described (43) and the medium was replaced once prior to screening colony supernatant by ELISA with sG glycoprotein antigen. To ensure clonal cultures, colonies were harvested from wells containing supernatant reactive with sG glycoprotein in ELISA and plated twice at limiting dilution (43). Cloned hybridoma lines were maintained in IMDM medium supplemented with 10% CCS, sodium hypoxanthine aminopterin thymidine (HAT; Invitrogen) and 100 U/ml recombinant mouse interleukin 6 (rIL-6; Roche).

#### *Monoclonal antibody preparation*

Purified mAb was prepared as previously described (43). Briefly, hybridoma cells were grown to high density in SFM4mAb medium (Hyclone) supplemented with HT and 100 U/ ml rIL-6. Supernatant from spent cultures was harvested, clarified by centrifugation, and filtered prior to storage at 4°C in the presence of protease inhibitor cocktail. mAb was purified using a Protein-G Sepharose (GE Healthcare, Piscataway, NJ) bead affinity chromatography and the elutant was concentrated with Centricon microconcentrator units (50,000 dalton molecular weight cut-off) while transferring purified mAb to PBS. The concentration of each preparation was determined using a Nanodrop spectrophotometer.



Purified human mAbs m101, m102.4, and m106.3 were prepared as previously described (169). Concentrated hybridoma supernatant containing murine mAbs 3A5.D2, 8H4, 17A5, and H2.1 were obtained from Dr. John White (157).

*Indirect ELISA and competitive-binding assay*

ELISA tests were performed using Immulon 2HB microtiter plates (Fisher Scientific, Hampton, NH) coated overnight at 4°C with 100 µl/well of PBS, 0.045 M sodium bicarbonate, 0.018 M sodium carbonate solution containing 0.5 µg/ml purified sG glycoprotein. Non-specific binding was reduced by pre-incubating coated microtiter wells with 5% bovine serum albumin, fraction V (BSA; Sigma Aldrich) in a solution of PBS containing 0.05% Tween-20 (BSA-PBST). A 100 µl aliquot of supernatant from hybridoma colony plates or mAb diluted in PBST buffer containing 1% BSA (1% BSA-PBST) was added to wells and labeled with horse radish-peroxidase (HRP) conjugated goat anti-mouse IgG (H+L) (1:10,000 dilution; Pierce). Microtiter plates were maintained at 37°C for 1 hr at each step and subsequently washed 6 times with PBST using a 96-well microtiter plate washer (Molecular Devices Corp., Sunnyvale, CA). Bound antibody/protein was detected with a 0.25 mg/ml solution of 2,2'-Azino-di-[3-ethylbenzthiazoline sulfonate (6)] diammonium substrate (ABTS; Roche) (100 µl/well). After 30 minute incubation with shaking at 25°C, the absorbance (405 nm) was determined using a Versamax microtiter plate reader (Molecular Devices) with SoftMax Pro software (104). The reported optical density (OD) represents the mean value of 3 or more replicate wells.

Competitive-binding assays with antibody and receptor were performed similarly to the basic ELISA assay described with the following modifications. Wells were

blocked with 5% BSA-PBST prior to adding 100 µl of 2.5 µg/ml unlabeled mAb or purified viral receptor in 1% BSA-PBST. The microtiter plates were incubated overnight at 4°C and, subsequently, 100 µl of biotinylated mAb, biotinylated ephrinB2/Fc (0.25 µg/ml), or biotinylated ephrinB3/Fc (0.5 µg/ml) was added to wells and incubated at 4°C for 45 min. To each well, 100 µl of HRP conjugated streptavidin (Pierce) was added at a final dilution of 1:10,000 in 1% BSA-PBST. Microtiter plates were developed with ABTS substrate and the absorbance (A) was determined as above. Competition was calculated as the percent decrease of the mean absorbance in the presence of the competitive mAb (A2) when compared to the mean absorbance in the absence of competitive antibody (A1) or  $((A1-A2)/A1)*100$ .

#### *Serology and data collection*

Serum samples and health information were collected from a cohort of Thai children attending 6 different schools in Kamphaeng Phet Province, Thailand to study the occurrence of Dengue virus (48, 49, 119). Subject enrollment, sample collection, and data analysis were completed in accordance with the rules and regulations set forth by the Walter Reed Institute of Research (WRAIR) Human Use Committee and the Thai Ethical Review Committee, Ministry of Public Health, Nonthaburi, Thailand (approved protocol “Prospective Study of Dengue Virus Transmission and Disease in Primary School Children,” WRAIR# 654) as well as the Uniformed Services University Human Use Committee (approved protocol “Serosurvey of Thai Children to Evaluate Potential henipavirus Exposure,” USUHS# HU73NK). Whole blood and a health questionnaire were obtained from children within 7 days of the onset of fever resulting in absence from school and 14 days following recovery. The serum fraction was isolated by standard

techniques and stored at  $-70^{\circ}\text{C}$  until use. Randomly selected serum samples were assayed at multiple dilutions (1:50, 1:250, and 1:1000) in triplicate by ELISA using plates coated with sG<sub>NiV</sub> glycoprotein. Captured henipavirus serum antibody was labeled with alkaline phosphatase (AP) conjugated goat anti-human IgG (Jackson ImmunoResearch, West Grove, PA) and detected with PNPP (p-Nitrophenyl Phosphate, Disodium Salt) in Diethanolamine Buffer (Thermo Scientific, Rockford, IL) for 30 min at  $25^{\circ}\text{C}$ . The absorbance at 405 nm was determined for each well and the mean absorbance value was calculated for each sample dilution. Positive samples were those with a mean absorbance at least twice the mean absorbance of non-immune normal human sera.

#### *Data analysis*

One way ANOVA and data graphical representations were developed using GraphPad Prism software for Windows (56). For each illness resulting in the collection of a blood sample, the public health worker documented the age, gender, school location, history of hospital admission, and clinical symptoms (specifically fever, headache, altered consciousness, vomiting, and breathing difficulties) of the child. The prevalence odds ratio (POR) was calculated for demographic factors and the Fischer's exact test was used to assess statistical differences among groups. Statistical analyses were performed using SPSS (141).

#### *Virus neutralization assays*

Neutralization of live virus was examined under BSL-4 level containment at the Australian Animal Health Laboratory (AAHL), Commonwealth Scientific and Research Organization (CSIRO) facility in Geelong, Australia as previously described (16). Briefly, mAbs were incubated with  $1.5 \times 10^3$  TCID<sub>50</sub>/ml or  $7.5 \times 10^2$  TCID<sub>50</sub>/ml of HeV

or NiV, respectively, in EMEM medium containing 10% CCS for 30 min and then added to Vero cell monolayers grown to 90% confluence. The cells were cultured with the virus inoculum for 24 hr. The Vero cell monolayers were fixed in methanol and stained for the viral P protein before imaging. All images were obtained using an Olympus IX71 inverted microscope coupled to an Olympus DP70 high resolution color camera.

*Viral glycoprotein mediated membrane fusion assays*

Recombinant vaccinia virus driven cell-cell fusion inhibition assays were performed as previously described (15). Briefly, HeLa-USU cells were infected with recombinant vaccinia virus or modified vaccinia virus ankera (MVA) encoding homotypic G and F glycoproteins (117) as well as vaccinia virus-encoding T7 RNA polymerase at a multiplicity of infection (MOI) of 10. Vero cell monolayers were infected with vaccinia virus encoding  $\beta$ -galactosidase ( $\beta$ -Gal) under the *Escherichia coli* (*E. coli*) T7 bacteriophage promoter at an MOI of 10. Protein expression was allowed to proceed overnight at 31°C. Dilutions of either polyclonal sera or purified mAbs were added to cells expressing the henipavirus F and G glycoproteins and allowed to bind for 30 min at 37°C. Following, an equivalent number ( $2 \times 10^5$  total cells per well) of receptor positive vaccinia infected Vero cells were added to the HeLa-USU effector cells in a 96 well microtiter plate. Cell fusion was allowed to proceed for 2.5 hr at 37°C before the addition of Nonidet P-40 alternative (Cal Biotech, San Diego, CA) to final concentration of 0.5%.

$\beta$ -Gal activity among aliquots of lysates was measured at 25°C with chlorophenol red-D-galactopyranoside (CPRG; Roche) substrate. Fusion was quantified and represented as the rate of  $\beta$ -Gal activity ([change in optical density at 570 nm per minute]

x 1,000) using a Versamax microtiter plate reader and SoftMax Pro software. The cell fusion results were normalized to the rate of fusion without antibody. The IC<sub>50</sub> for each mAb was determined by multivariate linear regression analysis using GraphPad Prism software for Windows.

#### *Immunoprecipitation assays*

HeLa-USU cells were infected with wild type (WT) vaccinia virus (vWR) or recombinant vaccinia virus encoding HeV G (vKB2) or NiV G (vKB6) glycoproteins at an MOI of 10 and incubated overnight at 37°C. Cells were lysed in lysis buffer (100 mM Tris-HCl [pH 8.0], 100 mM NaCl, and 1% Triton X-100) on ice and clarified by centrifugation. Protein G Sepharose beads (70 µl; GE Healthcare) were added to remove components of the cell-lysate that bound the beads non-specifically. Cleared lysates were incubated with 2 µl of mouse sG antiserum or 2 µg of mAb overnight at 4°C and precipitated with Protein G-Sepharose for 40 min at 25°C. Competitive-binding assays with viral receptors were performed with cleared lysate incubated with 1 µg unlabeled receptor overnight at 4°C followed by 0.5 µg biotinylated mAb for 45 min at 25°C. Samples were precipitated with either Protein G-Sepharose or avidin D-agarose beads (Vector Laboratories, Burlingame, CA) for 40 min at 25°C. The beads were precipitated by centrifugation (400 x g for 5 min).

The supernatant was aspirated and the precipitated beads were washed twice with lysis buffer and once in lysis buffer with 100 mM Tris-HCl (pH 8.0), 100 mM NaCl, 0.1% sodium deoxycholate, and 0.1% SDS (DOC wash buffer). Samples were boiled in LDL sample buffer (Invitrogen) with β-mercaptoethanol (BME) at a final concentration

of 2.5% and analyzed by SDS-PAGE electrophoresis using 4-12% NuPAGE BIS-Tris gels (Invitrogen).

Gels were transferred to 0.45  $\mu$ m nitrocellulose membranes (BioRad, Hercules, CA) and incubated at 4°C in 5% milk in 0.5% Tween-20/PBS (PBST) overnight. Blots were incubated with rabbit sG<sub>HeV</sub> antisera (1:20,000) in 1% milk-PBST for 1 hr at 25°C followed by HRP conjugated goat anti-rabbit antibody (Jackson ImmunoResearch) (1:20,000) in 5% milk-PBST for 1 hr at 25°C. Blots were washed 4 times for 15 min following each antibody step and developed using WestPico chemiluminescent substrate (Thermo Scientific) according to the manufacturer's directions. All blots were imaged on Kodak Biomax XAR film (Sigma Aldrich, St. Louis, MO).

#### *Metabolic labeling and receptor induced changes assays*

Metabolic labeling of full-length and soluble protein was performed as previously described (12). Briefly, sub-confluent monolayers of HeLa-USU cells were transfected overnight with 3  $\mu$ g of HeV F glycoprotein or NiV F glycoprotein as indicated in accordance with previously established methods (11). Cultures of HeLa-USU cells were infected with recombinant vaccinia virus for 3 hr at 37°C as above. Subsequently, the virus inoculum was aspirated and the monolayers washed 3 times with cysteine and methionine depleted DMEM medium. Cell monolayers were incubated overnight at 37°C in labeling media (cysteine/methionine depleted DMEM supplemented with 2.5% dialyzed fetal bovine serum (FBS) and 0.1  $\mu$ Ci/ml [<sup>35</sup>S]-cysteine/methionine (Promix; Amersham Pharmacia Biotech, Piscataway, NJ). Label media was aspirated and the cell monolayers were cultured with DMEM-10 for 1.5 hr at 37°C. After washing the monolayers with PBS, the cells were gently detached from the flask and lysed as above.

The cell lysate material was divided into 100  $\mu$ l aliquots and half were incubated with 2  $\mu$ g purified soluble human ephrinB2 per 100  $\mu$ l of lysate overnight at 4°C. An equivalent volume of PBS without purified protein was added to the remaining aliquots and incubated overnight at 4°C. Subsequently, the samples were transferred to 37°C for 1 hr before mAb (2  $\mu$ g per sample) was added. Following, samples were combined with 70  $\mu$ l of 20% Protein G-Sepharose for 45 min at 25°C with rotation. Samples were washed, as above, and boiled for 5 min in 20  $\mu$ l LDL sample buffer (Invitrogen) with or without 2.5% 2-mercaptoethanol. Reduced and non-reduced samples were analyzed by SDS-PAGE electrophoresis using either 4-12% NuPAGE Bis-Tris gels (reduced samples) or 3-8% Tris-Acetate gels (non-reduced samples) according to the manufacturer's directions (Invitrogen).

Resolving gels were soaked the gel in a solution containing 40% Methanol 10% glacial Acetic acid for 30 min followed by Enlightening solution (Perkin Elmer, Waltham, MA) for 20 min. The gels were dried using Model 583 Gel Dryer (BioRad, Hercules, CA) and imaged with XAR film. The ratio of the quantity of G glycoprotein precipitated in the presence versus absence of ephrinB2 normalized to the amount precipitated by the mAb nAH1.3 (control mAb) in the presence versus absence of ephrinB2 was calculated using Image J software (National Institutes of Health, Bethesda, MD) as follows:  $[(\text{adj. density}_{\text{sample mAb with ephrinB2}} / \text{adj. density}_{\text{control mAb with ephrinB2}}) / (\text{adj. density}_{\text{sample mAb without ephrinB2}} / \text{adj. density}_{\text{control mAb without ephrinB2}})]$ , where the adjusted (adj.) density is the density measure obtained following adjustment for the background density measure for each mAb.

## **Chapter 3: Characterizing the neutralizing epitopes of the henipavirus G glycoprotein**

### **Introduction**

Recombinant henipavirus sG glycoprotein is produced as a disulfide-linked homodimer along with lesser amounts of the tetrameric (dimer of dimers) oligomeric form, both of which can be purified to homogeneity by size exclusion chromatography (16). Recombinant sG<sub>HeV</sub>, and sG<sub>NiV</sub>, glycoproteins retain important native structural features necessary for binding ephrinB2/B3 and induce potent neutralizing antibody responses in rabbits (16). In addition, sG glycoprotein has been shown to be an effective subunit vaccine in challenge studies against NiV in a feline model of henipavirus infection (99, 110). The crystal structures of the sG<sub>NiV</sub> glycoprotein, alone and in complex with the ephrinB3 receptor as well as sG<sub>HeV</sub> glycoprotein in complex with ephrinB2 have detailed the receptor binding domain of the G glycoprotein (20, 162) and Xu and Nikolov, personal communication). The binding interface is composed of a polar docking region near the rim of the globular head with a smaller pocket that accepts residues of the G-H loop of the B class ephrin molecules (20, 162).

Passively administered antibody is an effective antiviral therapy or prophylaxis for some paramyxoviruses such as MeV and hRSV (reviewed in 25). In addition, passive transfer of polyclonal antibody from immunized donors has been used to treat hRSV, Rabies virus, Variola virus, among other (25). These reports demonstrate the antibody response to viruses, specifically the paramyxoviruses, is important in preventing and limiting morbidity resulting from infection.



As with several other paramyxoviruses, the prominent role the henipavirus G glycoprotein plays in virus attachment and in promoting F-mediated membrane fusion makes it an ideal target for the development of vaccine or therapeutic interventions. The current description of the antigenic structure of the henipavirus G glycoprotein is incomplete. White *et al.* reported the first anti-G glycoprotein neutralizing mAbs (5 mAbs targeting 4 epitopes) from mice immunized with inactivated HeV (157). More recently, Zhu *et al.* isolated 7 neutralizing human mAbs targeting 2 distinct antigenic sites by panning a large naïve human antibody phage library with recombinant sG glycoprotein (169). In addition, passive transfer studies of polyclonal or monoclonal antibodies to hamsters have shown them to be effective in preventing NiV and more recently HeV infection and disease (59-61), highlighting the dominant role for the G glycoprotein as a protective immunogen. Moreover, a fully-human and cross-reactive neutralizing mAb against the henipavirus G glycoprotein (m102.4) has been shown to be an effective post-exposure immunotherapy against lethal NiV challenge in a ferret model (18).

Further characterization is required to define the determinants of the G glycoprotein targeted during the protective humoral response. In addition, a more extensive evaluation of the antigenic structure of the henipavirus G glycoprotein will provide insight toward understanding the nature of the differential neutralizing antibody responses and will also aid in defining the structural and functional activities of the attachment glycoprotein.

## Results

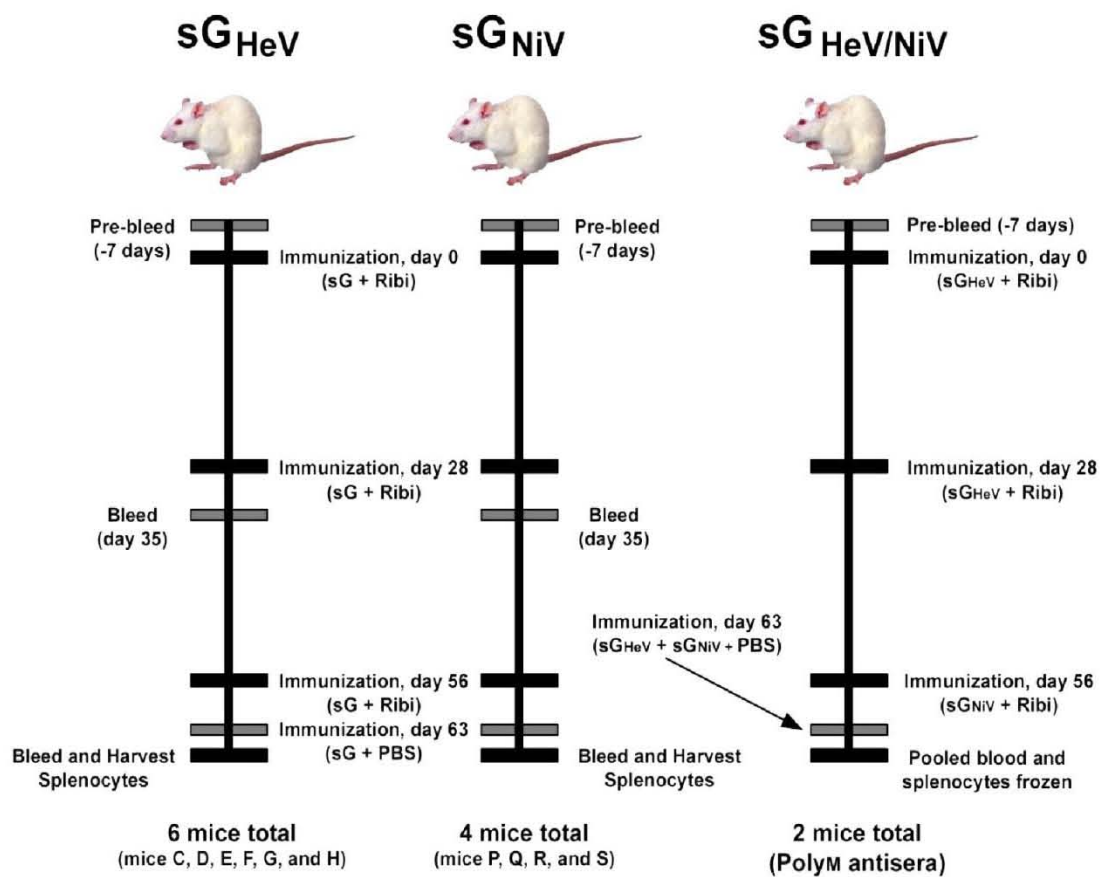
### *Murine polyclonal B cell response following sG glycoprotein immunization*

Previous reports have clearly demonstrated immunization of mammalian species from multiple taxa with the sG glycoprotein elicits a strong protective humoral response (16, 99). Here, Balb/cJ mice were immunized at 28-day intervals with purified sG<sub>HeV</sub> glycoprotein or sG<sub>NiV</sub> glycoprotein in RiBi adjuvant (**Figure 9**) and the polyclonal response was characterized. The ELISA endpoint titer determined for serum harvested from immunized animals demonstrated both soluble constructs induced a strong humoral response with similar magnitudes (endpoint ELISA titer >1:1,000,000) in mice (**Figure 10A**). The polyclonal antisera bound the heterotypic sG glycoprotein species slightly less efficiently in ELISA (endpoint titer >1:250,000) indicating the cross-reactive response was slightly less robust (**Figure 10B**). Serum from sG<sub>HeV</sub> glycoprotein or sG<sub>NiV</sub> glycoprotein immunized mice potently inhibited fusion (IC<sub>50</sub> dilution 1:2220 and 1:650, respectively) mediated by the envelope glycoproteins of the henipavirus species from which the immunogen was derived (homotypic G glycoprotein) and comparatively, less efficiently inhibited fusion (IC<sub>50</sub> dilution 1:150 and 1:80, respectively) mediated by mediated by the envelope glycoproteins of the alternate henipavirus species from which the immunogen was derived (heterotypic G glycoprotein).

Additional analysis was performed to evaluate the diversity and conservation of the epitopes targeted during the humoral response. Clarified lysate material was prepared from cells infected with WT vaccinia virus (vWR) or recombinant vaccinia virus encoding HeV G glycoprotein (vKB2) or NiV G glycoprotein (vKB6). Antisera from all mice bound native and denatured glycoprotein in immunoprecipitation and Western blot

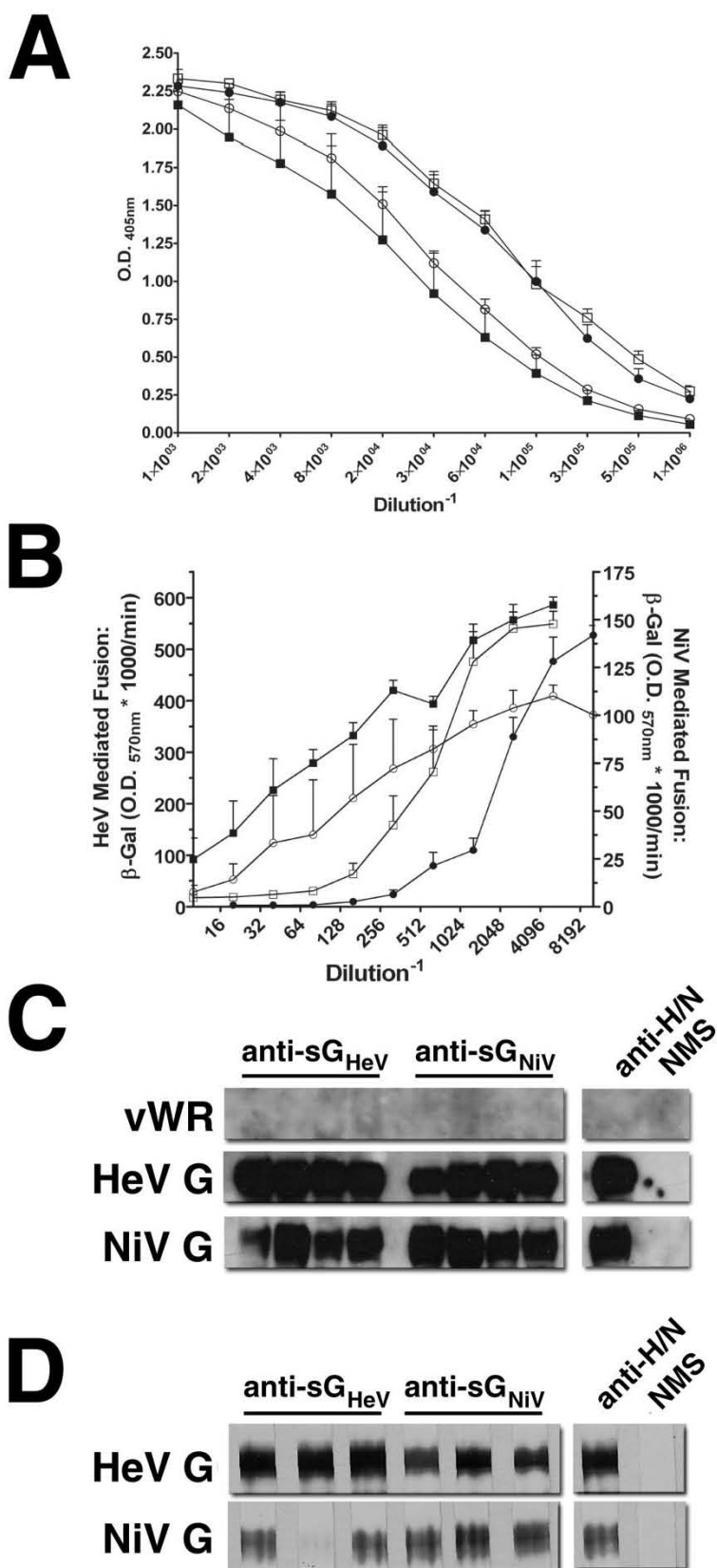
**Figure 9. Diagram of the immunization of mice with sG glycoprotein.**

Diagram showing the schedule of procedures for each of the mice immunized with the henipavirus sG glycoprotein antigens. Briefly, mice were immunized with Ribi adjuvant prepared with 10-15  $\mu$ g sG<sub>HeV</sub> glycoprotein (6 mice), sG<sub>NiV</sub> glycoprotein (4 mice), or both glycoprotein antigens (2 mice) at 28 day intervals and mice were given 10-15  $\mu$ g of sG glycoprotein antigen in PBS 7 days following the 3<sup>rd</sup> immunization. Three days following the final injection, a homogeneous suspension of splenocytes harvested from immunized mice was prepared for PEG-mediated fusion with Sp2/0 cells. Whole blood was collected from mice prior to the first immunization, 7 days following the second immunization, and at the time the animal was sacrificed. The serum fraction was collected by standard techniques and stored at -70°C until characterization.



**Figure 10. Polyclonal humoral response among mice immunized with purified henipavirus sG.**

(A) Serial dilutions of antiserum from mice immunized with sG<sub>HeV</sub> glycoprotein (squares) or sG<sub>NiV</sub> glycoprotein (circles) were prepared in BSA/PBST and analyzed by ELISA using plates coated with either sG<sub>HeV</sub> glycoprotein (open symbols) or sG<sub>NiV</sub> glycoprotein (closed symbols). The mean absorbance (405nm) was calculated for each serum dilution repeated in triplicate. (B) Inhibition of HeV (open symbols) or NiV (closed symbols) glycoprotein-mediated membrane fusion. Reactivity of antisera with WT G glycoprotein by (C) immunoprecipitation or (D) Western blot. Normal mouse sera (NMS) and polyclonal sera (Poly<sub>m</sub>) from mice immunized with sG<sub>HeV</sub> glycoprotein and boosted with sG<sub>NiV</sub> glycoprotein were included to demonstrate the specificity of the analyses.



assays (**Figure 10C and 10D**), respectively, indicating the humoral response recognizes diverse henipavirus G glycoprotein epitopes. Again, the antisera reacted most strongly with the homotypic G glycoprotein and less well with heterotypic G glycoprotein. Together, these results demonstrate the soluble constructs retained antigenic traits of the native glycoprotein and suggest there is considerable conservation of the antigenic structure among the henipaviruses.

#### *Generating the library of mAb-secreting hybridomas*

Splenocytes harvested from sG glycoprotein immunized mice were hybridized with Sp2/0 cells (murine myeloma) using standard practices. Hybridomas were plated in 96-well microtiter plates at limiting dilution and grown in HAT-supplemented selective growth medium. Supernatant from each well was screened for sG glycoprotein specific antibody by ELISA and colonies from positive wells were cloned by limiting dilution at least twice more. In summary, I isolated 27 stable hybridoma cell lines secreting mAb specific for the sG glycoproteins (mAbs and characteristics detailed in **Appendix A** and **Appendix B**). Of these, 14 hybridoma cell lines were derived from mice immunized with sG<sub>HeV</sub> glycoprotein and 13 from mice immunized with sG<sub>NiV</sub> glycoprotein.

#### *Identification of neutralizing mAbs*

To identify fusion inhibitory mAbs, supernatant harvested from each clonal hybridoma cell line was titrated in the surrogate viral glycoprotein-mediated membrane fusion assay. Reduced  $\beta$ -Gal activity was detected following addition of supernatant from 12 (6 anti-sG<sub>HeV</sub> glycoprotein and 6 anti-sG<sub>NiV</sub> glycoprotein) hybridoma lines. Linear regression analysis was used to estimate the 50% inhibitory concentration (IC<sub>50</sub>) and 95% confidence interval (95% CI) of the estimate from the titration curve of purified

preparations of each inhibitory mAb (**Table 4**). The  $IC_{50}$  varied extensively among the mAbs, from potent inhibitors nAH1.3 and hAH6.3 ( $IC_{50}$  0.5 and 0.73  $\mu$ g/ml respectively) to less potent inhibitory mAbs nAH7.3 and nAH10.1 ( $IC_{50}$  5.81 and 8.34  $\mu$ g/ml respectively). Consistently, the neutralizing efficacy was greatest when assayed with the homotypic G glycoprotein species and weakest with the heterotypic G glycoprotein species. Not surprisingly, when assayed with the heterotypic G glycoprotein species, the least effective mAbs, nAH7.3, nAH10.1, and nAH22.4, were not able to completely inhibit fusion at mAb concentrations as high as 200  $\mu$ g/ml.

Purified mAb was prepared from two hybridoma cell lines, mAbs hAH1.3 and hAH2.1, and was added to media containing either HeV or NiV to measure the neutralizing effects of each mAb with live virus. The HeV G glycoprotein-specific mAb hAH1.3 potently inhibited HeV infection of Vero cell monolayers and did not inhibit NiV infection at concentrations less than 200  $\mu$ g/ml (**Figure 11**). In addition, the non-neutralizing mAb hAH2.1 did not inhibit either HeV or NiV infection of Vero cell monolayers (at concentrations up to 100  $\mu$ g/ml). These results are consistent with the pattern of inhibition observed with the surrogate viral glycoprotein-mediated membrane fusion assay.

#### *Characterization of neutralizing mAbs*

Reactivity of the neutralizing mAbs with the henipavirus immunogens was quantified by ELISA to compare the conservation of the targeted epitopes between the henipavirus species. These analyses revealed 3 anti-sG<sub>HeV</sub> glycoprotein mAbs (hAH6.3, hAH11.2, and hAH14.2) and 4 anti-sG<sub>NiV</sub> glycoprotein mAbs (nAH1.3, nAH7.3, and nAH10.1) which bound both the homo- and heterotypic immunogens (**Figure 12A**). The



**Table 4. MAb inhibition of viral glycoprotein-mediated membrane fusion.<sup>a</sup>**

mAb <sup>b</sup>	HeV <sup>c</sup>		NiV <sup>c</sup>	
	IC <sub>50</sub>	(95% CI)	IC <sub>50</sub>	(95% CI)
hAH1.3	2.21	(1.72, 2.84)	--	
hAH5.1	1.59	(1.37, 1.84)	--	
hAH6.3	0.73	(0.51, 1.04)	1.49	(1.28, 1.73)
hAH8.2	1.70	(1.31, 2.20)	--	
hAH11.2	2.16	(1.78, 2.62)	3.84	(2.83, 5.20)
hAH14.2	1.79	(1.51, 2.12)	>100 <sup>d</sup>	
nAH1.3	1.15	(0.96, 1.34)	0.50	(0.43, 0.58)
nAH2.1	--		2.57	(1.65, 3.98)
nAH3.4	--		0.80	(0.68, 0.93)
nAH7.3	>100 <sup>d</sup>		5.81	(2.37, 14.25)
nAH10.1	>100 <sup>d</sup>		8.34	(7.35, 9.50)
nAH22.4	>100 <sup>d</sup>		1.24	(0.94, 1.63)
m102.4	2.07	(1.21, 3.55)	0.52	(0.49, 0.55)

<sup>a</sup> HeLa-USU cells expressing the homotypic HeV or NiV envelope glycoproteins mixed with Vero cells.

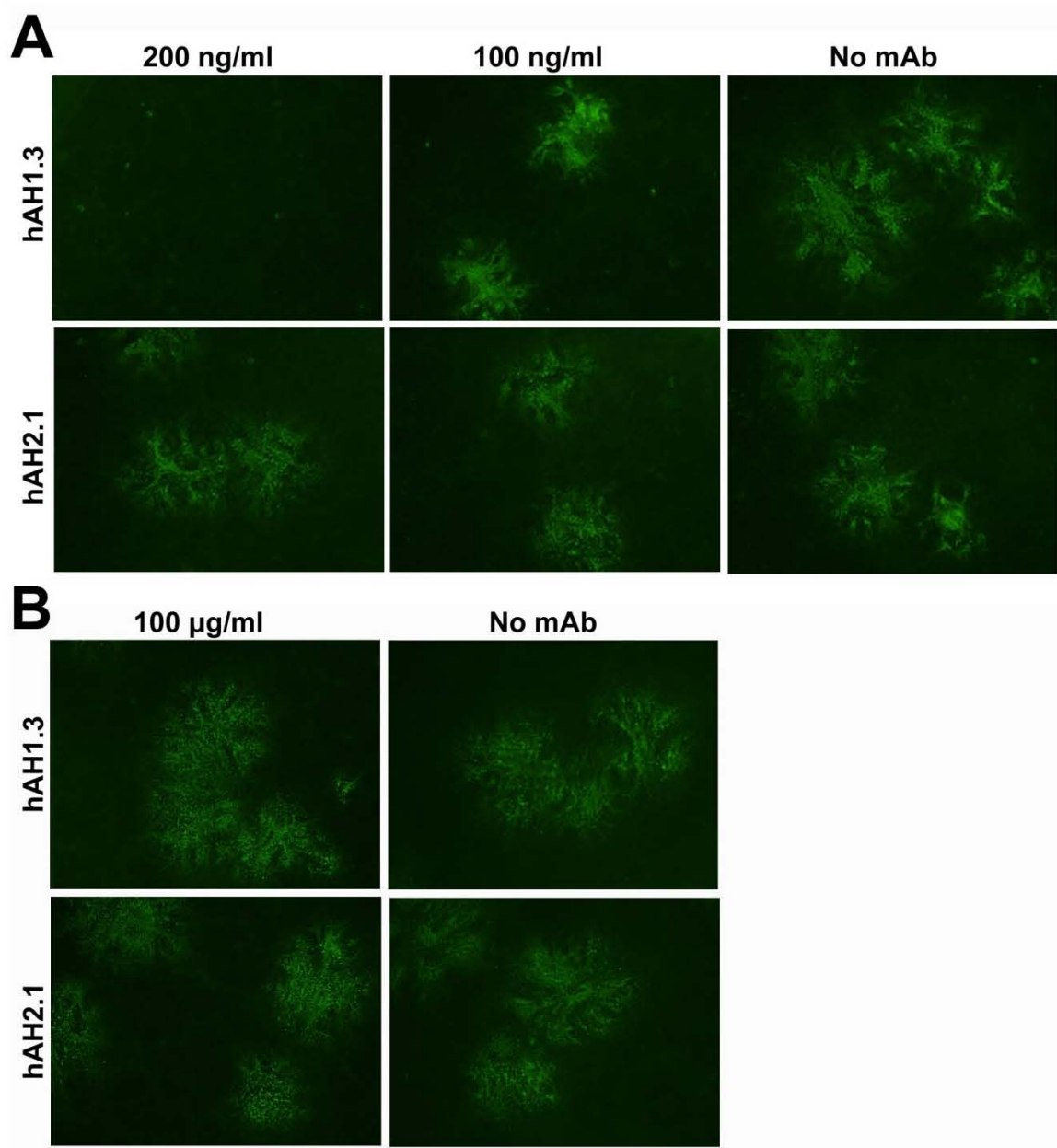
<sup>b</sup> Virus neutralizing mAb derived from mice immunized with either sG<sub>HeV</sub> glycoprotein (hAHX.X) or sG<sub>NiV</sub> glycoprotein (nAHX.X).

<sup>c</sup> The 50% Inhibitory concentration (μg/ml) and 95% confidence interval (95% CI) estimated by multivariate regression.

<sup>d</sup> The IC<sub>50</sub> could not be determined (maximum inhibition is not achieved at mAb concentrations ≤200 μg/ml)

**Figure 11. Inhibition of HeV- and NiV- entry by mAb hAH1.3.**

The mAbs hAH1.3 and hAH2.1 were diluted in EMEM-10 (100  $\mu$ l)  $1.5 \times 10^3$  TCID<sub>50</sub>/ml or  $7.5 \times 10^2$  TCID<sub>50</sub>/ml of HeV (A) or NiV (B), respectively. After 30 minutes, the virus/mAb inoculum was added to Vero cell monolayers and cultured at 37°C. After 24 hours, monolayers were fixed in methanol and expression of the viral P protein was detected with a mouse anti-P-FITC mAb. Stained monolayers were imaged with an Olympus IX71 inverted microscope coupled to an Olympus DP70 high resolution color camera.



**Figure 12. Neutralizing mAb reactivity with soluble and full-length recombinant G.**

(A) Neutralizing mAbs (200 ng) were diluted in BSA/PBST and added to microtiter plates coated with sG<sub>HeV</sub> glycoprotein (closed bars) and sG<sub>NiV</sub> glycoprotein (open bars). The plates were washed and incubated for 1 hr in BSA/PBST containing goat anti-mouse-HRP antibody (1:10,000) at 37°C. Peroxidase activity was estimated with ABTS as the mean absorbance (405 nm) of 3 repeats for each mAb. (B) Clarified lysates of HeLa-USU cells infected with vWR or recombinant vaccinia expressing HeV G glycoprotein or NiV G glycoprotein was incubated overnight at 4°C with mAb (2 µg). Protein G Sepharose beads (70 µl) were added to each sample and rotated for 45 min at 25°C. Precipitated sample material was separated by electrophoresis prior to western blot with polyclonal rabbit anti-sG glycoprotein and goat anti-rabbit-HRP (both diluted to 1:20,000). Blots were imaged with WestPico chemiluminescent substrate and Kodak XAR film.



mAbs were titrated by ELISA to compare the relative antigen avidity (**Table 5**).

Consistent with the previous data, the cross-reactive neutralizing mAbs bound homotypic G glycoprotein with greater avidity than the heterotypic G glycoprotein immunogen.

Comparatively, mAb nAH1.3 exhibited the strongest avidity for both antigens while mAbs nAH7.3 and nAH10.1 exhibited weak avidity for both henipavirus immunogens.

In all cases strength of mAb binding strongly correlated with the relative neutralizing potency of each mAb.

The resistance of the targeted epitopes to denaturing and reducing agents was explored by ELISA. The immunogens were treated with 0.25% SDS, 100 mM of  $\beta$ -mercaptoethanol (BME), or boiled for 10 min and added to microtiter plates. As shown in **Table 5**, the panel of neutralizing mAbs targeted conformational epitopes susceptible to both heat and mild SDS treatment; although the epitope(s) targeted by mAbs derived from sG<sub>HeV</sub> glycoprotein immunized mice were more resistant to mild treatment with SDS. In addition, treatment of the purified protein with a strong reducing agent disrupted the structure of target epitopes and inhibited mAb recognition. These results indicate the mAbs target conformation-dependent epitopes maintained structurally by the network of disulfide-linkages in the globular head of the G glycoprotein.

Native full-length and soluble G recombinant glycoproteins were precipitated with the neutralizing mAbs to compare the antigenic structure of the recombinant forms. The mAb precipitation results were consistent with the observed reactivities by ELISA and similar with both the full-length and soluble constructs (**Figure 12B**). Interestingly, mAbs hAH6.3 and hAH14.2 bound well to sG<sub>HeV</sub> glycoprotein and sG<sub>NiV</sub> glycoprotein in

**Table 5. Characteristics of neutralizing mAbs and the target epitopes of the sG glycoprotein.**

mAb	HC <sup>a</sup>	LC <sup>b</sup>	% Reduction <sup>c</sup>			sG <sub>HeV</sub> (μg/ml) <sup>d</sup>			sG <sub>NiV</sub> (μg/ml) <sup>d</sup>		
			SDS	Heat	BME	Max	50% Max	Min	Max	50% Max	Min
hAH1.3	G <sub>1</sub>	κ	23	98	98	0.125	0.010	0.001	--	--	--
hAH5.1	G <sub>1</sub>	κ	7	98	86	0.125	0.012	0.001	--	--	--
hAH6.3	G <sub>1</sub>	κ	11	93	90	0.125	0.009	5.0 x 10 <sup>-4</sup>	0.250	0.031	0.003
hAH8.2	G <sub>1</sub>	κ	11	97	90	0.200	0.015	0.001	--	--	--
hAH11.2	G <sub>1</sub>	κ	21	99	96	0.005	0.005	5.0 x 10 <sup>-7</sup>	0.500	0.005	3.0 x 10 <sup>-4</sup>
hAH14.2	G <sub>1</sub>	κ	13	98	87	0.100	0.100	9.5 x 10 <sup>-4</sup>	> 1.0	--	0.031
nAH1.3	G <sub>1</sub>	κ	97	98	97	0.008	1.3 x 10 <sup>-4</sup>	2.0 x 10 <sup>-6</sup>	0.008	7.0 x 10 <sup>-5</sup>	5.0 x 10 <sup>-7</sup>
nAH2.1	G <sub>1</sub>	κ	97	98	98	--	--	--	0.060	0.013	0.002
nAH3.4	G <sub>2b</sub>	κ	95	99	80	--	--	--	0.063	0.009	0.002
nAH7.3	G <sub>1</sub>	κ	99	99	97	2.0	0.200	0.016	0.125	0.013	0.002
nAH10.1	G <sub>1</sub>	κ	95	98	97	> 10.0	--	0.001	0.013	8.0 x 10 <sup>-5</sup>	2.0 x 10 <sup>-6</sup>
nAH22.4	G <sub>2a</sub>	κ	97	100	93	1.0	0.045	0.004	0.030	0.007	0.002

<sup>a</sup> Heavy chain<sup>b</sup> Light chain<sup>c</sup> Reduction (%) of antibody binding to the immunogen [(ABS<sub>405nm</sub> Untreated - ABS<sub>405nm</sub> treated)/ ABS<sub>405nm</sub> Untreated]\*100. Prior to coating, sG glycoprotein was treated with 0.25% SDS (SDS); boiled for 10 minutes (Heat); or 100 mM 2-mercaptoethanol (BME).<sup>d</sup> Concentration of mAb (μg/ml) corresponding to the maximum (Max), mid- (50% Max), and minimum (Min) point.

ELISA, but precipitated the full-length antigen less efficiently. These disparity of mAb hAH6.3 and hAH14.2 binding with sG glycoprotein and WT G glycoprotein observed here may result from differences in antigen preparation and/or artifacts of the different assays, although another supposition based on these observations is that the epitopes targeted by mAbs hAH6.3 and hAH14.2 may be partially hidden in the WT G glycoprotein and more exposed in the soluble constructs.

*Competitive-binding analysis of neutralizing mAbs*

Limited information is available comparing the anti-henipavirus G glycoprotein neutralizing mAbs reported from different studies. As a result, it is not possible to determine the number of independent neutralizing antigenic sites on the G glycoprotein represented among the panels of virus neutralizing anti-G glycoprotein mAbs. Here, competitive-binding ELISA test was developed to determine the number of competitive antigenic groups represented among the mAbs developed here as well as the 3 human mAbs (m101, m102.4, and m106.3) and 4 murine mAbs (3A5.D2, 8H4, 17A5, and H2.1) previously described (157, 169). Competition among pairs of mAbs was established as a greater than 25% reduction in the mean ELISA absorbance. Due to the potential for allosteric binding effects, a determination of competitiveness here required a reduction in mean absorbance regardless of the order of addition of the mAbs. That is, the specific interaction of one mAb may induce structural changes in the sG glycoprotein that, when first incubated with the sG glycoprotein, could influence the interaction of the sG glycoprotein with a non-competitive mAb added subsequently. Therefore, similar competitive binding effects, measured as a decrease in the mean absorbance, must be



measured with sG glycoprotein regardless of the order of the addition of mAb pairs during the course of the assay.

Competitive-binding analyses revealed the neutralizing mAbs targeted 7 distinct antigenic sites (**Figure 13**), which we have here termed antigenic sites I thru VII. These competitive binding analyses revealed that the virus neutralizing antibodies nAH3.4 and 8H4 were the only mAbs among the panel which bound antigenic sites I and IV, respectively. Multiple mAbs targeted each of the remaining 5 antigenic sites, as follows: epitope II (mAbs hAH5.1, hAH14.2, and hAH11.2), epitope III (mAbs hAH6.3 and m106.3), epitope V (mAbs 17A5, H2.1, and nAH1.3), epitope VI (mAbs m101, m102.4, nAH2.1, nAH7.3, nAH10.1, and nAH22.4), and epitope VII (mAbs hAH1.3 and 3A5.D2). Moreover, cross-reactive neutralizing mAbs bound 4 antigenic sites suggesting the sites were conserved between the henipavirus species. Antigenic site VI was bound by 6 of the 18 mAbs included in these analyses suggesting site VI may be an immunodominant epitope.

#### *Antigenicity of the receptor-binding domain*

The recent resolution of the sG<sub>NiV</sub> glycoprotein crystal structure in complex with ephrinB3 revealed the receptor-binding domain (RBD) is composed of a wide docking rim on the outermost face of the globular head ( $\beta_4$  and  $\beta_5$  regions) and a binding pocket formed by the  $\beta_{56}L$  and  $\beta_{6L23}$  loops (162). Previously, the human mAbs m102.4 and m101 were found to block or displace the receptor binding and disrupt virus attachment. Given the large expanse of the receptor docking region, mAbs targeting epitopes distinct from the region targeted by m101 and m102.4 (antigenic site VI) could also inhibit receptor binding (162). Prior incubation of the G glycoprotein with soluble viral

**Figure 13. Competitive-binding assays indicated the collection of neutralizing mAbs targeted 7 antigenic sites of the henipavirus G glycoprotein.**

Microtiter plates coated with 25 ng of purified sG<sub>HeV</sub> glycoprotein (A) or sG<sub>NiV</sub> glycoprotein (B) were incubated with a solution containing unlabeled competitive mAb (250 ng) at 4°C. The solution was removed the following day and replaced with a solution containing biotinylated mAb (25 ng) for 1 hr at 25°C. Finally, the plates were washed and incubated in a solution containing avidin-HRP (1:5,000) for 1 hour at 37°C. Peroxidase activity was quantified using ABTS substrate and the mean absorbance (405nm) was calculated. Included in these analyses are the mAbs derived from mice immunized with sG glycoprotein (reported here) as well as the human (m101, 102.4, and m106.3) and murine mAbs (3A5.D2, 8H4, 17A5, and H2.1) described previously (157, 169). The percent inhibition was estimated as:  $[(\text{absorbance}_{\text{no competition}} - \text{absorbance}_{\text{competitive mAb}}) / \text{absorbance}_{\text{no competition}}] \times 100$ . The % inhibition is represented as: - ( $\leq 25\%$ ), + ( $>25\%$  and  $\leq 50\%$ ), ++ ( $>50\%$  and  $\leq 75\%$ ), or +++ ( $>75\%$  inhibition).

**A**

	hAH1.3	hAH5.1	hAH6.3	hAH8.2	hAH11.2	hAH14.2	m101	m102.4	m106.3	3A5.D2	8H4	17A5	H2.1
hAH1.3	+++	—	—	—	—	—	—	—	—	+++	—	+	—
hAH5.1		+++	—	+++	+++	+++	—	—	—	—	—	—	—
hAH6.3			+++	—	—	—	—	—	+++	—	—	—	—
hAH8.2				+++	+++	+++	—	—	—	—	—	—	—
hAH11.2					+++	++	—	—	—	—	—	—	—
hAH14.2						+++	—	—	—	—	—	—	—
nAH1.3	—	—	—	—	—	—	—			—		—	
nAH7.3	—	—	—	—	—	—	+++			—		—	
nAH10.1	—	—	—	—	—	—	++			—		—	
nAH22.4	—	—	—	—	—	—	+++			—		—	

**B**

	nAH1.3	nAH2.1	nAH3.4	nAH7.3	nAH10.1	nAH22.4	m102.4	m106.3	8H4	H2.1
nAH1.3	+++	—	—	—	—	—	—	—	—	+++
nAH2.1		+++	—	—	++	+	+++	—	—	—
nAH3.4			+++	—	—	—	—	—	—	—
nAH7.3				+++	+	++	+++	—	—	—
nAH10.1					+++	++	++	—	—	—
nAH22.4						+++	+++	—	—	—
hAH6.3		nAH2.1	nAH3.4							
hAH11.2		—	—							
hAH14.2		—	—							

receptor reduced the precipitation of the G glycoprotein by 6 biotinylated mAbs: nAH2.1, nAH7.3, nAH10.1, nAH22.4, m101, and m102.4 (**Figure 14A and 14B**). All of the mAbs that were unable to precipitate the G glycoprotein in the presence of receptor targeted antigenic site VI, suggesting the RBD for ephrinB2 and -B3 consists of a single overlapping conformational site similar in both henipavirus species. Interestingly, the majority of neutralizing mAbs derived from sG<sub>HeV</sub> glycoprotein immunized mice did not target the RBD while the majority of neutralizing mAbs derived from sG<sub>NiV</sub> glycoprotein immunized mice inhibited binding with or displaced the viral receptor.

Incubation of G glycoprotein with sEphrinB3 reduced mAb binding only among antibodies of low avidity (such as mAbs nAH2.1, nAH7.3 and nAH10.1) indicating sEphrinB3 bound the G glycoprotein weakly (**Figure 14A and 14B**). Virus neutralizing mAbs derived from mice immunized with sG<sub>HeV</sub> glycoprotein bound the sG<sub>HeV</sub> glycoprotein well in ELISA assays and competition was not observed with either viral receptor (ephrinB2 or -B3) indicating the observed effects were not avidity related and the virus neutralizing mAbs targeted epitopes not directly associated with the RBD.

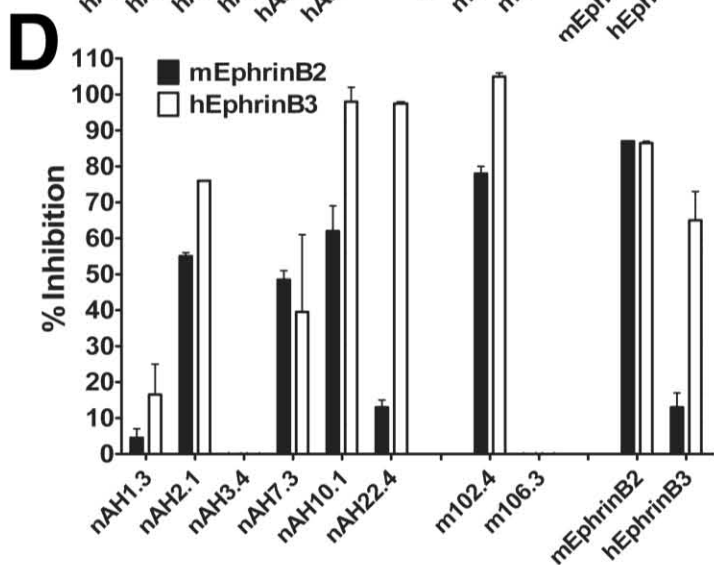
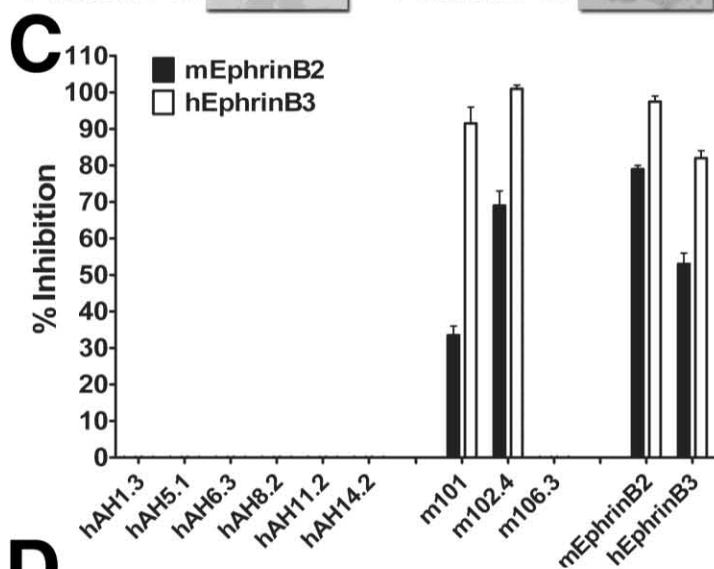
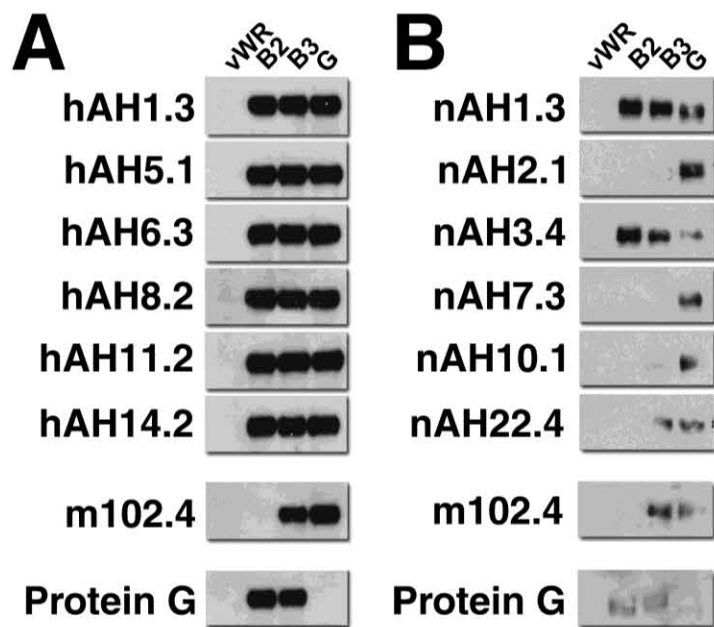
To partially circumvent avidity-associated effects, the competitive-binding ELISA was modified by maintaining the reaction at lower temperature (4°C) and shortening the final incubation period (40 min). The pattern of competitive binding was similar to that observed by immunoprecipitation; however, competition with both viral receptors was observed with all mAbs targeting antigenic site VI (**Figure 14C and 14D**).

#### *Model of the virus neutralizing henipavirus G glycoprotein antigenic sites*

Competitive-binding assays revealed the current collection of neutralizing mAbs target 7 antigenic sites in the ectodomain of the henipavirus G glycoprotein, including 4

**Figure 14. Neutralizing mAbs that block ephrinB2 and -B3 targeted a single antigenic site.**

Clarified lysate prepared from cells infected with vaccinia virus expressing HeV G (A) or NiV G (B) was incubated with sEphrinB2 or sEphrinB3 (1  $\mu$ g) overnight at 4°C followed by biotinylated mAb (0.5  $\mu$ g) for 45 min at 25°C. Subsequently, the samples were incubated with avidin D- agarose beads and precipitated. The material was then processed for SDS-PAGE and detected in Western blot analysis using rabbit antiserum. Shown is mAb precipitation of vWR lysate (vWR), G glycoprotein incubated with sEphrinB2 (B2), G glycoprotein incubated with sEphrinB3 (B3), and G glycoprotein in the absence of receptor (G). The competitive-binding ELISA assays were performed essentially as in figure 13. Briefly, microtiter plates coated with sG<sub>HeV</sub> (C) or sG<sub>NiV</sub> (D) were incubated with mAb prior to addition of biotinylated recombinant sEphrinB2/Fc (closed bars) or sEphrinB3/Fc (open bars). Receptor binding was quantified using avidin-HRP (1:5,000) with ABTS substrate.



common or cross-reactive and 3 HeV- or NiV-specific antigenic sites (**Figure 15**).

Furthermore, the neutralizing mAbs targeted 6 antigenic sites of HeV G glycoprotein and 5 of NiV G glycoprotein. However, given the extensive structural and functional homology between the henipaviruses it is probable that analogous antigenic sites exist for each of the virus-specific sites in the alternate henipavirus species. In fact, White *et al.* found mAb 8H4 inhibited HeV entry only, although we observed the mAb bound sG<sub>NiV</sub> glycoprotein at higher concentrations suggesting the differences observed in virus neutralization may result from differences in the binding specificity due to moderate divergence in the polypeptide sequence.

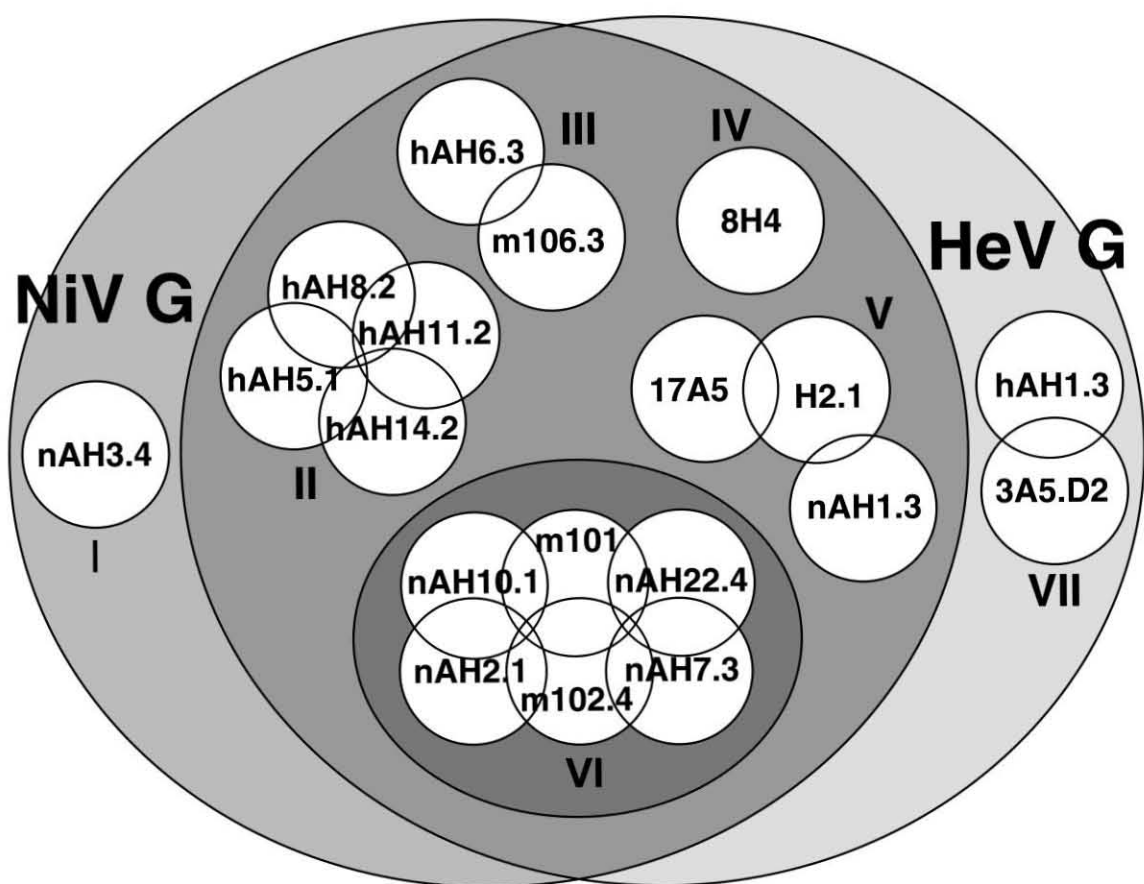
Under BSL-4 conditions, White *et al.* isolated virus mutants that escape neutralization by mAbs 3A5.D2, 8H4, 17A5, and H2.1 and then sequenced the coding region of the G glycoprotein to identify differences in the polypeptide sequence important to the neutralizing activity (157). Now, comparison of these mutated residues with the resolved crystal structure indicates the antigenic sites IV, V, and VII lie primarily within loops  $\beta_2L_{34}$ ,  $\beta_{61}L/\beta_5L_{12}/\beta_6L_{12}$ , and  $\beta_3L_{23}$ , respectively (157). Together, these results are consistent with some initial evidence that suggested the antigenic sites of the G glycoprotein would lie principally in the loops connecting  $\beta$ -strands in the globular head.

The henipavirus RBD consists of a single, and probably immunodominant, antigenic site targeted by neutralizing mAbs. The antigenic data confirm ephrinB2 and –B3 bind a single and overlapping conformational site that is common to both henipavirus species. Notably, the collection of neutralizing mAbs analyzed here target 6 distinct and additional antigenic sites not associated with receptor binding. Moreover, as

**Figure 15. Venn diagram of the henipavirus G glycoprotein antigenic sites.**

Neutralizing mAb targeted 7 antigenic sites (I through VII). Of the 7 sites, 4 antigenic sites were common to both henipavirus species, 6 antigenic sites present on the HeV G glycoprotein, and 5 antigenic sites found on the NiV G glycoprotein. Receptor (B class ephrin)-blocking virus neutralizing mAbs target a single conformational antigenic site (smaller central gray circle, VI) common to both species of the henipavirus G glycoprotein. Overlapping circles indicate competition between mAb pairs and the large circles indicate the target henipavirus (HeV G glycoprotein or NiV G glycoprotein) species.





the henipavirus G glycoprotein lacks both hemagglutinin and neuraminidase activities, these mAbs likely inhibit viral entry by a novel mechanism(s).

## Discussion

Although mice are resistant to henipavirus infection and disease, the murine model provided a convenient method to study the host humoral response to the G glycoprotein. Further, defining the protective antigenic sites in the G glycoprotein will aid in the structural and functional modeling of the G glycoprotein. Moreover, examination of the protective humoral response assists in evaluating vaccines and in potentially developing novel therapeutics for the henipaviruses. Therefore, I sought to characterize the humoral response in mice immunized with sG<sub>HeV</sub> glycoprotein and sG<sub>NiV</sub> glycoprotein with particular focus on detailing the neutralizing antibody response and repertoire.

Immunization of mice with recombinant sG glycoprotein derived from either virus generates a substantial and diverse polyclonal response. In addition, mice respond similarly to both viral antigens with significant cross-reactivity to the heterotypic viral antigen. Polyclonal serum binds both native and denatured viral glycoprotein, clearly demonstrating the humoral response to the sG glycoprotein is diverse, targeting conformation-dependent and -independent epitopes. These results demonstrate the antigenic structure of recombinant sG glycoprotein is quite similar to the native WT viral antigen found on virions or virus-infected cells further supporting the use of either soluble construct as a potential vaccine candidate. Indeed, immunization of cats with a sG<sub>HeV</sub> glycoprotein subunit vaccine has been demonstrated to completely protect against NiV -associated disease and mortality (99, 110).

Viral glycoprotein-mediated membrane fusion assays provide a surrogate for quantifying fusion under varying conditions when studies with live virus are impractical. While the magnitude of membrane fusion is often more robust than with virus, membrane fusion assays consistently exhibit proportional relationships to entry assays with virus. Although it was shown that serum from sG glycoprotein immunized mice inhibited fusion, the humoral response to sG<sub>HeV</sub> glycoprotein could more potently inhibit fusion with the heterotypic henipavirus antigen than antiserum from sG<sub>NiV</sub> glycoprotein immunized mice. However, and of greater significance, the extensive epitope conservation does suggest a univalent recombinant protein vaccine based on the HeV G glycoprotein may protect against morbidity or mortality associated with all known henipavirus isolates.

Molecular characterization of the henipavirus G glycoprotein has advanced significantly following the identification of the viral receptors ephrinB2 and -B3 as well as resolution of the crystal structures of sG<sub>NiV</sub> glycoprotein and sG<sub>HeV</sub> glycoprotein alone and in complex with receptor (20, 162), and Xu and Nikolov, personal communication). Defining the antigenic structure of the henipavirus G glycoprotein will compliment available information describing attachment and triggering the F glycoprotein-mediated membrane fusion process. Here we generated and characterized a panel of 27 henipavirus G glycoprotein-specific mAbs that target a diverse array epitopes. Among these mAbs, 12 antibodies inhibit henipavirus glycoprotein-mediated fusion and bind 7 distinct neutralizing epitopes.

Interestingly, additional characterization revealed neutralizing mAbs targeting only 1 of the 7 antigenic sites reduced receptor binding. Moreover, competitive-binding

assays are identical for both ephrinB2 and -B3 among mAbs that likely target the RBD, in agreement with the previous biochemical and structural characterization of the RBD. Taken together, these data clearly indicate both viral receptors target a single overlapping binding domain. In addition, competitive binding was identical for both HeV G glycoprotein and NiV G glycoprotein confirming the RBD is similar for both viral antigens.

It was also interesting that the neutralizing murine mAbs which block receptor binding exhibited the weakest avidity among all neutralizing antibodies studied. One speculation here would be that the structural composition of the RBD might augment viral resistance to antibody neutralization. The crystal structures of sG<sub>NiV</sub> glycoprotein in complex with sEphrinB2 or with sEphrinB3 indicate that receptor engagement does induce some induced fit interactions. The strongest site of interaction is found within the binding pocket comprised of multiple residues, including residues A558, Q559, E571, Y580, I581, and I588 (20, 21, 162). In addition, Xu *et al.* reported an outer binding groove mediating a weak interaction with sEphrinB3 (162). Strong neutralizing mAb binding to the RBD likely requires a distended variable loop, similar to potently neutralizing mAb m102.4 that inserts in the binding pocket mimicking the G-H loop of the B class ephrin molecules (169), Xu and Nikolov, personal communication). In comparison to human antibodies, the complementary determining region (CDR)-H3 loop of the Ig molecule is smaller, on average, among murine antibodies (78, 132). These species differences in antibody structure could limit the capacity the henipavirus sG glycoprotein immunogen to elicit murine antibodies with loop structure similar to the G-

H loop of the viral receptor or the human mAb m102.4 and, therefore, potentially limit antibody avidity.

Precipitation of WT G glycoprotein clearly demonstrates extensive antigenic conservation between the recombinant soluble constructs and native glycoprotein. This significant conservation of the antigenic structure indicates the soluble antigens are effective surrogates for studying the gross conformational structure of the glycoprotein.

Consistent with the description of neutralizing mAbs targeting other paramyxoviruses, the protective epitopes targeted by the host humoral response to henipavirus G glycoprotein are conformation-dependent. In addition, treatment of the viral antigen with reducing agents prevented mAb recognition of the viral antigen suggesting the disulfide linkages significantly contribute to maintaining the overall antigenic structure of the G glycoprotein. A reasonable speculation here is that the binding of neutralizing mAbs to functional sites may disrupt the conformation and/or alter the post-receptor-engagement sequence of events that lead to an inhibition of the activation of F glycoprotein-mediated membrane fusion.

Here, I describe the identification of multiple additional protective antigenic sites and characterize the relationships among a large panel of neutralizing mAbs. The majority of the mAbs isolated here bound epitopes common to both viral antigens indicating that the henipaviruses share significant antigenic homology. Depending on the henipavirus species, the strength of binding and inhibitory efficiency varies among the mAbs, but all cross-reactive mAbs inhibit hetero- and homotypic viral entry to some degree. Conservation of neutralizing determinants among the henipavirus G glycoproteins suggests the viruses contain homologous functional domains.

Not unexpectedly, the inhibitory effect of each of the mAbs was directly proportional to the antibody avidity observed by ELISA. While the majority of mAbs were cross-reactive, most neutralizing mAbs exhibited the strongest avidity and inhibitory activity against the homotypic immunizing viral antigen. However, several potent neutralizing mAbs strongly bound both viral antigens, specifically hAH6.3 and nAH1.3. Of particular note, neither mAb hAH6.3 nor nAH1.3 appears to target the RBD of the G glycoprotein. Further, mAb nAH1.3, a potent cross-neutralizing mAb inhibits henipavirus envelope glycoprotein mediated fusion at slightly lower concentrations of mAb than the most potent neutralizing mAb reported to date (mAb m102.4).

Surprisingly, neutralizing murine and human mAbs target six antigenic sites distinct from the receptor binding domain. Moreover, the lack of neuraminidase activity in the G glycoprotein suggests the mAbs inhibit the viral entry process by an uncharacterized/novel mechanism(s). Although the virus neutralizing mAbs may disrupt the entry process by steric hindrance during the attachment phase of the virus replication cycle, the neutralizing mAbs could alternatively target antigenic sites correlated with post-receptor binding functional domains of the G glycoprotein. However, the nature and contribution of such potential post-receptor binding functional domains of the G glycoprotein in triggering F glycoprotein activation remain unknown. Additional characterization with purified fAb fragments of these virus neutralizing mAbs could help demonstrate the mAbs do not sterically hinder the attachment of the virus to the host cell. Furthermore, more extensive characterization of the targeted protective antigenic sites may yield additional molecular and biochemical information about the G glycoprotein which would aid in refining the model of paramyxovirus class I viral fusion.

To date, the panel of mAbs described here is the most extensive and diverse collection of neutralizing mAbs to any henipavirus glycoprotein and has facilitated extensive evaluation of the henipavirus antigenic structure. However, the failure to isolate multiple neutralizing mAbs to each antigenic site suggests the panel, although large, may not be complete and additional more esoteric protective antigenic determinants of the G glycoprotein remain to be discovered. In addition, the extensive genetic and structural identity between HeV G glycoprotein and NiV G glycoprotein suggest epitopes targeted by type specific mAbs (antigenic sites I, IV, and VII) have analogous protective antigenic sites in the heterotypic viral antigen. At these sites, mAb specificity for a single viral antigen is probably the result of greater sequence variation and additional neutralizing henipavirus mAbs are necessary to complete the model of the antigenic structure.

Recognition of novel protective antigenic sites affords additional targets for therapeutic intervention, such as passive antibody therapy or small molecule inhibitors. Administration of mAb m102.4 to ferrets following a lethal challenge with NiV is protective (18). Potentially, the humanization of mAbs to additional antigenic sites could fortify passive antibody treatment and reduce the development of antibody-neutralization escape variants. Finally, these data clearly demonstrate immunization with recombinant soluble G glycoprotein generates a robust polyclonal B cell response to multiple protective targets. Identification of novel determinants of the G glycoprotein correlated with protection strengthens the vaccine competency and increases the likelihood that a monovalent subunit vaccine can protect against variant henipavirus species.

## **Chapter 4: Receptor induced changes in the antigenic structure of henipavirus G.**

### **Introduction**

Among paramyxoviruses, the attachment glycoprotein plays a critical role in initiating the membrane fusion process between the virion and target cell.

Conformational changes in the F glycoprotein that mediate membrane merger are irreversible and, therefore, must be tightly regulated by the attachment glycoprotein to maintain virus infectivity. Co-immunoprecipitation experiments have revealed that the F glycoprotein and its homotypic partner attachment glycoprotein are associated prior to virus attachment and entry, possibly by non-covalent interactions in the stalk and/or the  $\beta$ 2 sheet of the attachment glycoprotein (40, 102, 142, 143, 148, 150). Further, catalysis of membrane fusion requires the co-expression of homotypic or highly related paramyxovirus envelope glycoproteins (84). However, the region of the F glycoprotein that associates with an attachment glycoprotein in any paramyxovirus system has not been well defined. Several studies have shown that mutations in the globular head or stalk can inhibit fusion, without affecting ligand binding (89, 103, 145).

Current models of paramyxovirus fusion posit that receptor-binding alters the structure of the attachment glycoprotein resulting in the activation of the F glycoprotein to initiate the F glycoprotein mediated membrane merger process. Crennell *et al.* observed structural changes in the outer face of the NDV HN glycoprotein in the presence of sialic acid (37, 146). However, a similar phenomenon was not seen with the crystal structures of the HN derived from another paramyxovirus that utilizes sialic acid moieties on receptors (166). Whereas, as discussed earlier, interaction with the protein



ligand, sEphrinB3, induced only minor changes in the binding pocket of sG<sub>NiV</sub> (162). Although, it seems unlikely that the very minor structural changes observed in the NiV G glycoprotein upon receptor binding would be of sufficient magnitude to trigger the F glycoprotein conformational changes leading to fusion, the exact details of the process remain to be determined.

Interestingly, we recently demonstrated that single site (isoleucine to alanine) mutations in a heptad repeat-like structure of the HeV G glycoprotein stalk could completely abate its fusion promoting activity and the co-precipitation of the F/G glycoproteins, while not altering its receptor binding capacity (11). In addition, we identified multiple murine mAbs which bound and precipitated the HeV G glycoprotein stalk mutants better than wild type (WT) G glycoprotein and, similarly, could precipitate WT G glycoprotein to a greater extent in the presence of bound receptor. These data revealed that mutation of isoleucine residues in the stalk of HeV G exposed epitopes in a manner similarly seen in WT G following receptor binding. This report was the first description of conformational changes in a paramyxovirus attachment glycoprotein that uses a protein receptor (HeV G glycoprotein) occurring after receptor engagement. Further, analysis of the mAbs and the conformational changes resulting from receptor binding are incomplete and detailing these changes will aid in a better understanding of the receptor binding and fusion triggering process in paramyxovirus entry.

## Results

### *Conformational and antigenic changes in the henipavirus G glycoprotein following receptor binding*

To study the effect of receptor binding on the conformation of the henipavirus G glycoprotein, we evaluated epitope exposure modulation by precipitation of full-length G glycoprotein using a large panel of 27 murine and 3 human mAbs. Soluble viral receptor (sEphrinB2) was added to aliquots of clarified cell lysate preparations from cells infected with vaccinia virus encoding either HeV or NiV G glycoprotein. Purified mAb was then added to the samples and the complexes were precipitated with Protein G Sepharose beads. Analysis of the precipitates by SDS-PAGE revealed 12 mAbs among the panel differentially precipitate G glycoprotein in the presence or absence of sEphrinB2 binding. Five mAbs (nAH7.3, nAH10.1, nAh22.4, m102.4, and m101) precipitated much less G glycoprotein in the presence of receptor (data not shown). As shown earlier, all 5 of these mAbs form a single competition grouping and can inhibit receptor binding to the G glycoprotein (Hickey and Broder, unpublished). The crystal structure of Fab m102.3 (a light chain shuffled variant of m102 that possesses the identical heavy fragment as m102.4 and only scattered amino acid differences within the light chain) in complex with the G glycoprotein shows that the antibody contains a large loop within the heavy chain that inserts into the binding pocket of the G glycoprotein (Xu, Nikolov, and Broder, unpublished), and only the heavy chain engages the G glycoprotein. Taken together, these results indicate that mAbs that target the receptor binding domain (RBD) inhibit receptor-binding rather than targeting epitopes obscured by receptor-binding induced changes in the molecule.

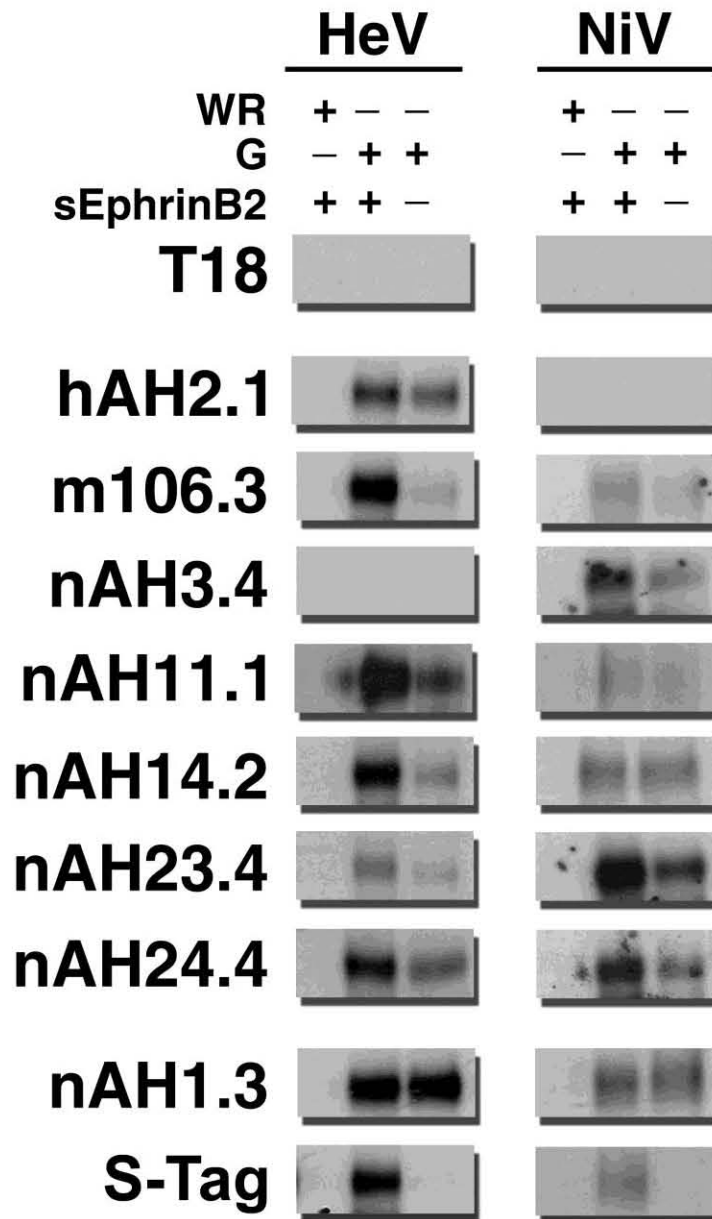
The remaining 7 mAbs tested in this group (hAH2.1, nAH3.4, nAH11.1, nAH14.2, nAH23.4, and nAH24.4) bound and precipitated the G glycoprotein more efficiently in the presence of bound sEphrinB2 receptor (**Figure 16**). The pattern of G glycoprotein precipitation was similar for both HeV and NiV G glycoproteins, although densitometry analysis revealed the ratio of NiV G glycoprotein precipitated by each mAb in the presence of ephrinB2 to the amount of NiV G glycoprotein precipitated by the mAb in the absence of ephrinB2 was slightly attenuated when compared with the similar measure for HeV G (**Table 6**). Further, although mAb hAH2.1 consistently precipitated more HeV G in the presence of ephrinB2 than in the absence of ephrinB2, receptor binding only minimally effected mAb binding with the G glycoprotein when compared with the strong effects of receptor binding observed with mAbs m106.3, nAH3.4, nAH11.1, nAH14.2, and nAH23.4 (**Table 6**). Overall, these data suggest the antigenic structure of both henipavirus G glycoproteins was similarly affected by receptor binding. In comparison, the cross-reactive neutralizing mAb nAH1.3 precipitated equivalent quantities of the G glycoprotein in the presence and absence of receptor (**Figure 16**). Further, characterization of this sub-panel of receptor modulated mAbs may provide new data on the receptor-induced henipavirus fusion process.

#### *Characterization of G glycoprotein specific mAbs*

The binding specificity of each mAb was further examined by ELISA using microtiter plates coated with sG<sub>HeV</sub> glycoprotein, sG<sub>NiV</sub> glycoprotein, or sEphrinB2. Consistent with the results obtained by immunoprecipitation, these analyses revealed that the majority of mAbs bound epitopes conserved between the henipavirus species (**Figure 17**), while mAbs hAH2.1 and nAH3.4 were type specific and reacted only with the

**Figure 16. Immunoprecipitation of HeV and NiV G glycoprotein in the presence and absence of sEphrinB2.**

Clarified lysate material was prepared from HeLa-USU cells infected with WT vaccinia virus (vWR) or recombinant vaccinia virus expressing WT HeV G (vKB2) or WT NiV G (vKB6) cultured in the presence of [ $^{35}\text{S}$ ]- cysteine/methionine. The material was divided equally and incubated overnight with sEphrinB2 at 4°C. Samples were warmed to 37°C for 1 hr and 2 µg of mAb was added to the sample. After 1 hour at 37 °C, Protein G Sepharose beads were added to the samples, incubated 45 min at 25°C and pelleted by centrifugation (400 x g, 5 min). The bead pellets were washed twice with lysis buffer and once with DOC buffer before the samples were boiled for 5 min in LDL sample buffer with BME. Precipitated antigen was analyzed by electrophoresis with 4-12% Bis-Tris NuPAGE gels prior to imaging. The HIV-1 gp120 mAb (T18) was used to demonstrate isotype-specific precipitation and a murine mAb targeting the S-peptide epitope (S-tag) shows sEphrinB2 associated with WT G.



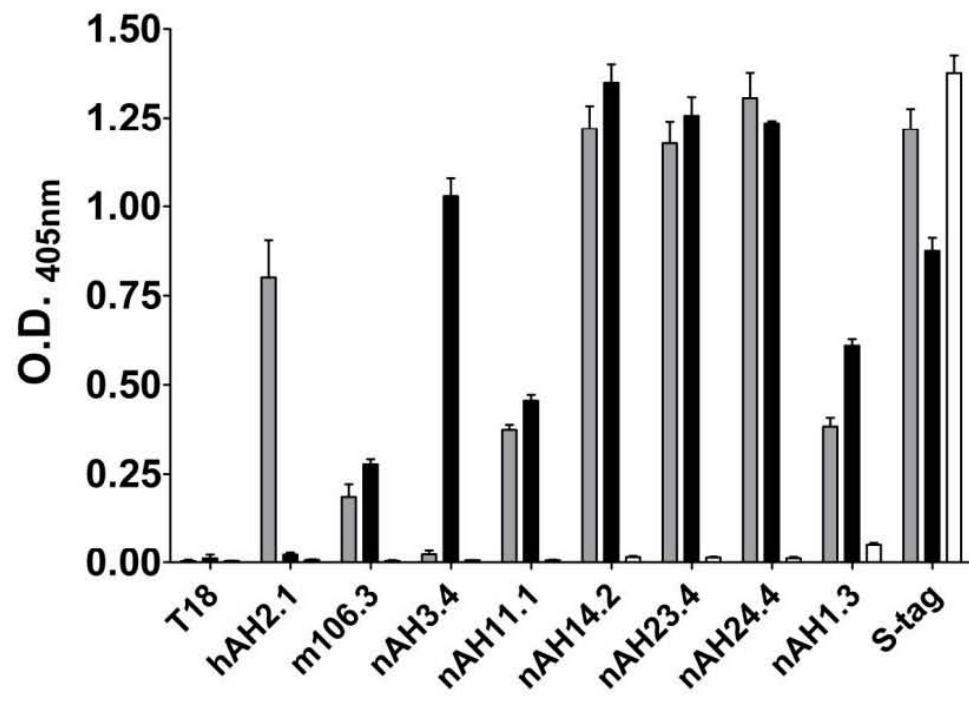
**Table 6. Ratio of G glycoprotein precipitated by each mAb in the presence and absence of ephrinB2.<sup>a</sup>**

mAb	HeV G	NiV G	sG <sub>HeV</sub>	sG <sub>NiV</sub>
hAH2.1	1.3	--	1.1	--
m106.3	6.4	1.5	0.9	0.5
nAH3.4	--	4.6	--	2.0
nAH11.1	2.3	1.9	1.1	0.8
nAH14.2	2.8	1.0	1.4	0.9
nAh23.4	2.4	1.9	1.0	1.0
nAH24.4	1.6	1.2	0.8	1.0

<sup>a</sup> Ratio comparing the normalized quantity of G glycoprotein ( $\text{density}_{\text{sample mAb}} / \text{density}_{\text{nAH1.3}}$ ) precipitated by each mAb in the presence of ephrinB2 with the normalized quantity precipitated by the mAb in the absence of ephrinB2. The density measures were adjusted for the background density measure of each mAb with the lysate material prepared from cells infected with WT vaccinia (vWR).

**Figure 17. The mAb specificity for the henipavirus G glycoprotein.**

The mAb reactivity with sG<sub>HeV</sub> glycoprotein (grey bars), sG<sub>NiV</sub> glycoprotein (black bars), and sEphrinB2, S-tag (open bars) was measured by indirect ELISA. Briefly, mAb (200 ng) diluted in 1% BSA/PBST was added to wells of microtiter plates coated with soluble antigen (50 ng) and blocked with 5% BSA/PBST. Goat anti-mouse-HRP or anti-human-HRP (1:10,000) in 1% BSA/PBST was added and the HRP activity was quantified using ABTS substrate. The absorbance (405nm) was determined and the mean OD of each dilution repeated in triplicate.





immunogen (*i.e.* sG<sub>HeV</sub> glycoprotein and sG<sub>NiV</sub> glycoprotein, respectively) to which each mAb was generated against. In addition, none of the mAbs in the panel interacted with sEphrinB2 demonstrating the mAbs specifically bound only the viral G glycoprotein.

Henipavirus sG glycoproteins were also treated with 0.25% SDS, 100 mM BME, or boiled for 10 min and added to microtiter plates to examine the sensitivity of the epitopes to denaturing and reducing conditions (data not shown). The mAbs hAH2.1, m106.3, nAH3.4, and nAH11.1 were unable to bind the G glycoprotein, and thus appeared to target epitopes susceptible to denaturing and reducing conditions suggesting the epitopes are conformation-dependent and maintained structurally by disulfide bridges and/or secondary structural interactions. Whereas the mAbs nAH14.2, nAH23.4, and nAH24.4 were able to bind denatured and reduced G glycoproteins, indicating the mAbs targeted epitopes which are at least partially linear or conformation-independent.

Interestingly, and of particular note, mAbs nAH3.4 and m106.3 potentially inhibit viral-glycoprotein mediated membrane fusion. Association of neutralizing mAbs with epitopes exposed following attachment suggests the mAbs inhibited fusion downstream of receptor-binding. Potentially, these mAbs interfere with post-attachment conformational steps which are crucial for the activation of the F glycoprotein.

#### *Competitive binding analysis of the G glycoprotein specific mAbs*

Competition analysis among pairs of mAbs was examined to define the number of independent antigenic groups targeted by the panel of mAbs. Competitive-pairs were defined as any two mAbs that exhibited a greater than 25% reduction in the mean ELISA absorbance. In addition, to demonstrate that the mAbs targeted overlapping epitopes and

the observed differences were not the result of allosteric effects, an observed decrease in the mean absorbance was required regardless of the order of addition of the mAbs.

The results of these competitive-binding analyses are shown with sG<sub>HeV</sub> glycoprotein (**Figure 18A**) and sG<sub>NiV</sub> glycoprotein (**Figure 18B**) antigens. Reduction of the mean absorbance was observed only among the mAbs hAH2.1, nAH14.2, nAH23.4, and nAH24.4, defining a single competitive group. The remaining mAbs did not exhibit competitive-binding suggesting mAbs m106.3, nAH3.4, and nAH11.1 target distinct non-overlapping epitopes. In summary, the competitive-binding analyses revealed that the panel of mAbs target 4 distinct antigenic sites (I, III, A, and B) on the G glycoprotein (**Figure 18C**), including the virus-neutralizing antigenic sites I and III as well as non-neutralizing antigenic sites A and B. The mAbs nAH14.2, nAH23.4, and nAH24.4 target a linear conformation-independent epitope while the epitope for hAH2.1 is conformational-dependent. Taken together, these data indicate antigenic site A is a complex epitope consisting both of conformation-dependent and -independent components.

The antigenic sites targeted by the mAbs have not been mapped to a specific region of the G glycoprotein; however, mAbs nAh14.2, nAH23.4, nAH23.4, nAH11.1, and m106.3 do target epitopes common to both HeV and NiV G glycoproteins that are more readily exposed following receptor-binding (1, 11). These results suggest that some structural and functional features of the G glycoprotein are conserved among the henipavirus species. The neutralizing mAb nAH3.4 specifically binds the NiV G glycoprotein and is unique as the only mAb that targets the neutralizing antigenic site I. As indicated previously, further study will be required to identify the target epitope and

**Figure 18. Competitive-binding assays indicate the subset of mAbs target 4**

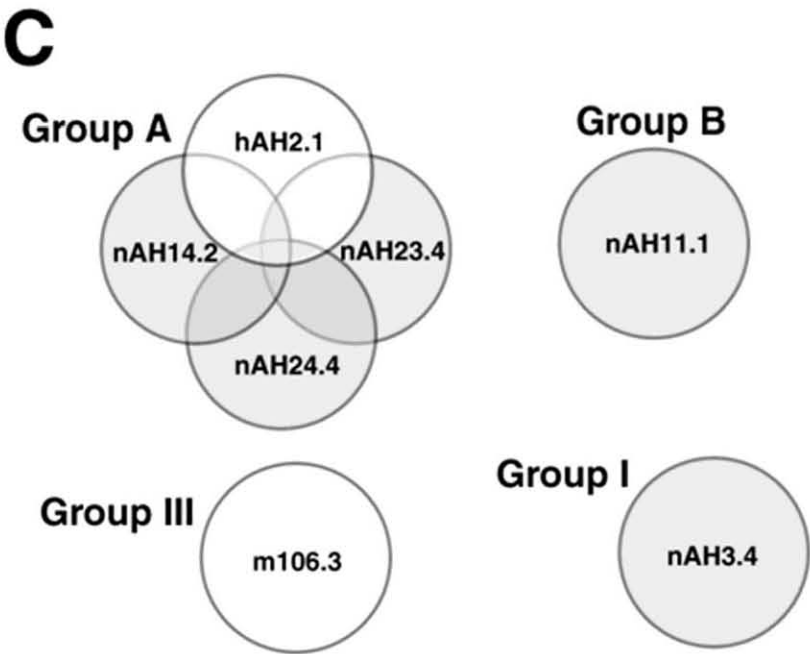
**antigenic sites.** Microtiter plates were coated overnight with 25 ng of purified sG<sub>HeV</sub> glycoprotein (A) or sG<sub>NiV</sub> glycoprotein (B) and blocked in a 5% BSA/PBST solution. Competitive mAb (250 ng) was diluted in 1% BSA/PBST and added to the wells and incubated overnight at 4°C. The competitive mAb was removed from the microtiter plates and biotinylated mAb (25 ng) in 1% BSA/PBST was added to the wells for one hour at 25°C. Bound biotinylated mAb was labeled with HRP conjugated avidin (1:5,000 dilution) in a solution of 1% BSA/PBST for 1 hour at 37°C and detected with ABTS substrate. The percent inhibition was calculated as  $[(\text{absorbance}_{\text{no competition}} - \text{absorbance}_{\text{competitive mAb}}) / \text{absorbance}_{\text{no competition}}] \times 100$ . The % inhibition is represented as: - ( $\leq 25\%$ ), + ( $>25\%$  and  $\leq 50\%$ ), ++ ( $>50\%$  and  $\leq 75\%$ ), or +++ ( $>75\%$  inhibition). (C) Venn diagram of the henipavirus G glycoprotein receptor-binding modulated antigenic sites. The panel of receptor binding modulated mAbs targeted 4 distinct antigenic sites (sites A, B, I, and III), including 2 antigenic sites (A and B) targeted by non-virus neutralizing mAbs as well as 2 antigenic sites (I and III) targeted by virus neutralizing mAbs. Overlapping circles indicate competition between pairs of mAbs derived from animals immunized with sG<sub>HeV</sub> glycoprotein (white circles) and sG<sub>NiV</sub> glycoprotein (grey circles).

**A**

	hAH2.1	m106.3	nAH11.1	nAH14.2	nAH23.4	nAH24.4
hAH2.1	+++	—	—	—	++	++
m106.3		++	—	—	—	—

**B**

	nAH3.4	nAH11.1	nAH14.2	nAH23.4	nAH24.4
nAH3.4	+++	—	—	—	—
nAH11.1		++	—	—	—
nAH14.2			+++	+++	—
nAH23.4				+++	+++
nAH24.4					+++



the features contributing to the species specificity for mAb nAH3.4.





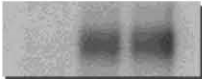



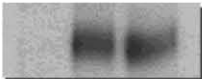

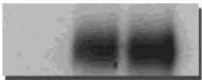
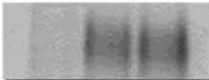




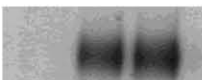

*Antigenic structural analysis of henipavirus sG glycoprotein*

Although comparison of the receptor-bound and -unbound crystal structures of sG<sub>NiV</sub> glycoprotein and sEphrinB3 did not reveal significant conformational changes in the sG<sub>NiV</sub> glycoprotein following receptor-binding (162), recent data suggested interaction with receptor protein could alter the conformation of WT henipavirus G glycoprotein (1, 11). Using the sub-panel of receptor-modulated mAbs identified here, an examination of the antigenic structure of the sG glycoprotein in the presence and absence of sEphrinB2 was carried out.

Interestingly, as shown in **Figure 19**, each of the mAbs precipitated near equivalent quantities of metabolically-labeled sG glycoprotein in the presence or absence of sEphrinB2. The neutralizing mAb nAH3.4 precipitated slightly more sG glycoprotein antigen in the presence of receptor; however, the magnitude of the effect was modulated when compared to the differences observed with WT G glycoprotein (**Figure 19**). Furthermore, densitometry showed the ratio comparing of the amount of G glycoprotein precipitated in the presence and absence of ephrinB2 was nearly equivalent among all of the mAbs suggesting the receptor modulated effects on the antigenic structure of the sG glycoprotein were unapparent (**Table 6**). When compared to the amount of sG glycoprotein precipitated by nAH1.3, all of the mAbs bound a significant portion of the total sG glycoprotein protein present in the absence of sEphrinB2 suggesting the epitopes recognized by the sub-panel were readily exposed on sG glycoprotein, and in sharp contrast to the binding characteristics for WT G glycoprotein (**Figure 16**). Further, these data suggest sG glycoprotein, in the presence or absence of exogenous sEphrinB2,

**Figure 19. EphrinB2 binding did not alter the amount of sG glycoprotein precipitated with the sub-panel of receptor-modulated mAbs.**

Supernatant was harvested from HeLa-USU cells infected with wild type (WT) vaccinia virus (vWR) or recombinant vaccinia virus expressing sG<sub>HeV</sub> glycoprotein (vKB16) and sG<sub>NiV</sub> glycoprotein (vKB22) cultured in media containing [<sup>35</sup>S]-cysteine/methionine and clarified by centrifugation (400 x g for 10 min). The supernatant was divided equally and incubated with sEphrinB2 overnight at 4°C and warmed to 37°C for 1 hr. Subsequently, the samples were incubated with 2 µg of mAb for 1 hour at 37°C and precipitated with Protein G Sepharose beads for 45 min at 25°C. Bead pellets were washed twice with lysis buffer and once with DOC buffer before the samples were boiled for 5 min in LDL sample buffer with BME. The precipitate was analyzed by electrophoresis with 4-12% Bis-Tris NuPAGE gels prior to imaging.

	HeV			NiV		
WR	+	-	-	+	-	-
sG	-	+	+	-	+	+
sEphrinB2	+	+	-	+	+	-
T18						
hAH2.1						
m106.3						
nAH3.4						
nAH11.1						
nAH14.2						
nAH23.4						
nAH24.4						
nAH1.3						

assumes a structure analogous to full-length WT G glycoprotein that is associated with receptor. These data also suggest the cytoplasmic tail and transmembrane domains of the henipavirus G glycoprotein may be necessary to maintain a pre-triggered G glycoprotein structure.

The details of the structural changes occurring in the WT G glycoprotein following receptor-binding are not fully understood. Aguilar *et al.* recently demonstrated that receptor binding induced conformational changes in the epitope targeted by mAb 45 (1). In addition, others have suggested the relationship of the globular heads within a dimer or the oligomeric structure (dimer of dimers) may change following receptor binding (166, 167, and reviewed in 89). Although sG glycoprotein competitively blocks receptor binding and its overall antigenic structure appears very similar to the WT G glycoprotein, examination by sucrose density gradient centrifugation revealed sG glycoprotein predominately form dimers whereas WT G glycoprotein was found, almost exclusively, as a tetramer (16). It is very likely that association of dimer pairs to form the tetrameric complex could obscure epitopes on the WT G glycoprotein that are otherwise readily exposed on dimeric sG glycoprotein. The subtle differences detected in each of the antigenic sites may indicate that receptor binding modifies henipavirus G glycoprotein in alternate manners, including conformation changes in a monomer as well as alterations in its oligomeric form.

#### *Antigenic changes in oligomeric forms of the henipavirus G glycoprotein*

Sucrose density gradient centrifugation has revealed the dimers of HeV G glycoprotein form a mixture of both covalently- and noncovalently associated tetrameric (dimer of dimers) oligomers (16). To examine the antigenic and functional



characteristics of the different oligomeric forms of the G glycoprotein, mAb precipitation analysis of covalently- and noncovalently associated WT G glycoprotein was conducted. Metabolically-labeled WT G glycoprotein pre-incubated with sEphrinB2 or PBS was precipitated with representative mAbs (site A, nAH24.4; site B, nAH11.1; site I, nAH3.4; site III, m106.3) from the sub-panel of receptor-modulated mAbs and compared following SDS-PAGE in the absence of reducing compounds followed by autoradiography.

Precipitation of the WT G glycoprotein with a murine mAb specific for the S-peptide tag fused to the C-terminal end of sEphrinB2 demonstrated the receptor could bind both covalently- and noncovalently associated dimer pairs (**Figure 20**). Moreover, the representative mAbs targeting antigenic sites A, B, I, and III precipitated both covalently- and noncovalently associated dimer pairs of WT G glycoprotein more efficiently in the presence of sEphrinB2 (**Figure 20**). Quantitation by densitometry demonstrated the ratio of G glycoprotein precipitated by the mAbs in the presence and absence of receptor was similar for both the covalently- and non-covalently associated G glycoprotein tetramers suggesting receptor binding had similar effects on both forms of the G glycoprotein (**Table 7**). These data demonstrate that receptor modulates antigenic changes in both covalently- and noncovalently associated pairs of dimers and suggests both oligomeric forms could function during virus attachment and initiation of the F glycoprotein-mediated fusion process.

*Receptor-induced antigenic changes in henipavirus G glycoprotein co-expressed with the F glycoprotein*

Multiple studies have shown that paramyxovirus attachment glycoproteins can

**Figure 20. Precipitation of covalently- and noncovalently associated henipavirus G glycoprotein.**

Clarified cell lysates of metabolically-labeled HeV and NiV G glycoproteins were prepared as before. Equivalent aliquots were incubated overnight with sEphrinB2 and moved to 37°C for 1 hr. Following, representative mAbs (A, nAH24.4; III, nAH3.4; B, nAH11.1; and I, nAH3.4) were added (2 µg) and the samples were held at 37°C for 1 hr prior to the addition of Protein G Sepharose beads. After 45 min at 25°C, the beads were pelleted by centrifugation (400 x g, 5 min) washed twice with lysis buffer and once with DOC buffer. Samples were boiled for 5 min in LDL sample buffer without reducing compounds and analyzed by electrophoresis with 3-8% Tris-Acetate NuPAGE gels prior to imaging. SDS-PAGE analysis of the G glycoprotein under non-reducing conditions was necessary to separately observe the henipavirus G glycoprotein tetrameric oligomer formed by covalently linked dimer pairs (T) and non-covalently associated dimer pairs (D).



**Table 7. Ratio of covalently and non-covalently associated tetramers of the G glycoprotein precipitated by each mAb in the presence and absence of ephrinB2.<sup>a</sup>**

Group	Oligomer <sup>b</sup>	G glycoprotein <sup>c</sup>		G & F glycoprotein <sup>d</sup>	
		HeV	NiV	HeV	NiV
A	T	1.2	2.5	1.7	1.5
	D	1.5	2.1	2.2	1.3
III	T	3.8	1.4	27.3	40.9
	D	3.4	1.3	14.4	67.4
B	T	1.0	7.8	1.5	1.9
	D	1.3	9.1	1.8	1.9
I	T	--	1.8	--	0.6
	D	--	1.5	--	1.1

<sup>a</sup> Ratio comparing the normalized quantity of G glycoprotein ( $\text{density}_{\text{sample mAb}} / \text{density}_{\text{nAH1.3}}$ ) precipitated by each mAb in the presence of ephrinB2 with the normalized quantity precipitated by the mAb in the absence of ephrinB2. The density measures were adjusted for the background density measure of each mAb with the lysate material prepared from cells infected with WT vaccinia (vWR).

<sup>b</sup> Covalently-linked tetramers (T) of the G glycoprotein and tetramers formed by the non-covalent association of a pair of disulfide-linked dimers (D) of the G glycoprotein.

<sup>c</sup> Expression of the full-length G glycoprotein

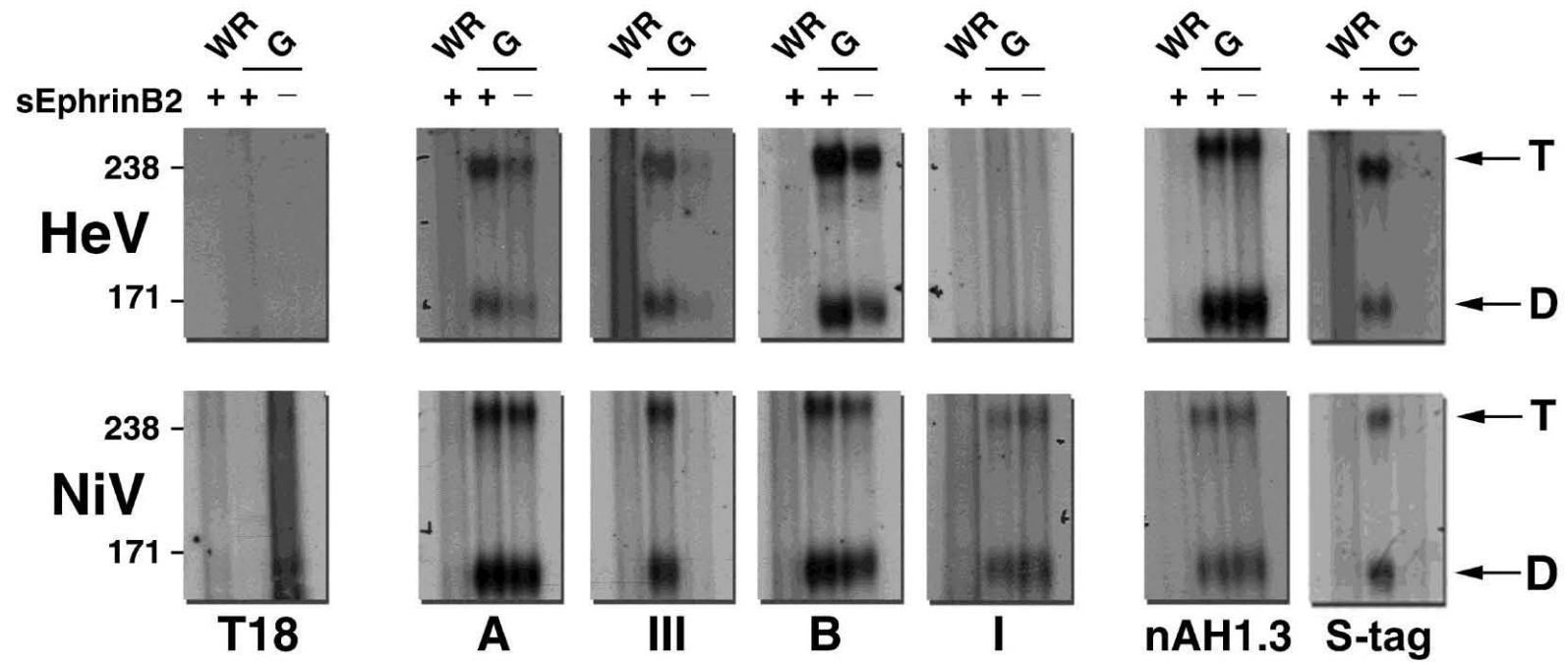
<sup>d</sup> Co-expression of the homotypic viral envelope glycoproteins (F and G glycoproteins)

modulate the activity of the F glycoprotein (reviewed in 76). Co-precipitation of henipavirus F and G glycoproteins demonstrates that the viral envelope glycoproteins associate on the cell surface prior to receptor binding. However, the region(s) or domains of the attachment and fusion glycoproteins that interact have not been well defined. In addition to the dimer of dimer relationship and its influence on epitope exposure following receptor binding just described, mAbs that recognize receptor induced antigenic changes in the G glycoprotein could also potentially target epitopes obscured by the F glycoprotein. To address this possibility, an analysis of the antigenic structure was repeated with metabolically-labeled henipavirus G glycoprotein co-expressed with its homotypic F glycoprotein.

Here, HeLa-USU cells were transfected with a plasmid encoding henipavirus F glycoprotein and subsequently infected with a recombinant vaccinia virus encoding the homotypic G glycoprotein. The cells were then cultured for 16 hours in labeling media followed by media without the <sup>35</sup>S radionucleotide-label for 1.5 hours. Cell lysates were then prepared and clarified by centrifugation. The amount of G glycoprotein precipitated in the presence and absence of sEphrinB2 using the same representative mAbs from the sub-panel of receptor-modulated mAbs was analyzed by SDS-PAGE under non-reducing conditions. These mAbs precipitated the G glycoprotein more efficiently in the presence of sEphrinB2 consistent with previous results (**Figure 21**); indicating that co-expression of the F glycoprotein does not appear to block the antigenic sites (A, B, I, or III) and, furthermore, that the F glycoprotein did not modulate the observed receptor induced alterations of the antigenic structure of WT G glycoprotein. Here, densitometry quantitation revealed the ratio of precipitated G glycoprotein in the presence and absence

**Figure 21. Co-expression of F glycoprotein does not alter mAb precipitation of henipavirus G glycoprotein.**

Clarified lysates were prepared from metabolically-labeled HeLa-USU cells transfected with henipavirus F and subsequently infected with vKB2 or vKB6 encoding HeV G or NiV G, respectively, or control vWR. Lysates were divided equally and incubated overnight with sEphrinB2 at 4°C and warmed to 37°C for 1 hr. Samples were incubated with 2 µg of representative mAbs (A, nAH24.4; III, nAH3.4; B, nAH11.1; and I, nAH3.4) for 1 hour at 37 °C and precipitated with Protein G Sepharose beads for 45 min at 25°C. Pelleted beads were washed twice with lysis buffer and once with DOC buffer before the samples were boiled for 5 min in LDL sample buffer without reducing compounds. Precipitated material was analyzed by electrophoresis using 3-8% Tris-Acetate NuPAGE gels prior to imaging. SDS-PAGE analysis of the G glycoprotein under non-reducing conditions was necessary to separately observe the henipavirus G glycoprotein tetrameric oligomer formed by covalently linked dimer pairs (T) and non-covalently associated dimer pairs (D).



of receptor was similar for both the covalently- and non-covalently associated G glycoprotein tetramers regardless of the co-expression of the F glycoprotein (**Table 7**), although, the effects of receptor binding shown here for antigenic site I were minimal. These data suggest the co-expression of the F glycoprotein did not inhibit structural changes in the G glycoprotein following receptor binding and, further, that receptor binding alone is sufficient to modulate the antigenic structure of the WT G glycoprotein, providing a possible mechanism to relate the F glycoprotein activation with receptor binding and virus attachment.

#### *Model of henipavirus fusion*

The observed changes in the antigenic structure of henipavirus G glycoprotein suggest a model for triggering the activation of the F glycoprotein (see **Figure 22**). The interaction of the G glycoprotein with the viral receptor (ephrinB2 or -B3) on the surface of the host cell initiates conformational and/or oligomeric changes in the G glycoprotein, as measured by modulation of the antigenic structure. Changes observed in covalently-linked dimer pairs of the henipavirus G glycoprotein also suggest that structural changes are not associated with a complete dissociation of dimer pairs, but rather may alter the spatial relationship of one dimer pair to another or between monomeric subunits.

Previously, it was shown the henipavirus G glycoprotein associates with the F glycoprotein on the cell surface prior to receptor binding (11). Furthermore, both co-precipitation of the envelope glycoprotein is only observed when the F glycoprotein is co-expressed with the G glycoprotein in the eukaryotic system (Broder, unpublished); however, the effect of receptor binding modulated activation of the F glycoprotein on the F/G glycoprotein hetero-oligomeric complex has not been conclusively determined.



These structural changes in the globular head of the G glycoprotein alter the association of the henipavirus envelope glycoproteins, promoting F glycoprotein dissociation or directly facilitating those conformational changes associated with F glycoprotein activation leading to F glycoprotein-mediated membrane fusion.

## **Discussion**

The paramyxovirus replication-cycle begins with the fusion of the virion envelope with the host cell membrane allowing the viral nucleoprotein complex to enter the cell. These steps provide an opportunity for intervention prior to virus infection of the host cell and consequently limit the spread of the virus and lower the viral burden within the host. The crystal structures of several paramyxovirus envelope glycoproteins have aided in molecular studies and in the development and refinement of models for membrane fusion. However, many important aspects of the fusion process remain enigmatic, including the post-attachment events promoting the fusogenic activity of the F glycoprotein.

With the exception of highly related species, heterotypic expression of the F glycoprotein and an attachment glycoprotein derived from different paramyxovirus species does not promote fusion suggesting the attachment glycoprotein is directly involved in regulating and triggering the F glycoprotein activation process (89, 106). However, detection of structural changes in the attachment glycoprotein following receptor binding has been difficult and the receptor-induced conformational changes observed in the crystal structures of the attachment glycoprotein have been limited primarily to the globular head and RBD. It seems unlikely that these minor observed changes would be sufficient to generate a triggering process of the F glycoprotein. Thus,

the precise mechanism(s) modulating conformational changes in the F glycoprotein remain ambiguous.

Here it was demonstrated that the antigenic structure of the henipavirus G glycoprotein is altered following receptor binding. The recognition of structural changes in multiple antigenic sites of the WT oligomeric G glycoprotein suggests receptor binding can induce significant alterations in the glycoprotein. Notably, these receptor induced structural changes were not observed with henipavirus sG glycoprotein suggesting the recombinant soluble glycoprotein lacking a TM and CT was not similarly “triggered” by ephrinB2 as observed in WT oligomeric (tetrameric) G glycoprotein. Moreover, it appears that the antigenic structure of the sG glycoprotein is somewhat analogous to the post-attachment (receptor-bound) conformation of WT henipavirus G glycoprotein. Indeed, soluble glycoproteins derived from MeV H, NDV HN, and PIV-5 HN glycoproteins similarly lack the TM and CT that limit protein solubility and also may assume a structure analogous to the post-attachment state of the WT protein. Under these considerations, the crystal structures of soluble attachment glycoproteins in complex with the appropriate ligand may likely not exhibit dramatic differences from the unbound form.

Henipavirus envelope glycoproteins also co-precipitate in the absence of ephrinB2 or -B3 demonstrating that these viral glycoprotein spikes are associated prior to attachment to the host cells. Further, the conformational changes associated with the activation of the F glycoprotein are irreversible and thus must be tightly regulated by the attachment glycoprotein to minimize any spurious or untimely activation of the F glycoprotein and maintain viral infectivity. The observed changes in the antigenic

structure of the G glycoprotein reported here provide a potential mechanism that physically link attachment and receptor binding with F glycoprotein activation. In addition, the co-expression of the F glycoprotein does not modulate receptor induced changes of the G glycoprotein suggesting the triggering mechanism operates in a unidirectional fashion to regulate this process. In addition, the F glycoprotein does not obscure the antigenic sites targeted by the subset of receptor binding modulated mAbs indicating that they do not target regions of the G glycoprotein that may be involved in facilitating the noncovalent association with its F glycoprotein partner.

Aguilar *et al.* reported on a mAb (mAb 45) that bound a conformational epitope in the  $\beta_6S_4$  /  $\beta_1H_1$  region of NiV G which undergoes structural changes induced by receptor binding (1) and is consistent with our results presented here. Mutations in this epitope also affected F/G glycoprotein association and NiV-glycoprotein mediated fusion suggesting the antigenic site appears associated with the structural changes that also promote the activation of conformational changes in the F glycoprotein. The attributes of the epitope targeted by mAb 45 are similar to the attributes of antigenic site III reported here and could indicate that these sites are the same or similar; however, additional studies will be necessary to determine the precise location of each of these sites with the G glycoprotein molecule. The studies here revealed multiple diverse epitopes associated with receptor-induced changes including a linear site targeted by non-neutralizing mAbs. Further studies with these mAbs will be needed to fully characterize the targeted epitopes recognized by these mAbs and to define the nature of the structural changes induced following receptor binding.

Mutation of several isoleucine residues in an HR-like structure of the HeV G glycoprotein stalk induced structural changes promoting a more efficient binding and precipitation by mAbs hAH2.1, nAH23.4, nAH24.4m and m106.3 (11). These data suggest the mutations altered the native structure of the G glycoprotein which exposed the epitopes similarly to that of a post-receptor bound conformation (1, 11). Repeated isoleucine and leucine residues in HR domains are important elements for the formation of coiled-coil structural motifs which facilitate the formation of both homo- and hetero-oligomeric complexes through electrostatic interaction between individual helical strands (reviewed in 81, 96). Disrupting the specific pattern of isoleucine and leucine can alter the hydrophobic faces that contribute to the  $\alpha$ -helices and, therefore, can also disrupt oligomeric structures (42, 81, 96). Expression of the stalk mutants along with HeV F glycoprotein revealed the G glycoprotein mutants did not associate with the F glycoprotein and could not promote F glycoprotein-mediated membrane fusion (11). These results were consistent with the effects (*i.e.* receptor binding and F glycoprotein association) of analogous isoleucine mutations in the stalk of NDV HN glycoprotein (1, 11, 143). However, in contrast, mutations in the HR-like region of the MeV H glycoprotein blocked fusion but did not impede the F/H glycoprotein interaction (36).

Sucrose density gradient centrifugation has revealed oligomeric differences between the WT full-length and soluble versions of the henipavirus G glycoprotein. Interestingly, differences in the antigenic structure between the full-length and soluble G glycoproteins was noted in the absence of receptor, with the sG form of the glycoprotein adopting a post-receptor bound conformation, yet in the absence of bound receptor. Together, these data suggest variation in the oligomeric conformation and/or spatial

arrangement of the G glycoprotein monomer subunits may, at least partially, account for the observed differences in the antigenic structure of the soluble versus WT constructs of the G glycoprotein. Sucrose density gradient analysis revealed that with the I83A, I112A, and I124A G glycoprotein mutants demonstrated a modest decrease in precipitation of noncovalently associated dimer pairs in the highest density fractions (11).

Together, these data suggest that, although the HeV G glycoprotein stalk mutants adopted a post-receptor bound antigenic structure, the mutants retained a tetrameric oligomeric conformation similar to the WT G glycoprotein. In addition, receptor binding induced alterations in the antigenic structure for both covalently and noncovalently associated pairs of dimers demonstrating that the antigenic differences do not appear to be the result of any complete dissociation of dimer pairs within the G glycoprotein tetramer. Rather, it could be that the association of dimers into tetrameric oligomers may constrain the spatial arrangement of individual monomeric G glycoprotein subunits that is later alleviated or modified by receptor-binding.

The observed differences between NDV HN and MeV H glycoproteins, particularly in respect to the interaction between HN/H glycoprotein and the F glycoprotein, prompted Iorio *et al.* to suggest paramyxoviruses may mediate fusion by divergent mechanisms that are influenced by the nature of their respective viral receptor (76). In addition, Iorio *et al.* related the type of receptor with the location of the RBD in the attachment glycoprotein globular head (76). The fusion defective isoleucine mutants of the HeV G glycoprotein discussed earlier did not associate with the F glycoprotein likely as a result of changes in the structure of the  $\alpha$ -helix of the stalk domain resulting from replacement of the isoleucine residues with non-conserved alanine residues.

Collectively, these observations are similar to the proposed model of the NDV HN glycoprotein which binds sialic acid residues. Surprisingly however, the crystal structure of the sG<sub>NiV</sub> glycoprotein revealed that the RBD was located distant to the dimer interface and very similar to the location of the sialic acid binding site on NDV HN glycoprotein. These results suggest the location of the RBD in the globular head may determine the nature and location of the structural changes in the attachment glycoprotein that signal the F glycoprotein to activate. Further, the observation that the HeV G glycoprotein isoleucine stalk mutants and sG glycoprotein assume a post-receptor bound like structure which also does not associate with the F glycoprotein would be consistent with the model whereby a triggering mechanism would induce the dissociation of the F glycoprotein from the tetrameric G glycoprotein complex.

Taken together, here, the most extensive characterization of the structural changes in the henipavirus G glycoprotein induced by interaction with its viral receptor, ephrinB2, is presented. These data suggest a model of G glycoprotein mediated activation of the F glycoprotein that follows a sequential series of steps in the process, which could be further investigated using antibody fragments (Fab) purified following digestion with the papasin cysteine-protease, and may uncover additional targets for therapeutic intervention. Further, these data support the paramyxovirus fusion models that propose a receptor binding event initiates the signals required to activate the F glycoprotein. Although both covalently and noncovalently associated dimer pairs of the G glycoprotein undergo similar antigenic modulation, we were not able to define the nature of the structural changes limiting the inferences that can be made in detailing the mechanism. Additional studies will be necessary to precisely map the location(s) of the observed

antigenic changes and characterize the structural features of each epitope affected by receptor binding. In addition, these analyses underscore the necessity to develop assays that can be used to reliably quantify the activation of the F glycoprotein and to further define and characterize the events preceding the F glycoprotein mediated fusion process in greater detail.

## Chapter 5: Discussion

### Preface

The henipaviruses are emerging paramyxoviruses that possess several characteristics which set them apart from all other members of the family. Foremost among these attributes is the henipaviruses are highly virulent and are broadly tropic often causing fatal disease in many infected mammalian species including humans. Among the important factors contributing to the increased virulence of the henipaviruses, the protein sequence of EphrinB2 and -B3 is highly conserved among mammals and widely expressed within multiple organ systems, including the respiratory system and CNS (reviewed in 45). Furthermore, the henipaviruses have evolved specific mechanisms to evade and/or diminish the host response in humans, including inhibition of the viral beta interferon response and JAK/STAT signaling pathway (reviewed in 47, 135). In addition, the data from recent outbreaks in Bangladesh has revealed that person-to-person aerosol transmission of NiV is possible (62), increasing the likelihood of sustained outbreak episodes of NiV in certain regions of the world.

Nucleic acid sequence analysis has shown that the henipaviruses are most closely related to members of the *Morbillivirus* and *Respirovirus* genera of the paramyxoviruses. The morbilliviruses, like the henipaviruses, can also be associated with neurovirulence and in some cases fatal disease in mammalian hosts. For example, CDV was identified as the etiologic agent of an acute neurologic illness that recently killed an estimated 30% of the population of African lions (*Panthera leo*) in Tanzania and Kenya (128). Most morbilliviruses, including MeV and CDV, target the signaling lymphocyte activation molecule (SLAM) as their host cell protein receptor for binding, a molecule that is



similar among many mammalian species (131). This conservation of the host receptor likely facilitated the repeated transmission events of CDV to lions allowing cross-species transmission and the subsequent epidemic, similar to the emergence of henipaviruses in Malaysia and Australia. These outbreaks of the henipaviruses and CDV demonstrate that species restrictions are not impregnable barriers to the emergence of deadly zoonotic viruses which pose a growing threat to both public and agricultural health. Indeed, the list of recently discovered paramyxoviruses continues to expand emphasizing the continued potential for emergence of novel and sometimes highly virulent viruses.

Paramyxoviruses mediate viral entry by a conserved general mechanism affording an opportunity to identify common points of susceptibility and areas for potentially developing therapeutic intervention strategies. In fact, examination of several crystal structures has revealed significant conformational and functional homologies in both the fusion and attachment envelope glycoproteins. As a result, modeling of the functional or inhibitory components across different virus species may facilitate a more rapid development of effective prophylactic and therapeutic modalities to address these emerging paramyxoviral threats.

The henipavirus G glycoprotein is the dominant viral determinant that is targeted by the host's protective humoral response. The crystal structure of the sG glycoprotein has revealed the protein possesses conformational attributes consistent with the general model of the paramyxovirus attachment glycoproteins, and molecular characterization has shown the antigenic structure of sG glycoprotein is analogous to the native, full-length G glycoprotein. Given the value of mAbs in the molecular characterization of the G glycoprotein and also use as potential therapeutic agents, I sought to develop a panel of

mAbs specific for the henipavirus G glycoprotein and this panel of mAbs was used to define the protective virus neutralizing epitopes on the G glycoprotein and aid in refining the model of henipavirus receptor binding and membrane fusion.

### **Experimental results in the context of the project aims**

Although previous attempts to develop a mouse model of henipavirus infection proved unsuccessful, White *et al.*, showed irradiated non-infectious HeV was immunogenic in mice and isolated 5 neutralizing mAbs from immunized animals (157). In addition, given the robust humoral response to the sG glycoprotein in both rabbits and cats, the immunization of mice with sG glycoprotein was expected to generate a similar robust humoral response targeting a variety of epitopes on the G glycoprotein.

Here, the immunization of mice with henipavirus sG glycoprotein did elicit a strong and diverse polyclonal humoral response. The mice developed high endpoint titers against the sG glycoprotein immunogen as well as against the heterotypic henipavirus sG glycoprotein species. The humoral response was shown to target both conformation-dependent and -independent epitopes and potently inhibited both HeV and NiV glycoprotein-mediated membrane fusion. Although either sG glycoprotein was highly immunogenic in mice, the response was strongest against the immunogen used and slightly less reactive against the heterotypic viral antigen. Together, these results indicated that the sG glycoprotein antigen displays diverse HeV- and NiV-specific and conserved epitopes also present on the native G glycoprotein.

In total, 27 mAbs specific for henipavirus G glycoprotein were isolated. Within this library, 12 mAbs targeted cross-reactive epitopes, 18 targeted conformation-dependent epitopes, and 12 mAbs targeted virus neutralizing epitopes. Beyond the

structural studies of the henipavirus G glycoprotein, the library of mAbs has become an important laboratory and clinical tool set for virus detection, speciation, diagnostic assay development, and may also be a source for the development of potential therapeutics.

Vaccination with sG glycoprotein elicits a strong protective response in experimental animals. The lack of cell-mediated immunity following subunit vaccination suggests the neutralizing antibody response is strongly correlated to resistance to henipavirus infection. Although several groups have reported some neutralizing henipavirus mAbs, the information has been limited and discontinuous. Here, a large panel of neutralizing mAbs composed of novel murine mAbs as well as previously described neutralizing murine and human mAbs reactive to the G glycoprotein was evaluated. Since previous reports have shown that neutralizing hPIV3 HN, NDV HN, MeV H, or Rinderpest virus (RPV) H glycoprotein-specific mAbs target multiple epitopes, I hypothesized that the protective humoral response to henipavirus G glycoprotein would similarly target multiple distinct epitopes. Further, I hypothesized that the neutralizing antigenic sites on the G glycoprotein would be highly conserved among both henipavirus species.

The data has revealed the mAbs from this panel target 6 distinct antigenic sites (I, II, III, V, VI, and VII) while mAb 8H4 targeted an additional antigenic site (site IV) distinct amongst the panel of neutralizing mAbs developed here. White *et al.*, reported neutralizing mAbs 17A5, H2.1, and 8H4 target a discontinuous epitope (157); however, our analysis here has further defined these characteristics showing the mAbs target 2 different yet related epitopes. It is probable that the antigen specificity of these neutralizing mAbs result from minor sequence variation rather than divergent

neutralizing sites among the henipaviruses. For example, the ELISA data suggests mAb 8H4 (targeting site IV) weakly binds the heterotypic NiV G glycoprotein suggesting the weak avidity may account for the failure to neutralize NiV-mediated fusion as previously reported. In addition, we demonstrated 4 of the antigenic sites were common to HeV and NiV G glycoproteins and 3 sites (I, IV, and VII) were defined by mAbs that were specific for either HeV or NiV G glycoprotein.

Although previous reports have shown that neutralizing mAbs target multiple antigenic sites of hPIV-3 HN glycoprotein and MeV H glycoprotein, the mechanism of virus neutralization by non-receptor blocking mAbs has not been thoroughly explored. Interestingly, the crystal structures for the attachment glycoproteins have shown the RBD is composed of a single but distinct conformational site. Although the RBD location and enzymatic activities vary across the lineages of the attachment glycoproteins, the published data to date suggests at least some neutralizing antibodies target analogous regions. From these data, I hypothesized that the neutralizing mAbs would target regions of the henipavirus G glycoprotein that mediate both receptor-binding as well as receptor independent domains.

The adaptation of competitive binding assays demonstrated that the neutralizing mAbs targeting antigenic site VI inhibit both ephrinB2 and -B3 binding suggesting the RBD consists of a single overlapping site conserved among henipaviruses. Interestingly, the majority of the neutralizing mAbs developed here bound and precipitated G glycoprotein at least as well in the presence of the viral receptor and these mAbs target multiple antigenic sites (sites I-V and VII) and inhibit fusion and infection by a novel and as yet uncharacterized mechanism(s).

As discussed earlier, the prevailing models of henipavirus fusion imply receptor binding results in conformational changes in G glycoprotein that trigger F glycoprotein activation. However, the published structural studies to date have not supported these theoretical models. The capacity for mAbs to detect changes in the structure of G glycoprotein makes them well suited to carry out comparisons between the structure of G glycoprotein in complex with and without the viral receptor (ephrinB2 and –B3). The final aim of these studies was to identify and characterize mAbs which could differentially bind native WT henipavirus G glycoprotein following receptor binding as a means of potentially identifying receptor induced structural changes that could be related to the F glycoprotein triggering and fusion process.

Among the entire panel of mAbs, the studies here identified 7 mAbs that could precipitate full-length G glycoprotein better in the presence of bound EphrinB2 receptor. Additional experiments subsequently showed that although receptor binding induced changes in WT G glycoprotein, the antigenic structure of sG glycoprotein did not change when in complex with receptor as measured by mAb binding. Bossart *et al.*, demonstrated the overall structure of sG glycoprotein and WT G glycoprotein were similar (15); however, the sG glycoprotein dimers were much less efficient in forming tetrameric complexes in comparison to WT G glycoprotein. One supposition is the transmembrane and/or cytoplasmic tail of the G glycoprotein are important domains for the interaction of the pairs of dimers and, ultimately, required for the formation and/or stabilization of the G glycoprotein tetrameric complex. Together, these results indicate receptor binding may induce changes in the oligomeric form and/or spatial arrangement of the individual monomeric subunits of the G glycoprotein and these alterations in

structure could play an important role in the model for the activation of F glycoprotein and subsequent membrane fusion process.

Consistent with this hypothesis, a series of competitive-binding assays revealed the mAbs targeted 4 distinct epitopes, 3 of which were common to both HeV and NiV. In addition, these changes were observed among all 4 of these antigenic sites in both the disulfide linked and noncovalently associated dimer pairs of the G glycoprotein. Furthermore, despite evidence suggesting the structure of the F glycoprotein is modulated by the G glycoprotein, a modulatory effect of F glycoprotein on the structure of the G glycoprotein is not known or been considered. The studies here indicate henipavirus F glycoprotein does not alter changes in the antigenic structure of the G glycoprotein following receptor binding and these observed antigenic changes occurred in both disulfide linked and noncovalently associated dimer pairs indicating the antigenic changes occur independent of any involvement of the F glycoprotein. A model of henipavirus fusion showing G-mediated activation of F is depicted in **Figure 22**.

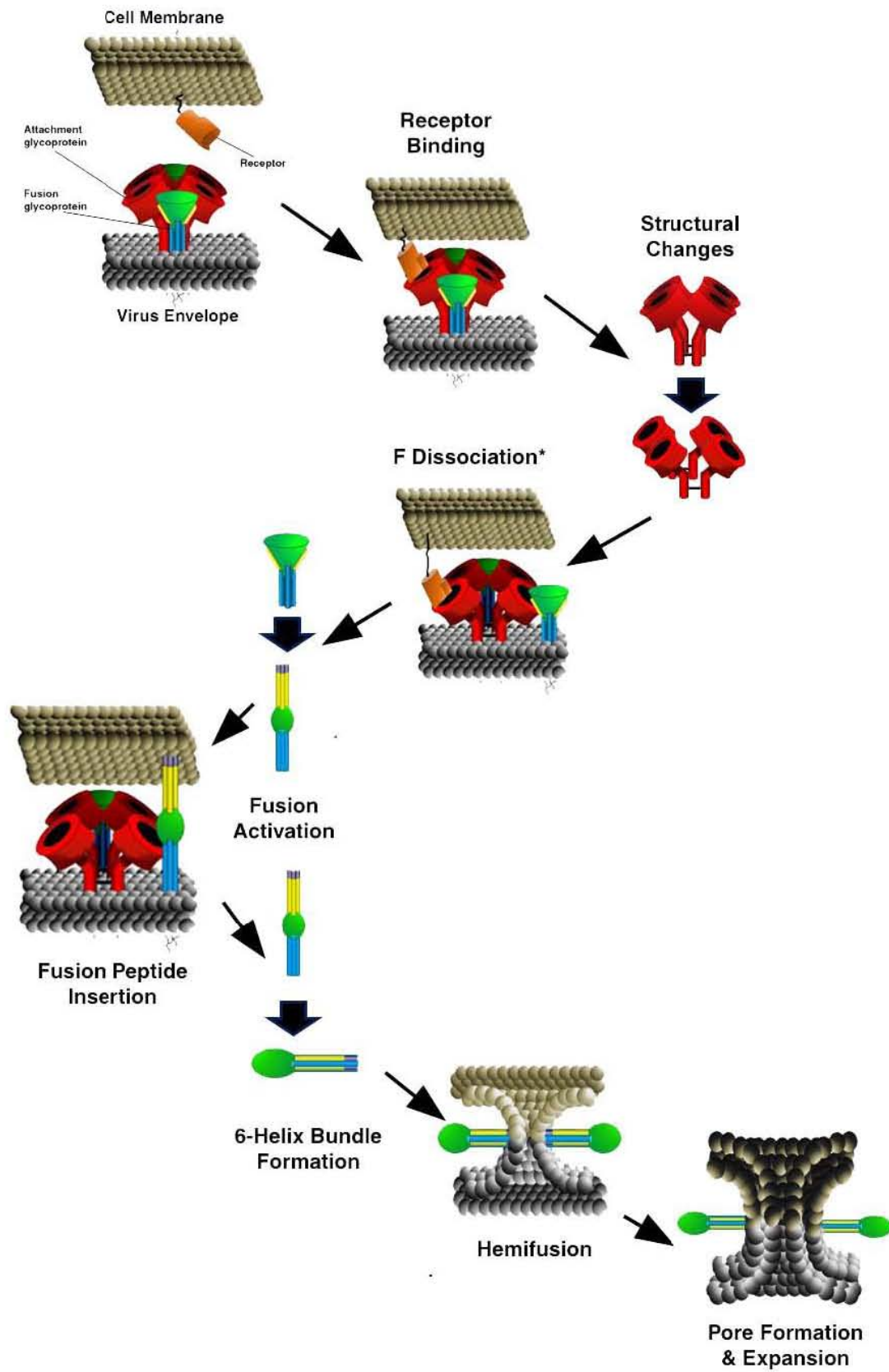
## **Contributions to the study of Paramyxoviruses**

### *Antibody library and assay development*

To date, the large panel of murine mAbs developed here is the largest and most diverse collection of henipavirus specific mAbs reported. The diversity of this mAb panel has provided a significant advantage in identifying and characterizing the structural and functional features of the henipavirus G glycoprotein. In addition, the mAb panel has provided essential tools for several henipavirus studies, including immunogold labeling of virus-like particles, *in situ* staining of virus-infected tissue samples, and FACS analysis

**Figure 22. Model of henipavirus receptor binding and membrane fusion.**

Henipavirus entry and infection begins with viral attachment and receptor engagement mediated by the interaction of the G glycoprotein with the host cell protein, ephrinB2 or -B3. Receptor binding induces structural changes in the G glycoprotein, altering the conformation and/or spatial relationship of the monomers within the G glycoprotein tetramer. These structural changes in the G glycoprotein provide a signal to trigger the dissociation (\*dissociation has not been reproducibly demonstrated) of the F/G glycoprotein hetero-oligomeric complex alleviating the presumed constraints to conformational changes associated with F activation. The hydrophobic F glycoprotein fusion peptide is inserted into the membrane of the target cell and additional conformational changes in the F glycoprotein lead to the formation of the 6-helix bundle structure. This form of the F glycoprotein positions the viral and target cell membranes into close proximity and is presumed to provide the energy needed to merge the viral and host cell membranes facilitating the progression from hemifusion to fusion pore formation. As the fusion pore expands, the contents of the infectious virion, including the viral genetic material, are deposited in the cytoplasm of the host cell initiating the replication phase of the virus replication-cycle.





of surface exposed viral glycoprotein. Some mAbs within the panel are also being used in structural characterization studies with the G glycoprotein to gain insight into the nature of non-receptor blocking or alternative neutralization mechanisms. The mAb panel has also been widely used in the development and validation of diagnostic and serologic assays such as in protein bioplexed luminescent and ELISA protocols employed in studying the epidemiology of henipaviruses in Southeast Asia, Oceania, and portions of Africa. Also, these mAbs have been used to develop an antigen capture ELISA, used to screen urine and fecal samples collected from bats in China and in the development of multivalent microchips for rapid identification of HeV, NiV, or related henipa-like viruses.

*The host virus neutralizing humoral response*

The data represented here is the most extensive characterization of the neutralizing antibody repertoire against the henipaviruses to date and clearly indicate the globular head subunit contains multiple protective antigenic sites. Previous reports concerning the virus-neutralizing response to different paramyxovirus species show minor differences in the number of independent protective antigenic sites targeted in paramyxovirus attachment glycoproteins during the humoral response, which may be related to lineage-specific enzymatic activity. The data here show the neutralizing antigenic structure of the henipavirus G glycoprotein is comparable in many ways with earlier studies suggesting the existence of several protective epitopes in other H glycoprotein and/or HN glycoprotein systems. In addition, our analyses have dramatically extended our current knowledge of the types and characteristics of the neutralizing epitopes of the henipavirus G glycoprotein, providing more details towards a

better understanding of the virus neutralization mechanisms targeting the G glycoprotein and its structure as it relates to the humoral neutralizing response, information which can also be compared to other well-characterized paramyxovirus species.

The B cell epitopes in viral glycoproteins of the *Morbillivirus* genus have been the most extensively characterized to date. Bouche *et al.* describe 8 antigenic sites in the MeV H glycoprotein targeted by neutralizing mAbs (reviewed in 19, 51). These epitopes partially overlap and lie predominantly on the surface of the globular head of the H glycoprotein (51, 72, 109). Additional studies with CDV H glycoprotein and RPV H glycoprotein identified virus neutralizing mAbs targeting 6 distinct antigenic sites (114, 124, 144).

Similar observations have also been reported on the host humoral response to paramyxovirus members possessing an HN attachment glycoprotein. Competitive binding analyses revealed the hPIV-3 HN glycoprotein specific mAbs targeted 5 independent antigenic epitopes (A,B,D, E, and F) and an overlapping antigenic site (C) (reviewed in 82). Of these, virus neutralizing activity was associated only with mAbs specific for antigenic sites A, B, and the overlapping site C (82). In another study, Iorio *et al.* identified 7 overlapping antigenic sites on the NDV HN glycoprotein (74, 75, 77). Among these sites, mAbs targeting 5 of 7 could neutralize NDV (77).

Although the number of neutralizing epitopes identified among these studies varies slightly, all demonstrated that the various neutralizing mAbs targeted a variety of antigenic sites. In addition, these studies revealed the neutralization mechanism of some of these mAbs, such as those associated with various functional activities of the attachment glycoprotein (e.g. receptor binding, hemagglutinating, and neuraminidase

activity) (77). However, the neutralizing mechanism of the majority of mAbs that target attachment glycoproteins has not been investigated.

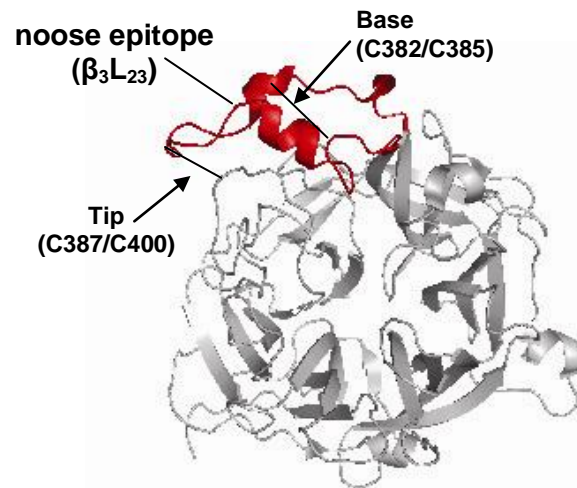
#### *Mechanisms of antibody-mediated virus neutralization*

Determining the virus neutralization mechanism of the various classes of mAbs may provide significant insight towards our understanding of the details of virus attachment, F glycoprotein activation, and the physical processes linking these events. The analysis here is the first to clearly demonstrate that the RBD of the G glycoprotein is composed of a single antigenic site. Information derived from the crystal structures of the henipavirus G glycoprotein has shown that the RBD is located similarly for many paramyxovirinae particularly those that possess an HN glycoprotein suggesting the characteristics of the RBD which elicit a protective response are likely similar. In contrast to the virus neutralizing mAbs which target the RBD, data suggests non-receptor blocking neutralizing mAbs also target poorly characterized antigenic sites in the paramyxovirus attachment glycoprotein species. Further, the henipavirus G glycoprotein lacks both enzymatic activities (i.e. neuraminidase and hemagglutinating activity) and consequently antibodies that bind to other virus neutralizing epitope groups that are independent of receptor binding can inhibit fusion and virus entry by a completely unknown mechanism(s).

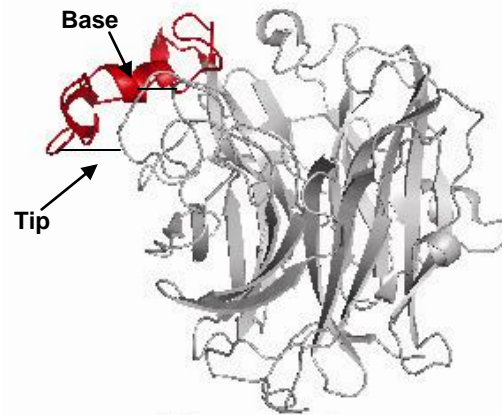
A particular neutralizing mAb described here, hAH1.3, was found to target a large loop of the G glycoprotein that protrudes from the solvent exposed face of the globular head and is formed by 2 disulfide linkages that are critical for antibody binding specificity (**Figure 23**). The disulfide bridges form a noose structure, linking the 2 distal cysteine residues (C382 and C395) near the base, and a disulfide bridge between the

**Figure 23. Ribbon diagram of the henipavirus G noose epitope.**

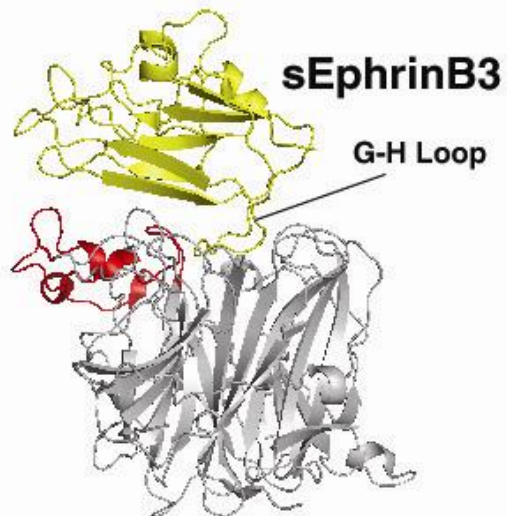
Ribbon diagram depicting the tertiary structure of the sG<sub>NiV</sub> (grey) glycoprotein globular head domain bound to sEphrinB3 (yellow). The noose epitope (red), B<sub>2</sub>L<sub>23</sub>, is a large loop formed by a disulfide bridge (arrows point to lines at the approx location) near the base (base) of the loop and a second bridge connecting the tip of the loop (tip) with a region near the RBD which accepts residues of the G-H loop. Ribbon diagram was created using the crystal structure of NiV G (PDB ID: 3D12) with Pymol software (39, 162).



**Top View**



**Side View**



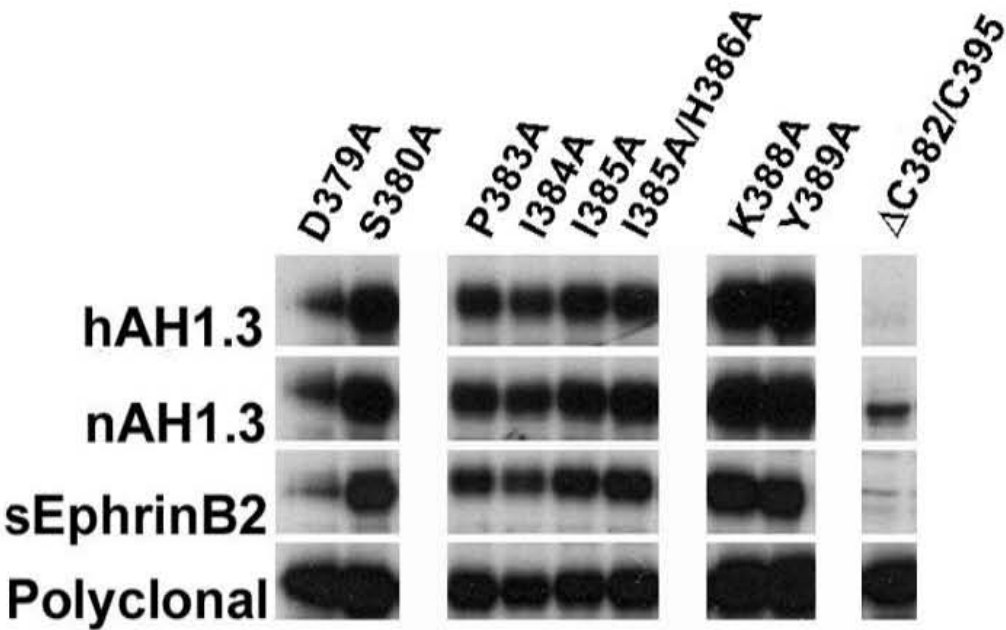
**Side View**

$\beta_3L_{23}$  and  $\beta_{45}L$  (C387 and C400). This structure, commonly referred to as a cysteine noose, is structurally analogous to the  $B_3L_{23}$  region of MeV H glycoprotein and hPIV-3 HN glycoprotein, both of which can be similarly targeted by virus neutralizing mAbs specific for those viral envelope glycoproteins. Cysteine noose domains are commonly involved in protein-protein interactions (90); however, the data here shows that mAb hAH1.3 does not inhibit receptor binding, yet exhibits potent virus neutralizing activity.

The crystal structure of the NiV G glycoprotein in complex with ephrinB3 shows a  $B_3L_{23}/B_{45}L$  disulfide link connecting the protruding loop to regions associated with the RBD. In addition, some of the residues of the loop are found in close proximity to portions of ephrinB3 when bound to the G glycoprotein. A scanning alanine mutagenesis study was carried out on this loop element of the HeV G glycoprotein and showed that most point mutations in the loop region did not greatly impact the antigenic structure of the G glycoprotein nor did they greatly impact receptor binding (**Figure 24**). However, the Y389 mutant (the noose epitope residue which lies closest to ephrinB3 in the crystal structure) promoted fusion to a level nearly 50% less in comparison to WT G glycoprotein when co-expressed with the HeV F glycoprotein (**Figure 25**). In addition, removal of the disulfide-bridges supporting this loop element disrupted receptor binding and fusion promotion activity as well as reduced binding among virus-neutralizing mAbs which specifically target the noose epitope (**Figure 24**). It is possible that mAb hAH1.3 inhibits structural changes in or blocks portions of the G glycoprotein that interact with alternate regions of the receptor following receptor binding. Conservation of the structural and neutralizing attributes of the attachment glycoprotein noose epitope among

**Figure 24. Deletion of cysteine residues forming a disulfide bridge near the base of the HeV G glycoprotein noose epitope disrupts hAH1.3 and receptor binding.**

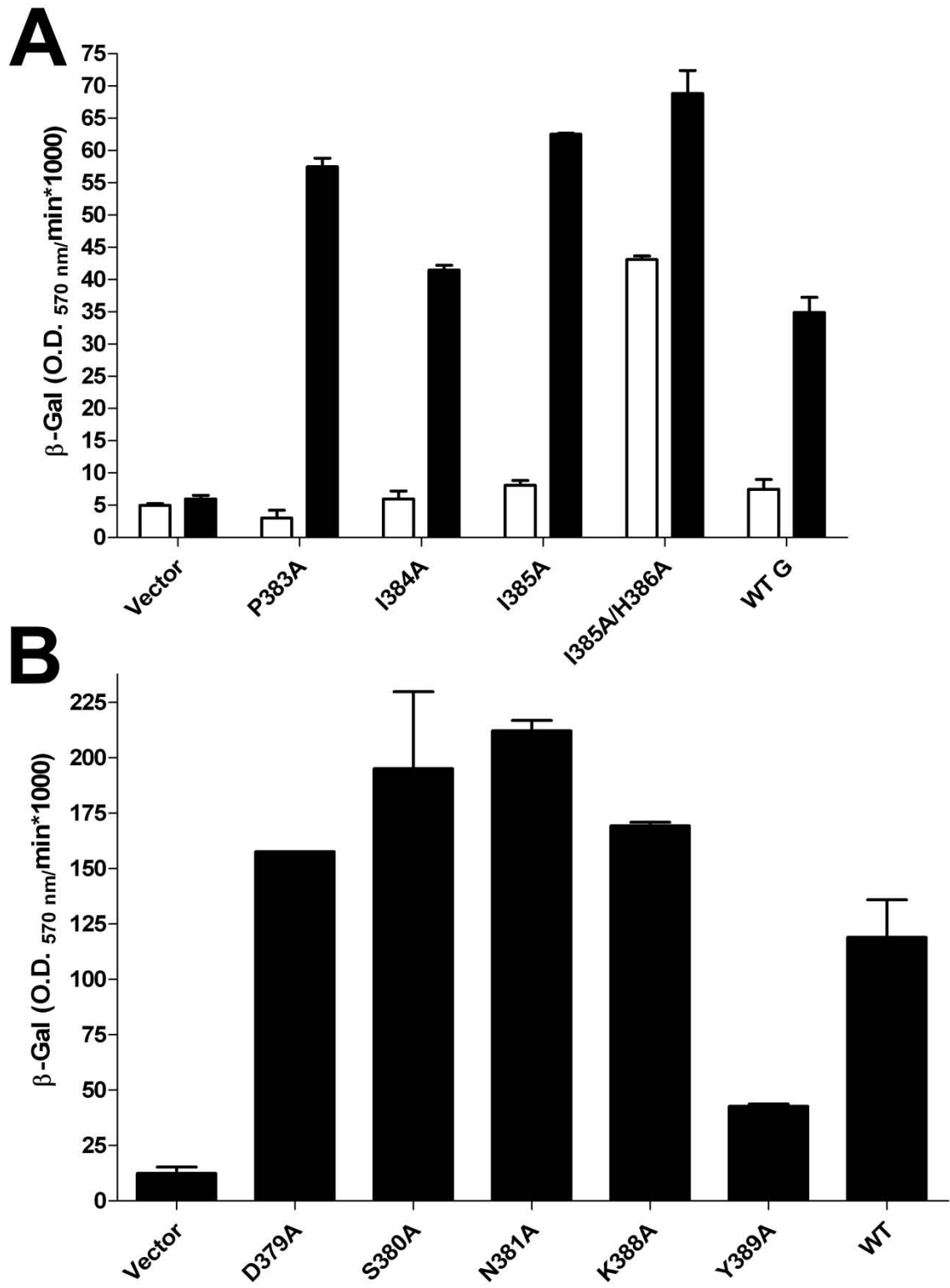
Clarified cell lysates were prepared as previously described and incubated overnight at 4°C with 2 µg of purified protein (mAb or sEphrinB2/Fc) or 2 µl of polyclonal antibody prepared from mice immunized with sG<sub>NiV</sub> glycoprotein. The samples were incubated at 37°C for 45 min with (100 µl) 20% Protein G Sepharose beads and precipitated by centrifugation (400 x g for 5 min). Bead pellets were washed twice with lysis buffer and once with DOC buffer before the samples were boiled for 5 min in LDS sample buffer with BME. The precipitate was analyzed by SDS-PAGE gel electrophoresis prior to imaging. The mAb hAH1.3 targets the noose epitope (antigenic site VII) and mAb nAH1.3 targets a distinct antigenic site (site V).





**Figure 25. Scanning alanine mutations of the HeV G glycoprotein noose epitope disrupt hAH1.3 virus neutralization and the fusogenic promoting activity of the viral envelope glycoproteins.**

HeLa-USU cells were co-transfected with 4  $\mu\text{g}$  of the mammalian expression plasmid vectors encoding the F glycoprotein (2  $\mu\text{g}$ ) as well as the WT or mutant G glycoprotein, as before. Transfected cell monolayers were subsequently infected with vaccinia virus-encoding T7 RNA polymerase and Vero cell monolayers were infected with vaccinia virus encoding  $\beta$ -galactosidase ( $\beta$ -Gal) under the T7 bacteriophage promoter. The cells were incubated overnight at 31°C and subsequently resuspended in DMEM media (1 x 10<sup>6</sup> cells/ml) and 50  $\mu\text{l}$  of the viral glycoprotein expressing HeLa-USU cells were added to 50  $\mu\text{l}$  of the viral receptor expressing 293T cells in a 96 well microtiter plate. The mixed cell populations were incubated for 2.5 hr at 37°C before the addition of Nonidet P-40 alternative to a final concentration of 0.5%.  $\beta$ -Gal activity among aliquots of the cell lysates was quantified with the CPRG substrate using a Versamax microtiter plate reader and the rate of  $\beta$ -Gal activity was calculated as: ([change in optical density at 570 nm per minute] x 1,000). Shown is the  $\beta$ -Gal activity for the G glycoprotein containing mutations in the central region between the C382 and C387 residues (A) incubated with 2  $\mu\text{g/ml}$  mAb hAH1.3 (open bars) or media without mAb (black bars) as well as for the G glycoprotein containing mutations in the regions flanking the C382 and C387 residues (B).



the morbilliviruses, respiroviruses, and henipaviruses may indicate a common structural and functional feature across many paramyxoviruses that is important for virus entry.

*Receptor induced antigenic changes in the paramyxovirus attachment glycoproteins*

Previous studies have shown the henipaviruses are ideal models for studying paramyxovirus class I viral fusion. Both sequence and structural homology between HeV and NiV allow functional expression of the homo- or heterotypic henipavirus envelope glycoproteins which are associated prior to receptor binding and can be co-precipitated (11, 17). Both soluble recombinant G (sG) glycoprotein and recently soluble F (sF) glycoprotein have been generated and extensively characterized (16) and Chan and Broder, unpublished). Both sG and sF glycoproteins resemble their native WT glycoprotein counterparts providing a means to study the structural organization and protective features. In addition, surrogate assays have been developed providing accurate and qualitative means to measure viral fusion and entry and together with the identification and cloning of the viral receptors has provided an opportunity to study specific interactions between the viral glycoproteins and the subsequent events related to virus infection under tightly controlled conditions. Taken together, the henipavirus systems developed here should yield information that may be broadly applicable to the paramyxovirinae in general.

Additional experiments identified a sub-panel of 7 mAbs which could detect receptor-induced structural modulations of the G glycoprotein occurring at 4 distinct antigenic sites. Moreover, the analysis here revealed important structural differences between WT G glycoprotein versus sG glycoprotein in the absence of receptor binding that offer an explanation for the observed inconsistencies between the available crystal

structures of the G glycoprotein alone and in complex with receptor and the proposed model of paramyxovirus fusion which posits of significant receptor induced conformational changes in the G glycoprotein as a trigger for fusion activation.

Overall, these studies suggest the henipavirus G glycoprotein and other paramyxovirus attachment glycoproteins in general are an important physical link between the receptor binding and fusion processes. The model of the neutralizing antigenic sites developed here shows the viral receptor contacts the henipavirus G glycoprotein at a single conserved RBD. Taken together, the molecular and structural analyses has shown that the location and form of the henipavirus RBD is similar to the sialic acid binding pocket of the HN glycoprotein suggesting a similar model of F glycoprotein activation may be applicable. The results here suggest the majority of antigenic sites targeted as part of the virus neutralizing humoral response for many paramyxoviruses are important for function(s) following the receptor binding step of entry.

Previously, we reported that single site mutation of a series of isoleucine residues within the stalk of HeV G glycoprotein disrupts its association with HeV F when co-expressed and consequently nullified its fusion promoting activity. Further, an examination of the antigenic structure of these G glycoprotein mutants showed the glycoprotein assumed a structure comparable to receptor bound WT G glycoprotein. Further experiments here demonstrate these antigenic changes are significant and may be a mechanism for transmitting signals for triggering F glycoprotein function. Indeed, the altered conformation of the HeV G glycoprotein resulting from mutation of isoleucine residues in the stalk domain may have other structural or oligomeric effects that cause the

glycoprotein to assume a form similar to the receptor-“triggered” form of the protein, accounting for its lack of functional activity in the virus entry process. The studies here provide further data in support of paramyxovirus fusion models that suggest F glycoprotein activation may be associated with its dissociation from the tetrameric oligomeric complex of G glycoprotein following receptor binding.

#### *Unanswered questions*

Significant gaps in our understanding of the paramyxovirus fusion mechanism still remain. Although a plethora of neutralizing mAbs have been isolated that target paramyxovirus attachment glycoproteins, surprisingly little information is available discerning the mechanisms of neutralization for most of them. The union of antigenic studies here and the recent crystal structures of MeV H, NiV G, and recently HeV G glycoproteins supply much new data allowing for the development of unique functional studies with a focus towards understanding of the important topological attributes of the attachment glycoprotein in relation to the entry process. Continued investigation of the mechanisms of mAb virus neutralization and the characterization of their target epitopes of not only henipaviruses, but also other paramyxovirus species will help detail and evaluate the structural and functional similarities between their attachment glycoproteins and identify both conserved neutralizing determinants as well as their conserved functional features.

Several long standing questions in the study of paramyxovirus fusion and entry have complicated the molecular characterization of the virus entry process. First, qualitative and quantitative measurement of F glycoprotein activation has been frustrated by a lack of reliable assays demonstrating or disproving the F glycoprotein dissociates

from the G glycoprotein following receptor binding. Although a few groups have provided some evidence showing the F glycoprotein dissociates from its attachment glycoprotein partner following receptor binding, these assays have not been accepted widely or shown to be highly reproducible (1 and Moscona, unpublished). No doubt a measure of dissociation of the F glycoprotein in such a manner would provide solid evidence for determining the relevance of attachment glycoprotein-mediated effects following receptor binding. Secondly, although some reports have implicated portions of both the stalk and/or outer face of the globular head of the attachment glycoprotein in their association with the F glycoprotein, convincing evidence has not provided the details to identify the precise regions of either envelope glycoprotein that facilitate the noncovalent interactions between them. Identification of the domains or elements important for the association of the F glycoprotein and the G glycoprotein for example would provide a greater understanding of the manner in which these proteins non-covalently interact and help detail the triggering process of F glycoprotein activation.

Here it was demonstrated that discrete epitopes of the G glycoprotein undergo structural changes as detected by mAb binding following receptor engagement. Defining the targeted epitopes recognized by these mAbs would provide a platform for developing additional hypotheses and molecular assays aimed at resolving some of these long standing questions regarding paramyxovirus entry. For example, mapping these targeted epitopes may reveal significant changes occur in one or few domains of the G glycoprotein and suggest that they could be important elements in facilitating the interaction(s) with the F glycoprotein. As a result, targeted mutations could be generated near these target epitopes followed by an investigation of the efficiency with which these

G glycoprotein mutants are able to associate with the F glycoprotein. In addition, a molecular assay could be envisioned to quantitatively measure triggering of the F glycoprotein (e.g. dissociation of the F/G complex) which would clearly demonstrate and relate the structural changes in the G glycoprotein linking receptor binding with activation of the conformational changes in the F glycoprotein leading to membrane fusion.

## **Limitations and future directions**

### *Limitations*

Although the present work has significantly advanced our understanding of henipavirus binding and entry, several limitations are present in the analysis. Here, the largest and most diverse panel of G glycoprotein specific mAbs has been developed and extensively characterized; however, the large panel is limited in number and diversity. Given the high degree of sequence and structural homology of the henipavirus envelope glycoproteins, additional studies will likely demonstrate that the antigenic sites targeted by species specific mAbs are in fact conserved among the henipaviruses.

Restriction of the henipaviruses to BSL-4 containment facilities limits the extent by which experiments can be carried out. Characterization of the function of the viral glycoproteins as well as fusion and inhibitory molecules against them often requires expression and manipulation of the viral envelope glycoproteins in surrogate systems that could affect the results and inferences drawn from the data. For example, the envelope glycoprotein determinants (F glycoprotein and G glycoprotein) are present in much greater quantity in viral glycoprotein mediated membrane fusion assays than in live virus infection, which can mask minor inhibitory and fusion defects. As a result, the reported

IC<sub>50</sub> concentrations of fusion inhibitors or the fusion activity measured for glycoprotein mutants are just proportional estimates and could be underestimated in comparison to direct measures of their effects or real virus entry.

#### *Future directions*

Here, we report the development of a large panel of mAbs and their use to characterize important epitopes of the henipavirus G glycoprotein. The presented analyses are only a starting point of a much more comprehensive research focus to describe the antigenic structure of the G glycoprotein and to refine the model of henipavirus enveloped glycoprotein mediated membrane fusion. Toward this end, the panel of mAbs will be used to further define the structural characteristics of the G glycoprotein and the relation of these regions to function as well as to develop additional assays that can be used to study the epidemiology and basic biologic features of the henipaviruses.

Recently, in a novel ferret model of NiV disease, post-challenge therapy with mAb m102.4 was clearly shown to reduce morbidity and mortality among challenged animals (18). These results, together with multiple recent spillover events of HeV and NiV, have spurred greater interest in the development and characterization of henipavirus neutralizing mAbs, including those virus-neutralizing mAbs detailed here. Although some data has been presented mapping the epitopes of a limited number of henipavirus specific mAbs, the targeted epitope(s) of the henipavirus G glycoprotein for many of the mAbs presented remain to be precisely mapped. One method for identifying residues potentially important for antibody binding is the generation of mAb neutralization escape



virus(es) and the characterization of the specific mutations of these viruses which contribute virus neutralization escape.

In general, the mAb virus neutralization escape mutants are developed by *in vitro* serial passage of the virus in culture with the virus neutralizing mAb at low concentration in the culture media. Over the course of multiple passages, growth of the virus in the presence of the neutralizing mAb selects for virus which contains mutations in the G glycoprotein that effect mAb binding or decreases the viral sensitivity to the inhibitory effects of mAb. The nucleotide sequence of the G glycoprotein for each of the mAb neutralization escape virus can be determined and these analyses may reveal specific residues important in the epitope of these virus-neutralizing mAb. Although generating neutralizing mAb virus mutants is a common and widely used method for epitope discovery, these experiments can only be efficiently employed to characterize the epitope(s) of mAbs that inhibit the viral replication process.

In order to determine the target epitopes for non-virus neutralizing mAbs, a panel of chimeric recombinant HeV G glycoprotein constructs is being developed. Specifically, the loops protruding from the outermost surface of the henipavirus G glycoprotein were identified based from the crystal structure of sG<sub>NIIV</sub> and will be replaced with the nucleotide sequence encoding the analogous loop region of the hPIV3 HN glycoprotein. These loops are solvent exposed, readily available on the viral G glycoprotein, and commonly are regions targeted by virus neutralizing mAbs among the paramyxoviruses. Furthermore, these loops of the G glycoprotein are commonly limited in size and, as a result, divergence in the loop between viral species is less likely to introduce conformation changes which significantly disrupt the overall structure of the

WT G glycoprotein. Chimeric HeV G glycoproteins containing the hPIV-3 HN glycoprotein loop substitutions can be expressed *in vitro* and precipitated with each of the murine mAbs to identify differences mAb binding and, thus, identify regions of the G glycoprotein strongly associated with the interaction with the mAb. Furthermore, the capacity of these chimeric constructs to bind receptor and promote activation of the F glycoprotein mediated fusion process and could uncover areas of the G glycoprotein that are important for the function of the viral protein and/or association with the F glycoprotein.

Although the effects of specific mutations of the henipavirus G glycoprotein were presented here, the nucleotide coding sequence and amino acid composition of the murine mAbs are not known. The dearth of mAb sequence information has limited the range of experiments performed, development of reagents, and conclusions that could be drawn during the course of these studies. Rapid amplification of cDNA ends (RACE), a technique used to amplify and sequence an unknown portion of a gene, will be employed to determine the unknown sequence of selected mAbs following the development of a suitable collection of oligonucleotide primers and purification high quality cellular RNA isolated from each of the target clonal hybridoma cell lines.

One such planned application of mAb nucleotide sequence data is for resolving the crystal structure of virus neutralizing mAbs bound to the target henipavirus G glycoprotein. Solution structures of the antibody/G glycoprotein complex can aid in determining the mechanism of mAb mediated virus neutralization when molecular techniques have not yielded clear evidence for a specific mechanism of virus neutralization. Recently, crystals of the Fab m102.3 (a derivative of m102.4) and a

hAH1.3 Fab in complex with the HeV G glycoprotein have been obtained and resolution of the solution structure would deliver the first solution structures of virus neutralizing antibodies complexed with the viral G glycoprotein antibody ligands and provide significant advancement of structural data for the henipavirus envelope glycoproteins furthering the utility of these organisms as model systems for studying the paramyxoviruses and class I viral fusion.

In addition, humanization of the neutralizing mAb nAH1.3, the most potent antibody inhibitor of henipavirus fusion and entry described to date, would provide additional therapeutic options and can be used to fortify the current investigational antibody therapies for henipavirus infection. The mAb nAH1.3 binds the G glycoprotein of both known henipaviruses, targeting a large discontinuous epitope (antigenic site V) first described by White *et al.* (157). Additional detailed mapping of the residues important for nAH1.3 binding and resolution of the mAb crystal structure in complex with the henipavirus sG glycoprotein would validate competitive-binding assays and help define its neutralizing mechanism. Furthermore, sequencing the CDR region of virus neutralizing mAb nAH1.3 is the first step in the process toward transferring the important variable loops of the murine mAb to a human IgG backbone in the process of "humanizing" the virus neutralizing murine mAb. Following the generation of a humanized form of nAH1.3 the virus neutralizing potency would again have to be verified using the standard *in vitro* surrogate assays and with live henipavirus before the utility of the potential therapeutic mAb could be investigated using an *in vivo* animal model system.

The data here clearly demonstrates the structure of the henipavirus G glycoprotein is modulated by the viral receptor. Furthermore, these data indicate the sG glycoprotein is structurally more similar to the post-receptor bound form of the WT henipavirus G

glycoprotein, potentially suggesting an important role of the TM and CT domains as well as oligomeric structure of the G glycoprotein. In the absence of crystal structures for the tetrameric WT henipavirus G glycoprotein in a "pre-attachment" conformation, the panel of mAbs is the most readily available and reliable method for characterizing receptor binding modulated effects on the structure of the henipavirus G glycoprotein. Beyond the necessity to precisely determine and characterize the targeted epitopes of the G glycoprotein, additional analyses should be undertaken comparing the structure of the henipavirus G glycoprotein in the presence and absence of viral receptor and evaluate varying conditions (ex. temperature) on the kinetics of receptor and/or mAb binding as well as receptor modulated structural changes. Specifically, these analyses could utilize molecular techniques such as circular dichroism, surface plasmon resonance, and immunoprecipitation assays to probe the structure and specifically quantify the reaction at various steps.

Previous characterizations suggested expression of the WT henipavirus G glycoprotein in mammalian tissue cultures resulted in a mixed population of both pairs of dimers that are covalently (form disulfide linked tetramers) and non-covalently associated (disulfide linked dimers that associate non-covalently to form tetramers), a largely uncharacterized trait not widely described in the paramyxovirus literature. Furthermore, it is unclear whether both covalently and non-covalently associated tetrameric G glycoprotein species are biologically relevant during henipavirus entry. Here, the data suggest both forms of the G glycoprotein tetramer (covalently and non-covalently associated) can bind the viral receptor(s) and receptor engagement modulates analogous antigenic and structural changes in both tetrameric species suggesting both forms of the

G glycoprotein tetramer may be active during attachment. Similar sucrose density gradient centrifugation analyses with HeV and NiV are necessary to determine if the observed phenomenon can be detected in virus particles or represents an artifact of the over-expression of the G glycoprotein from *in vitro* expression from mammalian vectors. In addition, examination of the effect of receptor binding on the oligomeric forms of the G glycoprotein should be conducted using native (non-denaturing and non-reducing) PAGE analysis to detect differences in the amount of each oligomeric species in the presence and absence of ephrinB2. The analyses would directly address limitations of the PAGE assays presented and minor differences and/or dissociation of the G glycoprotein tetrameric complex may be visible by this method.

Isolation of a panel of receptor modulated mAbs not only affords a means for the characterization of the structural aspects of the G glycoprotein under varied conditions, but also can facilitate the development of additional assays to observe and quantify activation of the F glycoprotein as well as study the predicted dissociation of the F glycoprotein trimer from the G glycoprotein complex. A variety of methods could be used to study receptor modulated antigenic changes in the G glycoprotein and, simultaneously, specific changes in the F glycoprotein. The direct association of native and activated forms of the F and G glycoproteins could be assayed in bead based precipitation assays using differentially labeled anti-sG and anti-sF mAb pairs. In addition, the panel of mAbs described here can be used to precipitate the G glycoprotein co-expressed with the F glycoprotein and quantify the amount of co-precipitated F glycoprotein in the presence or absence of the viral receptor. Alternatively, dissociation of the F/G glycoprotein complex following receptor binding can be imaged by

fluorescence resonance energy transfer (FRET) or split green fluorescent protein (GFP) labeling of the F and G glycoproteins. Regardless of the specific techniques employed for these studies, the extensive panels of virus neutralizing and receptor modulated mAbs are essential tools for developing these assays and identifying subtle differences in the structure and state of the henipavirus envelope glycoproteins mediating membrane fusion.

#### *Concluding remarks*

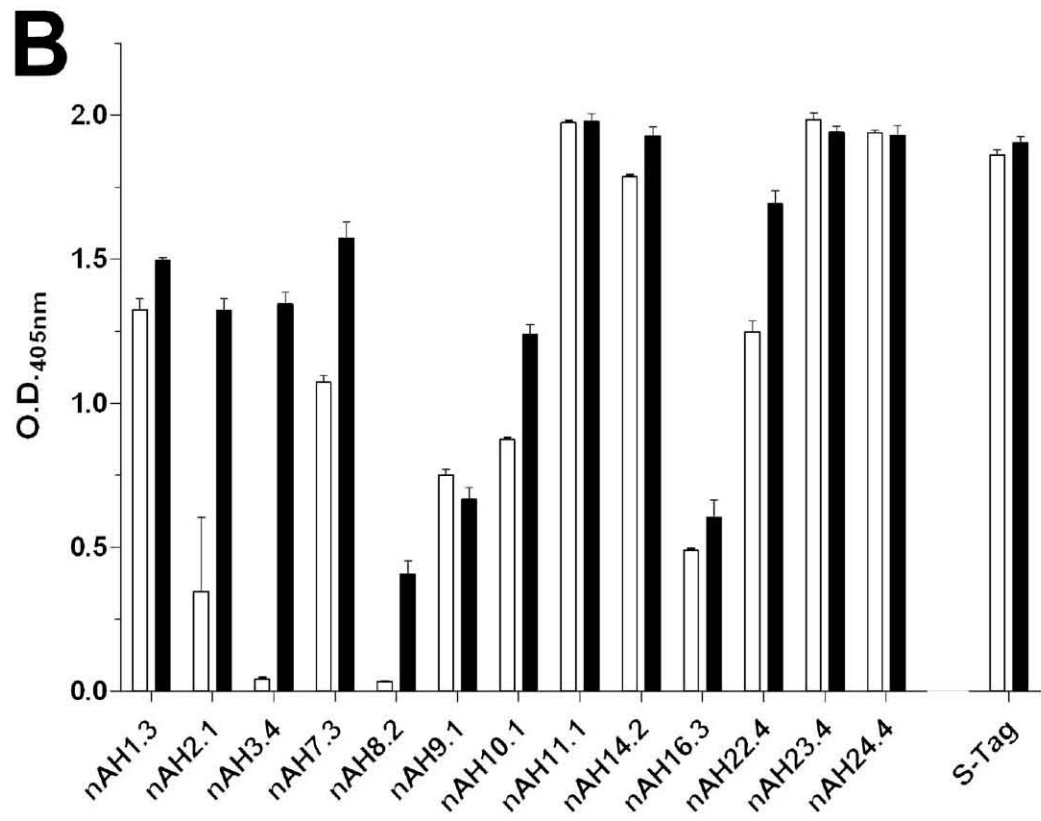
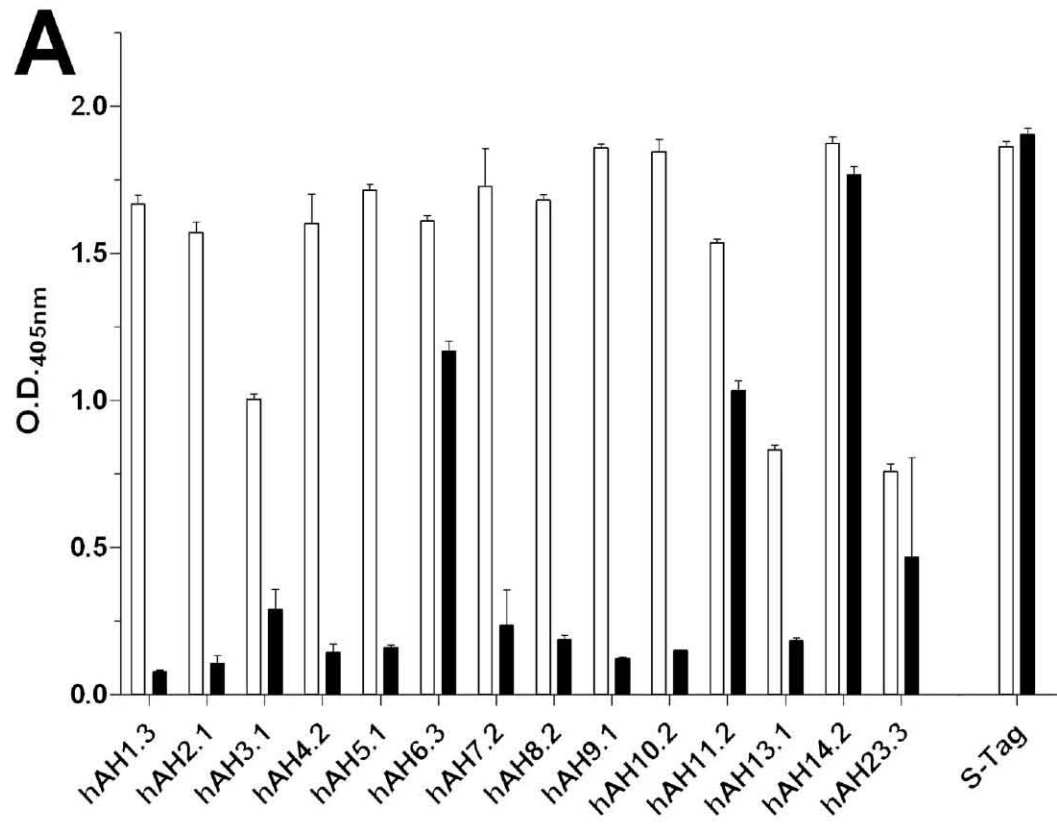
This work reports the most extensive characterization of the virus neutralizing epitopes and antigenic structure for any of the henipavirus envelope glycoproteins to date. The size and diversity of the panel of mAbs generated for these studies was advantageous in probing the virus neutralizing epitopes and structural features of the henipavirus G glycoprotein and aided in further elucidating the role of the G glycoprotein in henipavirus fusion and entry. Furthermore, the panel of mAbs generated here has become an invaluable tool that has been widely used in henipavirus research. The panel of mAb along with the information presented here will provide the basis for continue studies that will yield new information for on both henipavirus and paramyxovirus biology in the future.

## **Chapter 6: Appendices**

**Appendix A. Binding of mAbs with henipavirus sG antigens in ELISA.**

The mAbs (200 ng) derived from mice immunized with sG<sub>HeV</sub> (A) or sG<sub>NiV</sub> (B) were diluted in 1% BSA/PBST and added to microtiter plates coated with sG<sub>HeV</sub> (closed bars) and sG<sub>NiV</sub> (open bars). The plates were washed and incubated for 1 hr in 1% BSA/PBST containing goat anti-mouse-HRP antibody (1:10,000) at 37°C. Peroxidase activity was estimated with ABTS as the mean absorbance (405nm) of 3 repeats for each mAb.





**Appendix B. Characteristics of the mAbs derived from mice immunized with henipavirus sG antigens and the targeted epitopes.**

## Appendix B: Part 1

mAb <sup>1</sup>	Isotype <sup>2</sup>	Amt <sup>3</sup>	Original Well	Immunoprecipitation <sup>4</sup>		Western Blot <sup>4</sup>		Neutralizing <sup>5</sup>		Comp Group <sup>6</sup>	Epitope <sup>7</sup>	Notes
				HeV	NiV	HeV	NiV	HeV	NiV			
hAH1.3	G <sub>1</sub>	H	C16F9	S	NB	NB	NB	S	N	VII	B3L23	Used in diagnostic assays to identify HeV Used in diagnostic assays to identify HeV; epitope undergoes receptor induced changes
hAH2.1	G <sub>2a</sub>	M	C2B4	M	NB	NB	NB	N	N	A		
hAH3.1	G <sub>2b</sub>	M	F2F6	W	M	M	NB	N	N			
hAH4.2		H	F6F2	W	M	M	NB	N	N			
hAH5.1	G <sub>1</sub>	H	F2E7	S	NB	NB	NB	S	N	II		
hAH6.3	G <sub>1</sub>	M	F1D8	M	W	NB	NB	S	N	III		
hAH7.2		VL	F6C5									produces very little antibody, not well characterized
hAH8.2	G <sub>1</sub>	H	F6E7	S	NB	NB	NB	N	N	II		
hAH9.1		H	F8C4	W	NB	M	NB	S	N			
hAH10.2	G <sub>1</sub>	M	F8G4	W	NB	M	NB	N	N			
hAH11.2	G <sub>1</sub>	VL	H6E11	S	M	NB	NB	S	M	II		
hAH13.1		H	H8G2	W	NB	M	NB	N	N			
hAH14.2	G <sub>1</sub>	H	F6F7	S	W	NB	NB	S	W	II		
hAH23.3		L	H7G10	W	NB	W	NB	N	N			

<sup>1</sup>mAbs denoted hAHXX.X refer to mAbs isolated from mice immunized with sG<sub>HeV</sub> and those denoted nAHXX.X refer to mAbs derived from mice immunized with sG<sub>NiV</sub>

<sup>2</sup>Immunoglobulin isotype (Ig)

<sup>3</sup>Amount of antibody produced (yield) by the hybridoma: very little (VL), low (L), medium (M), High (H)

<sup>4</sup>Reactivity of the mAb: no binding (NB), weak (W), medium (M), strong (S)

<sup>5</sup>Inhibition of viral glycoprotein-mediated membrane fusion: non neutralizing at conc. < 200 µg/ml (N), weak (W), medium (M), strong (S)

<sup>6</sup>Competitive-binding groups determined by ELISA, neutralizing groups (I-VII) and non-neutralizing (A and B)

<sup>7</sup>The region of G targeted by the mAb using standard notation for the 6-bladed propeller model; receptor binding domain (RBD)

## Appendix B: Part 2

nAH1.3	G <sub>1</sub>	H	S1B2	S	S	NB	NB	S	S	V		Most potent published neutralizing mAb targeting HeV/NiV G; used in capture ELISAs
nAH2.1	G <sub>1</sub>	H	S1E5	NB	S	NB	NB	N	S	IV	RBD	
nAH3.4	G <sub>2b</sub>	M	R9C8	NB	S	NB	NB	N	S	I		epitope undergoes conformational induced changes
nAH7.3	G <sub>1</sub>	L	S5F6	W	W	NB	NB	W	M	IV	RBD	
nAH8.2		VL	S3E2									produces very little antibody, not well characterized
nAH9.1		M	S1D6	W	NB	S	W	N	N			
nAH10.1	G <sub>1</sub>	L	S1F5	W	W	NB	NB	W	W	IV	RBD	
nAH11.1	G <sub>1</sub>	VL	R3G4	M	M	NB	NB	N	N	B		epitope undergoes conformational induced changes
nAH14.2		H	S9B6	M	M	S	S	N	N	A		epitope undergoes conformational induced changes
nAH16.3		L	S12G9	W	W	NB	NB	N	N			
nAH22.4	G <sub>2b</sub>	H	R8B5	M	S	NB	NB	W	S	IV	RBD	
nAH23.4		H	S2E11	W	W	S	S	N	N	A		epitope undergoes conformational induced changes
nAH24.4		H	S5F11	W	W	S	S	N	N	A		epitope undergoes conformational induced changes

## Chapter 7: References

1. **Aguilar, H. C., Z. A. Ataman, V. Aspericueta, A. Q. Fang, M. Stroud, O. A. Negrete, R. A. Kammerer, and B. Lee.** 2009. A novel receptor-induced activation site in the Nipah virus attachment glycoprotein (G) involved in triggering the fusion glycoprotein (F). *J Biol Chem* **284**:1628-35.
2. **Aguirre, A. A., and G. M. Tabor.** 2008. Global factors driving emerging infectious diseases. *Ann N Y Acad Sci* **1149**:1-3.
3. **Ali, R., A. W. Mounts, U. D. Parashar, M. Sahani, M. S. Lye, M. M. Isa, K. Balathevan, M. T. Arif, and T. G. Ksiazek.** 2001. Nipah virus among military personnel involved in pig culling during an outbreak of encephalitis in Malaysia, 1998-1999. *Emerg Infect Dis* **7**:759-61.
4. **Anonymous.** 2006. Hendra virus, equine - Australia (New South Wales): suspected 20061109.3222. International Society for Infectious Diseases.
5. **Anonymous.** 2009. Hendra Virus, human, equine - Australia (04): (Queensland) fatal 20090903.3098. International Society for Infectious Diseases.
6. **Anonymous.** 2008. Hendra virus, human, equine - Australia (07): (QLD) 20080821.2606. International Society for Infectious Diseases.
7. **Anonymous.** 2007. Hendra virus, human, equine - Australia (QLD) 20070830.2851. International Society for Infectious Diseases.
8. **Anonymous.** 2008. Nipah virus, fatal - Bangladesh (Dhaka) 20080311.0979. International Society for Infectious Diseases.
9. **Backovic, M., and T. S. Jardetzky.** 2009. Class III viral membrane fusion proteins. *Curr Opin Struct Biol* **19**:189-96.

10. **Bishop, K. A., and C. C. Broder.** 2008. Hendra and Nipah viruses: Lethal Zoonotic Paramyxoviruses, p. 155-187. *In* W. M. Scheld, S. M. Hammer, and J. M. Hughes (ed.), *Emerging Infections* 8. ASM Press, Washington DC.
11. **Bishop, K. A., A. C. Hickey, D. Khetawat, J. R. Patch, K. N. Bossart, Z. Zhu, L. F. Wang, D. S. Dimitrov, and C. C. Broder.** 2008. Residues in the stalk domain of the Hendra virus G glycoprotein modulate conformational changes associated with receptor binding. *J Virol* **82**:11398-409.
12. **Bishop, K. A., T. S. Stantchev, A. C. Hickey, D. Khetawat, K. N. Bossart, V. Krasnoperov, P. Gill, Y. R. Feng, L. Wang, B. T. Eaton, L. F. Wang, and C. C. Broder.** 2007. Identification of Hendra virus G glycoprotein residues that are critical for receptor binding. *J Virol* **81**:5893-901.
13. **Bonaparte, M. I., A. S. Dimitrov, K. N. Bossart, G. Crameri, B. A. Mungall, K. A. Bishop, V. Choudhry, D. S. Dimitrov, L. F. Wang, B. T. Eaton, and C. C. Broder.** 2005. Ephrin-B2 ligand is a functional receptor for Hendra virus and Nipah virus. *Proc Natl Acad Sci U S A* **102**:10652-7.
14. **Bossart, K. N., and C. C. Broder.** 2009. Paramyxovirus Entry. *In* S. Pohlmann and G. Simmons (ed.), *Viral Entry into Host Cells*. Landes Bioscience, Austin, TX.
15. **Bossart, K. N., and C. C. Broder.** 2004. Viral glycoprotein-mediated cell fusion assays using vaccinia virus vectors. *Methods Mol Biol* **269**:309-32.
16. **Bossart, K. N., G. Crameri, A. S. Dimitrov, B. A. Mungall, Y. R. Feng, J. R. Patch, A. Choudhary, L. F. Wang, B. T. Eaton, and C. C. Broder.** 2005. Receptor binding, fusion inhibition, and induction of cross-reactive neutralizing antibodies by a soluble G glycoprotein of Hendra virus. *J Virol* **79**:6690-702.

17. **Bossart, K. N., L. F. Wang, M. N. Flora, K. B. Chua, S. K. Lam, B. T. Eaton, and C. C. Broder.** 2002. Membrane fusion tropism and heterotypic functional activities of the Nipah virus and Hendra virus envelope glycoproteins. *J Virol* **76**:11186-98.
18. **Bossart, K. N., Z. Zhu, D. Middleton, J. Klippel, G. Crameri, J. Bingham, J. A. McEachern, D. Green, T. J. Hancock, Y. P. Chan, A. C. Hickey, D. S. Dimitrov, L. F. Wang, and C. C. Broder.** 2009. A neutralizing human monoclonal antibody protects against lethal disease in a new ferret model of acute Nipah virus infection. *PLoS Pathog* **5**:e1000642.
19. **Bouche, F. B., O. T. Ertl, and C. P. Muller.** 2002. Neutralizing B cell response in Measles. *Viral Immunol* **15**:451-71.
20. **Bowden, T. A., A. R. Aricescu, R. J. Gilbert, J. M. Grimes, E. Y. Jones, and D. I. Stuart.** 2008. Structural basis of Nipah and Hendra virus attachment to their cell-surface receptor ephrin-B2. *Nat Struct Mol Biol* **15**:567-72.
21. **Bowden, T. A., M. Crispin, D. J. Harvey, A. R. Aricescu, J. M. Grimes, E. Y. Jones, and D. I. Stuart.** 2008. Crystal structure and carbohydrate analysis of Nipah virus attachment glycoprotein: a template for antiviral and vaccine design. *J Virol* **82**:11628-36.
22. **Brown, C.** 2004. Emerging zoonoses and pathogens of public health significance--an overview. *Rev Sci Tech* **23**:435-42.
23. **Büchen-Osmond, C.** 2006. Index to ICTVdB virus descriptions, ICTVdB - The Universal Virus Database, version 4. Management, Mailman School of Public Health, Columbia University, New York, NY.

24. **Carbone, K. M., and S. Rubin.** 2007. Mumps Virus, p. 1527-1550. *In* D. Knipe and P. M. Howley (ed.), *Fields Virology*, vol. 1. Lippincott Williams and Wilkins, Philadelphia.
25. **Casadevall, A., E. Dadachova, and L. A. Pirofski.** 2004. Passive antibody therapy for infectious diseases. *Nat Rev Microbiol* **2**:695-703.
26. **Chan, Y. P., L. Yan, Y. R. Feng, and C. C. Broder.** 2009. Preparation of recombinant viral glycoproteins for novel and therapeutic antibody discovery. *Methods Mol Biol* **525**:31-58, xiii.
27. **Childs, J. E., J. A. Richt, and J. S. Mackenzie.** 2007. Introduction: conceptualizing and partitioning the emergence process of zoonotic viruses from wildlife to humans. *Curr Top Microbiol Immunol* **315**:1-31.
28. **Chua, K. B.** 2003. Nipah virus outbreak in Malaysia. *J Clin Virol* **26**:265-75.
29. **Chua, K. B., W. J. Bellini, P. A. Rota, B. H. Harcourt, A. Tamin, S. K. Lam, T. G. Ksiazek, P. E. Rollin, S. R. Zaki, W. Shieh, C. S. Goldsmith, D. J. Gubler, J. T. Roehrig, B. Eaton, A. R. Gould, J. Olson, H. Field, P. Daniels, A. E. Ling, C. J. Peters, L. J. Anderson, and B. W. Mahy.** 2000. Nipah virus: a recently emergent deadly paramyxovirus. *Science* **288**:1432-5.
30. **Chua, K. B., B. H. Chua, and C. W. Wang.** 2002. Anthropogenic deforestation, El Nino and the emergence of Nipah virus in Malaysia. *Malays J Pathol* **24**:15-21.
31. **Chua, K. B., K. J. Goh, K. T. Wong, A. Kamarulzaman, P. S. Tan, T. G. Ksiazek, S. R. Zaki, G. Paul, S. K. Lam, and C. T. Tan.** 1999. Fatal encephalitis due to Nipah virus among pig-farmers in Malaysia. *Lancet* **354**:1257-9.



32. **Chua, K. B., C. L. Koh, P. S. Hooi, K. F. Wee, J. H. Khong, B. H. Chua, Y. P. Chan, M. E. Lim, and S. K. Lam.** 2002. Isolation of Nipah virus from Malaysian Island flying-foxes. *Microbes Infect* **4**:145-51.
33. **Chua, K. B., S. K. Lam, K. J. Goh, P. S. Hooi, T. G. Ksiazek, A. Kamarulzaman, J. Olson, and C. T. Tan.** 2001. The presence of Nipah virus in respiratory secretions and urine of patients during an outbreak of Nipah virus encephalitis in Malaysia. *J Infect* **42**:40-3.
34. **Cleaveland, S., D. T. Haydon, and L. Taylor.** 2007. Overviews of pathogen emergence: which pathogens emerge, when and why? *Curr Top Microbiol Immunol* **315**:85-111.
35. **Collins, P. L., and J. E. J. Crowe.** 2007. Respiratory Syncytial Virus and Metapneumovirus, p. 1601-1646. *In* D. Knipe and P. M. Howley (ed.), *Fields Virology*, 5th ed, vol. 2. Lippincott Williams and Wilkins, Philadelphia.
36. **Corey, E. A., and R. M. Iorio.** 2007. Mutations in the stalk of the Measles virus hemagglutinin protein decrease fusion but do not interfere with virus-specific interaction with the homologous fusion protein. *J Virol* **81**:9900-10.
37. **Crennell, S., T. Takimoto, A. Portner, and G. Taylor.** 2000. Crystal structure of the multifunctional paramyxovirus hemagglutinin-neuraminidase. *Nat Struct Biol* **7**:1068-74.
38. **Daszak, P.** 2009. The Ecology and Causes of Nipah and Hendra Virus Emergence. Presented at the Bats and Emerging Viral Diseases Workshop, Rockville, MD.
39. **DeLano Scientific LLC.** 2008. PyMOL Molecular Viewer, V1.1. Palo Alto, CA.

40. **Deng, R., Z. Wang, A. M. Mirza, and R. M. Iorio.** 1995. Localization of a domain on the paramyxovirus attachment protein required for the promotion of cellular fusion by its homologous fusion protein spike. *Virology* **209**:457-69.
41. **Drescher, U.** 2002. Eph family functions from an evolutionary perspective. *Curr Opin Genet Dev* **12**:397-402.
42. **Dubay, J. W., S. J. Roberts, B. Brody, and E. Hunter.** 1992. Mutations in the leucine zipper of the Human Immunodeficiency virus type 1 transmembrane glycoprotein affect fusion and infectivity. *J Virol* **66**:4748-56.
43. **Earl, P. L., C. C. Broder, D. Long, S. A. Lee, J. Peterson, S. Chakrabarti, R. W. Doms, and B. Moss.** 1994. Native oligomeric Human Immunodeficiency virus type 1 envelope glycoprotein elicits diverse monoclonal antibody reactivities. *J Virol* **68**:3015-26.
44. **Earp, L. J., S. E. Delos, H. E. Park, and J. M. White.** 2005. The many mechanisms of viral membrane fusion proteins. *Curr Top Microbiol Immunol* **285**:25-66.
45. **Eaton, B. T., C. C. Broder, D. Middleton, and L. F. Wang.** 2006. Hendra and Nipah viruses: different and dangerous. *Nat Rev Microbiol* **4**:23-35.
46. **Eaton, B. T., C. C. Broder, and L. F. Wang.** 2005. Hendra and Nipah viruses: pathogenesis and therapeutics. *Curr Mol Med* **5**:805-16.
47. **Eaton, B. T., J. S. Mackenzie, and L.-F. Wang.** 2007. Henipaviruses, p. 1587-1600. *In* D. Knipe and P. M. Howley (ed.), *Fields Virology*, 5th ed, vol. 2. Lippincott Williams and Wilkins, Philadelphia.

48. **Endy, T. P., S. Chunsuttiwat, A. Nisalak, D. H. Libraty, S. Green, A. L. Rothman, D. W. Vaughn, and F. A. Ennis.** 2002. Epidemiology of inapparent and symptomatic acute Dengue virus infection: a prospective study of primary school children in Kamphaeng Phet, Thailand. *Am J Epidemiol* **156**:40-51.
49. **Endy, T. P., A. Nisalak, S. Chunsuttiwat, D. H. Libraty, S. Green, A. L. Rothman, D. W. Vaughn, and F. A. Ennis.** 2002. Spatial and temporal circulation of Dengue virus serotypes: a prospective study of primary school children in Kamphaeng Phet, Thailand. *Am J Epidemiol* **156**:52-9.
50. **Epstein, J. H., S. Abdul Rahman, J. A. Zambriski, K. Halpin, G. Meehan, A. A. Jamaluddin, S. S. Hassan, H. E. Field, A. D. Hyatt, and P. Daszak.** 2006. Feral cats and risk for Nipah virus transmission. *Emerg Infect Dis* **12**:1178-9.
51. **Ertl, O. T., D. C. Wenz, F. B. Bouche, G. A. Berbers, and C. P. Muller.** 2003. Immunodominant domains of the Measles virus hemagglutinin protein eliciting a neutralizing human B cell response. *Arch Virol* **148**:2195-206.
52. **Field, H., P. Young, J. M. Yob, J. Mills, L. Hall, and J. Mackenzie.** 2001. The natural history of Hendra and Nipah viruses. *Microbes Infect* **3**:307-14.
53. **Field, H. E., P. C. Barratt, R. J. Hughes, J. Shield, and N. D. Sullivan.** 2000. A fatal case of Hendra virus infection in a horse in north Queensland: clinical and epidemiological features. *Aust Vet J* **78**:279-80.
54. **Fleming, A.** 2001. On the antibacterial action of cultures of a penicillium, with special reference to their use in the isolation of *B. influenzae*. 1929. *Bull World Health Organ* **79**:780-90.

55. **Goh, K. J., C. T. Tan, N. K. Chew, P. S. Tan, A. Kamarulzaman, S. A. Sarji, K. T. Wong, B. J. Abdullah, K. B. Chua, and S. K. Lam.** 2000. Clinical features of Nipah virus encephalitis among pig farmers in Malaysia. *N Engl J Med* **342**:1229-35.
56. **GraphPad Software.** 2007. GraphPad Prism, Version 5.0, La Jolla, CA.
57. **Griffin, D. E.** 2007. Measles Virus, p. 1551-1586. *In* D. Knipe and P. M. Howley (ed.), *Fields Virology*, 5th ed, vol. 2. Lippincott Williams and Wilkins, Philadelphia.
58. **Guillaume, V., H. Aslan, M. Ainouze, M. Guerbois, T. F. Wild, R. Buckland, and J. P. Langedijk.** 2006. Evidence of a potential receptor-binding site on the Nipah virus G protein (NiV G): identification of globular head residues with a role in fusion promotion and their localization on an NiV-G structural model. *J Virol* **80**:7546-54.
59. **Guillaume, V., H. Contamin, P. Loth, M. C. Georges-Courbot, A. Lefeuvre, P. Marianneau, K. B. Chua, S. K. Lam, R. Buckland, V. Deubel, and T. F. Wild.** 2004. Nipah virus: vaccination and passive protection studies in a hamster model. *J Virol* **78**:834-40.
60. **Guillaume, V., H. Contamin, P. Loth, I. Grosjean, M. C. Courbot, V. Deubel, R. Buckland, and T. F. Wild.** 2006. Antibody prophylaxis and therapy against Nipah virus infection in hamsters. *J Virol* **80**:1972-8.
61. **Guillaume, V., K. T. Wong, R. Y. Looi, M. C. Georges-Courbot, L. Barrot, R. Buckland, T. F. Wild, and B. Horvat.** 2009. Acute Hendra virus infection:

Analysis of the pathogenesis and passive antibody protection in the hamster model. *Virology* **387**:459-65.

62. **Gurley, E. S., J. M. Montgomery, M. J. Hossain, M. Bell, A. K. Azad, M. R. Islam, M. A. Molla, D. S. Carroll, T. G. Ksiazek, P. A. Rota, L. Lowe, J. A. Comer, P. Rollin, M. Czub, A. Grolla, H. Feldmann, S. P. Luby, J. L. Woodward, and R. F. Breiman.** 2007. Person-to-person transmission of Nipah virus in a Bangladeshi community. *Emerg Infect Dis* **13**:1031-7.
63. **Hall, L., and G. Richards.** 2000. *Flying Foxes: Fruit and Blossom Bats of Australia*. University of New South Wales Press Ltd, Sydney.
64. **Hanna, J. N., W. J. McBride, D. L. Brookes, J. Shield, C. T. Taylor, I. L. Smith, S. B. Craig, and G. A. Smith.** 2006. Hendra virus infection in a veterinarian. *Med J Aust* **185**:562-4.
65. **Harcourt, B. H., L. Lowe, A. Tamin, X. Liu, B. Bankamp, N. Bowden, P. E. Rollin, J. A. Comer, T. G. Ksiazek, M. J. Hossain, E. S. Gurley, R. F. Breiman, W. J. Bellini, and P. A. Rota.** 2005. Genetic characterization of Nipah virus, Bangladesh, 2004. *Emerg Infect Dis* **11**:1594-7.
66. **Harit, A. K., R. L. Ichhpujani, S. Gupta, K. S. Gill, S. Lal, N. K. Ganguly, and S. P. Agarwal.** 2006. Nipah/Hendra virus outbreak in Siliguri, West Bengal, India in 2001. *Indian J Med Res* **123**:553-60.
67. **Harrison, S. C.** 2008. Viral membrane fusion. *Nat Struct Mol Biol* **15**:690-8.
68. **Hayman, D. T., R. Suu-Ire, A. C. Breed, J. A. McEachern, L. Wang, J. L. Wood, and A. A. Cunningham.** 2008. Evidence of Henipavirus infection in West African fruit bats. *PLoS One* **3**:e2739.

69. **Herlihy, D.** 1997. *The Black Death and the Transformation of the West*. Harvard University Press, Cambridge, Massachusetts.
70. **Heroult, M., F. Schaffner, and H. G. Augustin.** 2006. Eph receptor and ephrin ligand-mediated interactions during angiogenesis and tumor progression. *Exp Cell Res* **312**:642-50.
71. **Hossain, M. J., E. S. Gurley, J. M. Montgomery, M. Bell, D. S. Carroll, V. P. Hsu, P. Formenty, A. Croisier, E. Bertherat, M. A. Faiz, A. K. Azad, R. Islam, M. A. Molla, T. G. Ksiazek, P. A. Rota, J. A. Comer, P. E. Rollin, S. P. Luby, and R. F. Breiman.** 2008. Clinical presentation of Nipah virus infection in Bangladesh. *Clin Infect Dis* **46**:977-84.
72. **Hummel, K. B., and W. J. Bellini.** 1995. Localization of monoclonal antibody epitopes and functional domains in the hemagglutinin protein of Measles virus. *J Virol* **69**:1913-6.
73. **Indoh, T., S. Yokota, T. Okabayashi, N. Yokosawa, and N. Fujii.** 2007. Suppression of NF-kappaB and AP-1 activation in monocytic cells persistently infected with measles virus. *Virology* **361**:294-303.
74. **Iorio, R. M., R. L. Glickman, A. M. Riel, J. P. Sheehan, and M. A. Bratt.** 1989. Functional and neutralization profile of seven overlapping antigenic sites on the HN glycoprotein of Newcastle disease virus: monoclonal antibodies to some sites prevent viral attachment. *Virus Res* **13**:245-61.
75. **Iorio, R. M., R. L. Glickman, and J. P. Sheehan.** 1992. Inhibition of fusion by neutralizing monoclonal antibodies to the haemagglutinin-neuraminidase glycoprotein of Newcastle disease virus. *J Gen Virol* **73 ( Pt 5)**:1167-76.

76. **Iorio, R. M., and P. J. Mahon.** 2008. Paramyxoviruses: different receptors - different mechanisms of fusion. *Trends Microbiol* **16**:135-7.
77. **Iorio, R. M., R. J. Syddall, J. P. Sheehan, M. A. Bratt, R. L. Glickman, and A. M. Riel.** 1991. Neutralization map of the hemagglutinin-neuraminidase glycoprotein of Newcastle disease virus: domains recognized by monoclonal antibodies that prevent receptor recognition. *J Virol* **65**:4999-5006.
78. **Ivanov, II, R. L. Schelonka, Y. Zhuang, G. L. Gartland, M. Zemlin, and H. W. Schroeder, Jr.** 2005. Development of the expressed Ig CDR-H3 repertoire is marked by focusing of constraints in length, amino acid use, and charge that are first established in early B cell progenitors. *J Immunol* **174**:7773-80.
79. **Joint United Nations Programme on HIV/AIDS (UNAIDS).** 2008. Report on the HIV/AIDS epidemic 2008 p. 211-234. UNAIDS, Geneva, Switzerland.
80. **Jones, K. E., N. G. Patel, M. A. Levy, A. Storeygard, D. Balk, J. L. Gittleman, and P. Daszak.** 2008. Global trends in emerging infectious diseases. *Nature* **451**:990-3.
81. **Kammerer, R. A.** 1997. Alpha-helical coiled-coil oligomerization domains in extracellular proteins. *Matrix Biol* **15**:555-65; discussion 567-8.
82. **Karron, R. A., and P. L. Collins.** 2007. Parainfluenza Viruses, p. 1497-1526. *In* D. Knipe and P. M. Howley (ed.), *Fields Virology*, 5th ed, vol. 1. Lippincott Williams and Wilkins, Philadelphia.
83. **Kielian, M., and F. A. Rey.** 2006. Virus membrane-fusion proteins: more than one way to make a hairpin. *Nat Rev Microbiol* **4**:67-76.

84. **Komatsu, T., K. Takeuchi, J. Yokoo, and B. Gotoh.** 2002. Sendai virus C protein impairs both phosphorylation and dephosphorylation processes of Stat1. *FEBS Let* **511**:139-44.
85. **Krishanan, S., and K. Biswas.** 2007. Nipah Outbreak in India and Bangladesh. World Health Organization-South East Asia regional office.
86. **Lam, S. K., and K. B. Chua.** 2002. Nipah virus encephalitis outbreak in Malaysia. *Clin Infect Dis* **34 Suppl 2**:S48-51.
87. **Lamb, R., and D. P. Griffith.** 2007. Paramyxoviridae: The Viruses and their Replication, p. 1449-1296. *In* D. Knipe and P. M. Howley (ed.), *Fields Virology*, 5th ed, vol. 1. Lippincott Williams and Wilkins, Philadelphia.
88. **Lamb, R. A., and T. S. Jardetzky.** 2007. Structural basis of viral invasion: lessons from paramyxovirus F. *Curr Opin Struct Biol* **17**:427-36.
89. **Lamb, R. A., R. G. Paterson, and T. S. Jardetzky.** 2006. Paramyxovirus membrane fusion: lessons from the F and HN atomic structures. *Virology* **344**:30-7.
90. **Lapthorn, A. J., R. W. Janes, N. W. Isaacs, and B. A. Wallace.** 1995. Cystine nooses and protein specificity. *Nat Struct Biol* **2**:266-8.
91. **Lashley, F. R.** 2004. Emerging infectious diseases: vulnerabilities, contributing factors and approaches. *Expert Rev Anti Infect Ther* **2**:299-316.
92. **Lawrence, M. C., N. A. Borg, V. A. Streltsov, P. A. Pilling, V. C. Epa, J. N. Varghese, J. L. McKimm-Breschkin, and P. M. Colman.** 2004. Structure of the haemagglutinin-neuraminidase from Human Parainfluenza virus type III. *J Mol Biol* **335**:1343-57.



93. **Lederberg, J., R. Shope, and S. C. Oaks, Jr., ed.** 1992. Emerging Infections: Microbial Threats to Health in the United States. Institute of Medicine, National Academy Press.
94. **Li, Y., J. Wang, A. C. Hickey, Y. Zhang, Y. Wu, H. Zhang, J. Yuan, Z. Han, J. McEachern, C. C. Broder, L. F. Wang, and Z. Shi.** 2008. Antibodies to Nipah or Nipah-like viruses in bats, China. *Emerg Infect Dis* **14**:1974-6.
95. **Li, Z., M. Yu, H. Zhang, D. E. Magoffin, P. J. Jack, A. Hyatt, H. Y. Wang, and L. F. Wang.** 2006. Beilong virus, a novel paramyxovirus with the largest genome of non-segmented negative-stranded RNA viruses. *Virology* **346**:219-28.
96. **Liu, J., Q. Zheng, Y. Deng, C. S. Cheng, N. R. Kallenbach, and M. Lu.** 2006. A seven-helix coiled coil. *Proc Natl Acad Sci U S A* **103**:15457-62.
97. **Lu, L. L., M. Puri, C. M. Horvath, and G. C. Sen.** 2008. Select paramyxoviral V proteins inhibit IRF3 activation by acting as alternative substrates for inhibitor of kappaB kinase epsilon (IKKe)/TBK1. *J Biol Chem* **283**:14269-76.
98. **Luby, S. P., M. Rahman, M. J. Hossain, L. S. Blum, M. M. Husain, E. Gurley, R. Khan, B. N. Ahmed, S. Rahman, N. Nahar, E. Kenah, J. A. Comer, and T. G. Ksiazek.** 2006. Foodborne transmission of Nipah virus, Bangladesh. *Emerg Infect Dis* **12**:1888-94.
99. **McEachern, J. A., J. Bingham, G. Crameri, D. J. Green, T. J. Hancock, D. Middleton, Y. R. Feng, C. C. Broder, L. F. Wang, and K. N. Bossart.** 2008. A recombinant subunit vaccine formulation protects against lethal Nipah virus challenge in cats. *Vaccine* **26**:3842-52.

100. **McIlhatton, M. A., M. D. Curran, and B. K. Rima.** 1997. Nucleotide sequence analysis of the large (L) genes of Phocine Distemper virus and Canine Distemper virus (corrected sequence). *J Gen Virol* **78 ( Pt 3)**:571-6.
101. **McMichael, A. J.** 2004. Environmental and social influences on emerging infectious diseases: past, present and future. *Philos Trans R Soc Lond B Biol Sci* **359**:1049-58.
102. **Melanson, V. R., and R. M. Iorio.** 2006. Addition of N-glycans in the stalk of the Newcastle disease virus HN protein blocks its interaction with the F protein and prevents fusion. *J Virol* **80**:623-33.
103. **Melanson, V. R., and R. M. Iorio.** 2004. Amino acid substitutions in the F-specific domain in the stalk of the Newcastle Disease virus HN protein modulate fusion and interfere with its interaction with the F protein. *J Virol* **78**:13053-61.
104. **Molecular Devices Inc.** 2008. SoftMax Pro, version 4.6, Sunnyvale, CA.
105. **Morens, D. M., G. K. Folkers, and A. S. Fauci.** 2008. Emerging infections: a perpetual challenge. *Lancet Infect Dis* **8**:710-9.
106. **Morrison, T. G.** 2003. Structure and function of a paramyxovirus fusion protein. *Biochim Biophys Acta* **1614**:73-84.
107. **Morrison, T. G.** 2001. The three faces of paramyxovirus attachment proteins. *Trends Microbiol* **9**:103-5.
108. **Morse, S. S.** 1995. Factors in the emergence of infectious diseases. *Emerg Infect Dis* **1**:7-15.
109. **Muller, C. P., T. Schroeder, R. Tu, N. H. Brons, G. Jung, F. Schneider, and K. H. Wiesmuller.** 1993. Analysis of the neutralizing antibody response to the

- Measles virus using synthetic peptides of the haemagglutinin protein. *Scand J Immunol* **38**:463-71.
110. **Mungall, B. A., D. Middleton, G. Cramer, J. Bingham, K. Halpin, G. Russell, D. Green, J. McEachern, L. I. Pritchard, B. T. Eaton, L. F. Wang, K. N. Bossart, and C. C. Broder.** 2006. Feline model of acute Nipah virus infection and protection with a soluble glycoprotein-based subunit vaccine. *J Virol* **80**:12293-302.
  111. **Murphy, F. A.** 2008. Emerging zoonoses: the challenge for public health and biodefense. *Prev Vet Med* **86**:216-23.
  112. **Naniche, D.** 2009. Human immunology of Measles virus infection. *Curr Top Microbiol Immunol* **330**:151-71.
  113. **Negrete, O. A., E. L. Levroney, H. C. Aguilar, A. Bertolotti-Ciarlet, R. Nazarian, S. Tajyar, and B. Lee.** 2005. EphrinB2 is the entry receptor for Nipah virus, an emergent deadly paramyxovirus. *Nature* **436**:401-5.
  114. **Orvell, C., H. Sheshberadaran, and E. Norrby.** 1985. Preparation and characterization of monoclonal antibodies directed against four structural components of Canine Distemper virus. *J Gen Virol* **66 ( Pt 3)**:443-56.
  115. **Parashar, U. D., L. M. Sunn, F. Ong, A. W. Mounts, M. T. Arif, T. G. Ksiazek, M. A. Kamaluddin, A. N. Mustafa, H. Kaur, L. M. Ding, G. Othman, H. M. Radzi, P. T. Kitsutani, P. C. Stockton, J. Arokiasamy, H. E. Gary, Jr., and L. J. Anderson.** 2000. Case-control study of risk factors for human infection with a new zoonotic paramyxovirus, Nipah virus, during a 1998-1999 outbreak of severe encephalitis in Malaysia. *J Infect Dis* **181**:1755-9.

116. **Pasquale, E. B.** 2004. Eph-ephrin promiscuity is now crystal clear. *Nat Neurosci* **7**:417-8.
117. **Patch, J. R., G. Crameri, L. F. Wang, B. T. Eaton, and C. C. Broder.** 2007. Quantitative analysis of Nipah virus proteins released as virus-like particles reveals central role for the matrix protein. *Virol J* **4**:1.
118. **Patch, J. R., Z. Han, S. E. McCarthy, L. Yan, L. F. Wang, R. N. Harty, and C. C. Broder.** 2008. The YPLGVG sequence of the Nipah virus matrix protein is required for budding. *Virol J* **5**:137.
119. **Pavlin, J. A., A. C. Hickey, N. Ulbrandt, Y. P. Chan, T. P. Endy, M. S. Boukhvalova, S. Chunsuttiwat, A. Nisalak, D. H. Libraty, S. Green, A. L. Rothman, F. A. Ennis, R. Jarman, R. V. Gibbons, and C. C. Broder.** 2008. Human metapneumovirus reinfection among children in Thailand determined by ELISA using purified soluble fusion protein. *J Infect Dis* **198**:836-42.
120. **Peetermans, W. E., and P. De Munter.** 2007. Emerging and re-emerging infectious diseases. *Acta Clin Belg* **62**:337-41.
121. **Plempner, R. K., A. L. Hammond, D. Gerlier, A. K. Fielding, and R. Cattaneo.** 2002. Strength of envelope protein interaction modulates cytopathicity of Measles virus. *J Virol* **76**:5051-61.
122. **Poliakov, A., M. Cotrina, and D. G. Wilkinson.** 2004. Diverse roles of eph receptors and ephrins in the regulation of cell migration and tissue assembly. *Dev Cell* **7**:465-80.
123. **Pringle, C. R.** 1997. The order Mononegavirales--current status. *Arch Virol* **142**:2321-6.

124. **Renukaradhya, G. J., S. Mitra-Kaushik, G. Sinnathamby, M. Rajasekhar, and M. S. Shaila.** 2002. Mapping of B-cell epitopes of hemagglutinin protein of Rinderpest virus. *Virology* **298**:214-23.
125. **Reynes, J. M., D. Counor, S. Ong, C. Faure, V. Seng, S. Molia, J. Walston, M. C. Georges-Courbot, V. Deubel, and J. L. Sarthou.** 2005. Nipah virus in Lyle's flying foxes, Cambodia. *Emerg Infect Dis* **11**:1042-7.
126. **Rima, B. K., and W. P. Duprex.** 2009. The Measles virus replication cycle. *Curr Top Microbiol Immunol* **329**:77-102.
127. **Rodriguez, J. J., C. D. Cruz, and C. M. Horvath.** 2004. Identification of the nuclear export signal and STAT-binding domains of the Nipah virus V protein reveals mechanisms underlying interferon evasion. *J Virol* **78**:5358-67.
128. **Roelke-Parker, M. E., L. Munson, C. Packer, R. Kock, S. Cleaveland, M. Carpenter, S. J. O'Brien, A. Pospischil, R. Hofmann-Lehmann, H. Lutz, and et al.** 1996. A Canine Distemper virus epidemic in Serengeti lions (*Panthera leo*). *Nature* **379**:441-5.
129. **Russell, C. J., T. S. Jardetzky, and R. A. Lamb.** 2001. Membrane fusion machines of paramyxoviruses: capture of intermediates of fusion. *EMBO J* **20**:4024-34.
130. **Sahani, M., U. D. Parashar, R. Ali, P. Das, M. S. Lye, M. M. Isa, M. T. Arif, T. G. Ksiazek, and M. Sivamoorthy.** 2001. Nipah virus infection among abattoir workers in Malaysia, 1998-1999. *Int J Epidemiol* **30**:1017-20.
131. **Sarkar, J., V. Balamurugan, A. Sen, P. Saravanan, B. Sahay, K. K. Rajak, T. J. Rasool, V. Bhanuprakash, and R. K. Singh.** 2009. Sequence analysis of

- morbillivirus CD150 receptor-signaling lymphocyte activation molecule (SLAM) of different animal species. *Virus Genes* **39**:335-41.
132. **Schroeder, H. W., Jr.** 2006. Similarity and divergence in the development and expression of the mouse and human antibody repertoires. *Dev Comp Immunol* **30**:119-35.
  133. **Selvey, L. A., R. M. Wells, J. G. McCormack, A. J. Ansford, K. Murray, R. J. Rogers, P. S. Lavercombe, P. Selleck, and J. W. Sheridan.** 1995. Infection of humans and horses by a newly described morbillivirus. *Med J Aust* **162**:642-5.
  134. **Shaffer, J. A., W. J. Bellini, and P. A. Rota.** 2003. The C protein of Measles virus inhibits the type I interferon response. *Virology* **315**:389-97.
  135. **Shaw, M. L., W. B. Cardenas, D. Zamarin, P. Palese, and C. F. Basler.** 2005. Nuclear localization of the Nipah virus W protein allows for inhibition of both virus- and toll-like receptor 3-triggered signaling pathways. *J Virol* **79**:6078-88.
  136. **Sherman, I. W.** 2006. Six Plagues of Antiquity, p. 43-66, *The Power of Plagues*. ASM Press, Washington, DC.
  137. **Shingai, M., M. Azuma, T. Ebihara, M. Sasai, K. Funami, M. Ayata, H. Ogura, H. Tsutsumi, M. Matsumoto, and T. Seya.** 2008. Soluble G protein of Respiratory Syncytial virus inhibits Toll-like receptor 3/4-mediated IFN-beta induction. *Int Immunol* **20**:1169-80.
  138. **Skiadopoulos, M. H., L. Vogel, J. M. Riggs, S. R. Surman, P. L. Collins, and B. R. Murphy.** 2003. The genome length of Human Parainfluenza virus type 2 follows the rule of six, and recombinant viruses recovered from non-polyhexameric-length

- antigenomic cDNAs contain a biased distribution of correcting mutations. *J Virol* **77**:270-9.
139. **Smith, E. C., A. Popa, A. Chang, C. Masante, and R. E. Dutch.** 2009. Viral entry mechanisms: the increasing diversity of paramyxovirus entry. *FEBS J.*
  140. **Snowden, F. M.** 2008. Emerging and reemerging diseases: a historical perspective. *Immunol Rev* **225**:9-26.
  141. **SPSS Inc.** 2007. SPSS, Version 16.0. IBM, Chicago, IL.
  142. **Stone-Hulslander, J., and T. G. Morrison.** 1997. Detection of an interaction between the HN and F proteins in Newcastle disease virus-infected cells. *J Virol* **71**:6287-95.
  143. **Stone-Hulslander, J., and T. G. Morrison.** 1999. Mutational analysis of heptad repeats in the membrane-proximal region of Newcastle disease virus HN protein. *J Virol* **73**:3630-7.
  144. **Sugiyama, M., N. Ito, N. Minamoto, and S. Tanaka.** 2002. Identification of immunodominant neutralizing epitopes on the hemagglutinin protein of Rinderpest virus. *J Virol* **76**:1691-6.
  145. **Takimoto, T., G. L. Taylor, H. C. Connaris, S. J. Crennell, and A. Portner.** 2002. Role of the hemagglutinin-neuraminidase protein in the mechanism of paramyxovirus-cell membrane fusion. *J Virol* **76**:13028-33.
  146. **Takimoto, T., G. L. Taylor, S. J. Crennell, R. A. Scroggs, and A. Portner.** 2000. Crystallization of Newcastle disease virus hemagglutinin-neuraminidase glycoprotein. *Virology* **270**:208-14.

147. **Tan, C. T., K. J. Goh, K. T. Wong, S. A. Sarji, K. B. Chua, N. K. Chew, P. Murugasu, Y. L. Loh, H. T. Chong, K. S. Tan, T. Thayaparan, S. Kumar, and M. R. Jusoh.** 2002. Relapsed and late-onset Nipah encephalitis. *Ann Neurol* **51**:703-8.
148. **Tanabayashi, K., and R. W. Compans.** 1996. Functional interaction of paramyxovirus glycoproteins: identification of a domain in Sendai virus HN which promotes cell fusion. *J Virol* **70**:6112-8.
149. **Taylor, L. H., S. M. Latham, and M. E. Woolhouse.** 2001. Risk factors for human disease emergence. *Philos Trans R Soc Lond B Biol Sci* **356**:983-9.
150. **Tsurudome, M., M. Kawano, T. Yuasa, N. Tabata, M. Nishio, H. Komada, and Y. Ito.** 1995. Identification of regions on the hemagglutinin-neuraminidase protein of Human Parainfluenza virus type 2 important for promoting cell fusion. *Virology* **213**:190-203.
151. **Vainionpaa, R., and T. Hyypia.** 1994. Biology of parainfluenza viruses. *Clin Microbiol Rev* **7**:265-75.
152. **Vorou, R. M., V. G. Papavassiliou, and S. Tsiodras.** 2007. Emerging zoonoses and vector-borne infections affecting humans in Europe. *Epidemiol Infect* **135**:1231-47.
153. **Wang, B., N. Zhang, K. X. Qian, and J. G. Geng.** 2005. Conserved molecular players for axon guidance and angiogenesis. *Curr Protein Pept Sci* **6**:473-8.
154. **Wang, L.-F., and B. T. Eaton.** 2001. Emerging Paramyxoviruses. *Infect Dis Rev* **3**:52-69.



155. **Weingartl, H. M., Y. Berhane, and M. Czub.** 2009. Animal models of henipavirus infection: a review. *Vet J* **181**:211-20.
156. **Weiss, R. A., and A. J. McMichael.** 2004. Social and environmental risk factors in the emergence of infectious diseases. *Nat Med* **10**:S70-6.
157. **White, J. R., V. Boyd, G. S. Crameri, C. J. Duch, R. K. van Laar, L. F. Wang, and B. T. Eaton.** 2005. Location of, immunogenicity of and relationships between neutralization epitopes on the attachment protein (G) of Hendra virus. *J Gen Virol* **86**:2839-48.
158. **Wolinsky, J. S., M. N. Waxham, and A. C. Server.** 1985. Protective effects of glycoprotein-specific monoclonal antibodies on the course of experimental mumps virus meningoencephalitis. *J Virol* **53**:727-34.
159. **Wong, K. T., W. J. Shieh, S. Kumar, K. Norain, W. Abdullah, J. Guarner, C. S. Goldsmith, K. B. Chua, S. K. Lam, C. T. Tan, K. J. Goh, H. T. Chong, R. Jusoh, P. E. Rollin, T. G. Ksiazek, and S. R. Zaki.** 2002. Nipah virus infection: pathology and pathogenesis of an emerging paramyxoviral zoonosis. *Am J Pathol* **161**:2153-67.
160. **Woolhouse, M., and E. Gaunt.** 2007. Ecological origins of novel human pathogens. *Crit Rev Microbiol* **33**:231-42.
161. **Woolhouse, M. E., and S. Gowtage-Sequeria.** 2005. Host range and emerging and reemerging pathogens. *Emerg Infect Dis* **11**:1842-7.
162. **Xu, K., K. R. Rajashankar, Y. P. Chan, J. P. Himanen, C. C. Broder, and D. B. Nikolov.** 2008. Host cell recognition by the henipaviruses: crystal structures of the

- Nipah G attachment glycoprotein and its complex with ephrin-B3. *Proc Natl Acad Sci U S A* **105**:9953-8.
163. **Yin, H. S., R. G. Paterson, X. Wen, R. A. Lamb, and T. S. Jardetzky.** 2005. Structure of the uncleaved ectodomain of the paramyxovirus (hPIV3) fusion protein. *Proc Natl Acad Sci U S A* **102**:9288-93.
  164. **Yin, H. S., X. Wen, R. G. Paterson, R. A. Lamb, and T. S. Jardetzky.** 2006. Structure of the Parainfluenza virus 5 F protein in its metastable, prefusion conformation. *Nature* **439**:38-44.
  165. **Yu, M., E. Hansson, J. P. Langedijk, B. T. Eaton, and L. F. Wang.** 1998. The attachment protein of Hendra virus has high structural similarity but limited primary sequence homology compared with viruses in the genus Paramyxovirus. *Virology* **251**:227-33.
  166. **Yuan, P., T. B. Thompson, B. A. Wurzburg, R. G. Paterson, R. A. Lamb, and T. S. Jardetzky.** 2005. Structural studies of the Parainfluenza virus 5 hemagglutinin-neuraminidase tetramer in complex with its receptor, sialyllactose. *Structure* **13**:803-15.
  167. **Zaitsev, V., M. von Itzstein, D. Groves, M. Kiefel, T. Takimoto, A. Portner, and G. Taylor.** 2004. Second sialic acid binding site in Newcastle disease virus hemagglutinin-neuraminidase: implications for fusion. *J Virol* **78**:3733-41.
  168. **Zhang, J., and S. Hughes.** 2006. Role of the ephrin and Eph receptor tyrosine kinase families in angiogenesis and development of the cardiovascular system. *J Pathol* **208**:453-61.

169. **Zhu, Z., A. S. Dimitrov, K. N. Bossart, G. Crameri, K. A. Bishop, V. Choudhry, B. A. Mungall, Y. R. Feng, A. Choudhary, M. Y. Zhang, Y. Feng, L. F. Wang, X. Xiao, B. T. Eaton, C. C. Broder, and D. S. Dimitrov. 2006.**  
Potent neutralization of Hendra and Nipah viruses by human monoclonal antibodies. *J Virol* **80**:891-9.

